NMR STUDIES
OF MIXED TETRAHALOBORATES
AND SOME RELATED BORON TRIHALIDE COMPLEXES

by

Gary John Schrobilgen, B.S.

A Thesis
Submitted to the Faculty of Graduate Studies
in Partial Fulfillment of the Requirements
for the Degree of
Master of Science

Brock University
St. Catharines, Ontario

January, 1971

To Lynn and Erik

ABSTRACT

Nuclear magnetic resonance spectroscopy has been used to study donor-acceptor complexes of boron trifluoride with several ureas, tetramethylthiourea, tetramethylselenourea, and tetramethylquanidine as well as adducts of tetramethylurea with BF_2Cl, $BFCl_2$, and BCl_3.

A large number of mixed tetrahaloborate ions, including some of the ternary ones such as BF_2ClBr^-, have been obtained by ligand exchange reactions and studied by NMR techniques. The bonding in these ions is of the same inherent interest as the bonding in the isoelectronic tetrahalomethanes which have been the subject of many detailed studies and have been involved in a controversy concerning the existence of and the nature of "fluorine hyperconjugation" or C-F p_π- p_π bonding.

Ligand exchange reactions also gave rise to the difluoroboron cation, $(TMU)_2 \cdot BF_2^+$. The difluoroboron cation has been observed in solutions of $TMU \cdot BF_3$, and has been proposed as a possible intermediate for fluorine exchange reactions in BF_3 adducts.

ACKNOWLEDGEMENTS

The author wishes to thank his research director, Dr. J. S. Hartman, for his advice and encouragement in the course of these investigations.

Thanks should also go to Dr. J. M. Miller, Dr. G. F. Lanthier, and Mr. C. V. Raman for many helpful discussions and assistance.

The author would also like to thank the entire technical staff in the Department of Chemistry, with special mention to Mr. J. M. Vandenhoff.

Special thanks should also go to Professor R. J. Gillespie and Mr. J. I. A. Thompson for the generous use of their NMR facilities at McMaster University.

Much appreciation is also extended to my wife, Lynn, for her patient and able preparation of this manuscript.

Financial assistance from Brock University and the National Research Council of Canada, which provided a Scholarship for 1970-71, is gratefully acknowledged.

TABLE OF CONTENTS

TABLE OF CONTENTS

TABLE OF CONTENTS

TABLE OF CONTENTS

TABLE OF CONTENTS

TABLE OF CONTENTS

TABLE OF CONTENTS

LIST OF TABLES

LIST OF FIGURES

CHAPTER I

INTRODUCTION

(A) NUCLEAR MAGNETIC RESONANCE

(i) General

High resolution nuclear magnetic resonance spectroscopy (NMR) has become a major technique of chemistry since the discovery of the "chemical shift" in 1949 and has facilitated the solution of a wide variety of chemical problems. Several good reviews on high resolution NMR are now available and provide outlines of the principles of nuclear magnetism (1-3). This thesis describes high resolution NMR studies which have yielded information on the stoichiometry, structure, relative stabilities, and reactions of some donor-acceptor complexes of boron trihalides and tetrahaloborate anions.

Nuclear magnetic resonance spectroscopy depends on the existence of nuclear magnetic moments. A nucleus of spin quantum number I possesses a magnetic moment μ given by

$$\mu = \gamma I\hbar \qquad (1)$$

where γ is the gyromagnetic ratio, I is the maximum observable component of the nuclear angular momentum, and $\hbar$ is $h/2\pi$, where h is Planck's constant. When a nucleus with a magnetic moment is placed in a uniform magnetic field H_o in the z direction, its energy relative to that in a field of zero is

$$E = -\mu_z H_o \tag{2}$$

where μ_z is the component of the magnetic moment in the same direction. For a nucleus of spin I, 2I+1 distinct values for μ_z exist,

$$-\mu H_o, -\frac{I-1}{I}\mu H_o, \cdots, \frac{I-1}{I}\mu H_o, \mu H_o \tag{3}$$

The corresponding energy levels are equally spaced, the separation being $\mu H_o/I$. The energy of any level relative to the nucleus in a zero magnetic field is

$$E = -\frac{m\mu}{I}H_o \tag{4}$$

where m is the magnetic quantum number and can take the values I, I-1,$\cdots$, -I+1, -I. This splitting of energy levels in a magnetic field is referred to as "nuclear Zeeman splitting". The NMR experiment consists of inducing transitions between the levels, subject to the selection rule

$$\Delta m = \pm 1 \tag{5}$$

so that the energy change in any allowed transition is $\frac{\mu H}{I}$. Thus, the frequency ν of the radiation required can be found from the Bohr frequency condition

$$\nu = \frac{\mu H_o}{Ih} = \frac{\gamma H_o}{2\pi} \tag{6}$$

(ii) Chemical Shift

Any atom or molecule placed in a magnetic field acquires a diamagnetic moment arising from induced orbital motion of

its electrons. These electronic motions constitute effective currents within the molecule and give rise to a secondary magnetic field which also acts on all the nuclei present.

Since the induced motions of the electrons, and hence the local magnetic interactions, are proportional to the applied field H_o, the magnetic field H at the position of a nucleus is given by

$$H = H_o(1-\sigma_d) \tag{7}$$

where σ_d is a dimensionless constant known as the diamagnetic screening constant. The screening constant is independent of H_o, but dependent on the chemical environment.

The effect of σ_d is to bring the nuclear Zeeman levels closer together resulting in a smaller required energy to effect a transition between states. If the experiment is performed in the usual manner, that is, by varying the field H_o at a fixed frequency until resonance conditions are satisfied, the applied field will have a larger value than would have been the case if the nucleus were unscreened. In practice the magnetic field at a nucleus is not measured with respect to the applied field but instead with respect to the reference magnetic field H_r corresponding to a screening constant σ_r of a reference substance. The chemical shift δ with respect to the reference substance is given by

$$\delta = \sigma-\sigma_r = \frac{H-H_r}{H_r} \tag{8}$$

It is customary and convenient to quote chemical shifts in

terms of the dimensionless parameter δ in units of parts per million (ppm). Tetramethylsilane (TMS) is the usual reference substance for ^{1}H NMR while trichlorofluoromethane is often used as a reference in ^{19}F NMR.

(iii) Spin-Spin Coupling

The local magnetic field H at a nucleus can be affected by electron-coupled spin interactions elsewhere in the molecule. These interactions can be transmitted through several bonds but generally attenuate rapidly as the number of intervening bonds increases. In the case of two non-equivalent nuclei, A and X, bonded by a covalent bond, the interaction may be described in the following manner. The interaction of nucleus A with its bonding electron will make the electron spin lie more frequently antiparallel than parallel to the nuclear spin of A. Since the two electron spins in the covalent bond must be antiparallel to one another, the electron spin of X will tend to lie more frequently parallel to the spin of nucleus A. The electron of atom X interacts magnetically with the nucleus of this atom; as a result, the spin of nucleus X tends to be antiparallel to that of A. If perfect pairing of electrons takes place there will be only one relative nuclear configuration, *i.e.*, with nuclear spins antiparallel. For there to be more than one energy level, and hence fine structure, it is necessary to invoke excited electronic states of the molecule in which other relative orientations of the nuclei can exist. Using the above rigid mechanism, this means that there must be spin states in which the electrons are paired with spins

parallel.

The interaction energy of two magnetic nuclei A and X is of the form $J_{AX}\vec{I}_A \cdot \vec{I}_B$ in the above coupling mechanism and is independent of the applied field. The spin coupling constant J_{AX} has the dimensions of energy and is usually expressed in Herz. The interaction energy is dependent both upon the total product and the relative spatial orientation of the nuclear magnetic moments; J_{AX} is defined to be positive if the spin states in which the nuclei have antiparallel spins are lowered in energy, and those in which they have parallel spins are raised in energy, by the interaction. The converse is true if J_{AX} is negative. In practice the absolute sign of J_{AX} cannot be determined under the usual conditions of high resolution NMR; it can be determined by a special technique (4). In this thesis, J_{AX} shall be taken as meaning $|J_{AX}|$.

The number and relative intensities of multiplets depends on the relative spin configurations of the interacting groups of nuclei. As an example, the ion $^{11}BF_4^-$ is considered. The ^{19}F nucleus has I = 1/2 and the ^{11}B nucleus has I = 3/2, therefore the possible spin states are those for m = ±1/2 in the case of the ^{19}F nucleus and m = ±1/2, ±3/2 in the case of the ^{11}B nucleus. The possible ^{19}F nuclear spin configurations are given in Table I where m = +1/2 and m = -1/2 are designated by α and β, respectively.

Table I

Spin States of Four Equivalent Fluorine Nuclei

^{19}F Nucleus				Total Spin	Statistical
1	2	3	4	(I_z)	Weight
α	α	α	α	+2	1
α	α	α	β	+1	4
α	α	β	α	+1	
α	β	α	α	+1	
β	α	α	α	+1	
α	α	β	β	0	6
α	β	β	α	0	
β	β	α	α	0	
α	β	α	β	0	
β	α	β	α	0	
β	α	α	β	0	
β	β	β	α	-1	4
β	β	α	β	-1	
β	α	β	β	-1	
α	β	β	β	-1	
β	β	β	β	-2	1

The ^{11}B nucleus sees five energy states of the ^{19}F nuclei corresponding to the five values of the total spin. The two states with total spin ±1 are each four times as numerous as those with total spin ±2 while the single state with total spin 0 is six times as numerous as either of the ±2 spin states. Hence, a quintet is observed in the ^{11}B NMR spectrum with relative band intensities 1:4:6:4:1. Similarly, the spin states of the four ^{19}F nuclei are determined by the four possible total spin values of ^{11}B, ±1/2 and ±3/2, all possessing equal statistical weights. Thus, the ^{19}F resonance is split into four equally spaced lines with relative intensities 1:1:1:1.

In general, for a set of n_A equivalent nuclei of type A interacting with n_X equivalent nuclei of type X, the A signal has $2n_XI_X+1$ components and the X signal has $2n_AI_A+1$ components separated by J_{AX}. The relative intensities of each group of signals are in the ratio of the corresponding binomial coefficients.

(iv) Effects of Rapid Exchange

Chemical shift and spin-spin coupling patterns may be modified if a rate process involving the magnetic nuclei is present. For example, rapid exchange of magnetic nuclei between different environments causes coalescence of resonances due to these environments in accordance with

$$T\Delta\nu \simeq \frac{1}{2\pi} \qquad (9)$$

where $\Delta\nu$ is the separation of the resonance lines in the absence of the rate process and τ is the smallest lifetime of a magnetic nucleus in the different environments for which separate resonances can be distinguished. When the mean lifetimes of the nuclei in the different environments are much greater than this, separate signals are obtained with the chemical shifts and fine structure that would be observed in the absence of exchange. When the mean lifetimes are of the same order of magnitude as τ in Equation (9), the observed signal shape changes systematically with exchange rate. As the lifetimes decrease, the separate peaks broaden and their maxima draw closer together until they coalesce yielding a single broad peak in an averaged position. This peak sharpens as the mean lifetimes are further decreased, so that for very short lifetimes a single sharp peak is obtained in the averaged position.

The components of a spin multiplet can be collapsed under conditions of rapid chemical exchange of one of the spin-coupled nuclei, even among identical molecules or ions. In the case of the BF_3 multiplet, the relative chemical shifts of the fluorine nuclei absorptions are determined by the spin state of the boron nucleus. A rapid intermolecular exchange of fluorine nuclei, yielding in any molecule a series of fluorine nuclei with random spin states, causes rapid changes in the environment at the boron nucleus and collapse of the multiplet components.

(v) Quadrupole Effects

Spin-spin multiplets can be collapsed by rapid transitions among spin spin states of one of the coupled nuclei. Spin-1/2 nuclei generally do not relax sufficiently rapidly to cause collapse of spin-spin multiplets, although such rapid relaxation can be induced by the technique of double irradiation (5). However, nuclei with $I > 1/2$ possess electric quadrupole moments arising from charge distributions which are not spherically symmetric, which in many cases allow very rapid relaxation of the nuclear spin states though interactions with fluctuating electric field gradients. In such cases, a second nucleus with $I = 1/2$, coupled to the high-spin nucleus, yields a spectrum in which the nuclei appear to be decoupled. In other cases quadrupole relaxation of the high-spin nucleus is not as effective so that partially collapsed multiplets are observed in the NMR spectrum of the spin-1/2 nucleus.

The degree of quadrupole relaxation is dependent upon the magnitude of the nuclear quadrupole moment Q, the electric field gradient q at the nucleus, and the correlation time τ_q for molecular reorientation. It has been shown (2) that the spin-lattice relaxation time T_1, due to quadrupole coupling with a high-spin nucleus, is given to a good approximation by

$$T_1 = \frac{40}{3} \frac{I^2(2I-1)}{(2I+1)} \left[\frac{\hbar}{e^2qQ} \right]^2 \frac{1}{\tau_q} \qquad (10)$$

The electric field gradient at the nucleus is strongly dependent upon the molecular environment, so that a given nucleus of high spin can undergo widely differing degrees of quadrupole relaxa-

tion in different environments. A high degree of symmetry about the nucleus results in a low electric field gradient and only a small degree of quadrupole relaxation. Thus, the spectrum of a ^{19}F nucleus coupled to a single ^{11}B nucleus should be dependent on the symmetry about the ^{11}B nucleus. If the latter is in a highly symmetrical environment, the ^{19}F NMR spectrum is likely to be split into a spin multiplet consisting of four equally spaced lines of equal intensities. If the ^{11}B nucleus is in an environment of low symmetry, the spin multiplet structure in the ^{19}F spectrum is likely to be partially or fully collapsed.

(vi) Isotope Shift

Fluorine-on-boron isotope shifts are the small difference in chemical shift between fluorine atoms on ^{10}B and those on ^{11}B. Previous examples of fluorine isotope shifts (6-10) have shown that the fluorine attached to the heavier boron nucleus absorbs at higher field. The relative peak areas are to be in agreement with the natural abundance ratio of $^{11}B/^{10}B$ = 3.95 - 4.10 (11). This range of values represents the natural variation of the boron isotope ratio.

(B) DONOR-ACCEPTOR COMPLEXES OF THE BORON TRIHALIDES

(i) General

The boron trihalides possess trigonal planar symmetry; in such a configuration the boron atom has only a sextet of electrons, the $2p_z$ orbital being at 90^o to the plane of the molecule. Since the trihalides are electron deficient compounds they behave as Lewis acids, or electron-pair acceptors. The boron trihalides are among the strongest Lewis acids known, and form donor-acceptor complexes with a wide variety of electron-pair donors. The application of various physical methods, as outlined by Coyle and Stone (12), Stone (13), and Greenwood and Martin (14), has led to a considerable degree of understanding of structural types of complexes and of their relative stabilities. Other reviews of boron trihalide and their complexes are available as well (15-17). All donor molecules have a lone pair of electrons in the valence shell of at least one atom; in other respects donor molecules can be of widely varying structural types. Donors include many neutral molecules such as amides (18,19), amines (20), and ureas (21) as well as ions such as chloride ion (22) and tetrafluoroborate ion (23,24).

The short B-X distance in the boron trihalides has been taken as evidence for p_π- p_π bonding (back-bonding) caused by the overlap of filled halogen p orbitals with the empty boron $2p_z$ orbital (16). Considerable effort has been expended to obtain further evidence for this π bonding since it has important consequences when attempts are made to correlate the

relative Lewis acid strengths of the trihalides. Several independent studies have shown the relative Lewis acid strengths of the boron trihalides increase in the order BF_3 < BCl_3 < BBr_3 < BI_3 (16). This is in contrast to the order expected from either electronegativity or steric considerations alone and is attributed to p_π- p_π bonding in the trihalides. This π bonding, which allows some electron density to be present in the $2p_z$ orbital on boron, should be most effective in BF_3 where the boron $2p_z$ orbitals are all in the same principal valence shell. The expectation of greater orbital overlap, and hence stronger π bonding in the case of BF_3, has been supported by molecular orbital calculations (25, 26).

In a recent study of the energetics of adduct formation, Drago and co-workers (26) concluded that π bonding is not destroyed on going from planar to pyramidal geometry in BF_3 and BCl_3. The critical factor appears to be residual π bonding which ties up the $2p_z$ orbital of boron so that it will not accept electron density as readily. In the pyramidal BX_3 series, BF_3 apparently has much stronger π bonds than other members of the series, making the p_z orbital less available for accepting electrons. Since there is a competition between the donor lone pair and the fluorine electrons for the boron $2p_z$ orbital, there can still be appreciable B-F π bonding in the adduct molecule. Boron trifluoride is the weakest Lewis acid in the BX_3 series, not because stronger π bonds must be broken, but because the residual π bonding determines

the response of BF_3 to added electron density. Thus, the amount of π bonding destroyed upon adduct formation is not a constant quantity but is determined by the donor's strength.

Relative strengths of donor-acceptor bonds are best determined directly from the heats of dissociation of the adducts in the gas phase, giving a direct measure of the enthalpy of the donor-acceptor bond. Since many complexes are completely dissociated in the gas phase, such measurements are often not obtainable. Alternative methods involving displacements and equilibria in solution are generally more applicable, but give a measure of the free energy change rather than of the enthalpy change, so that results are not strictly comparable. However, it is found that estimates of relative bond strengths obtained in the gas phase and in solution agree reasonably will in a series of related compounds in which entropy changes on complex formation are similar (16). In the present work, it therefore seems justified to draw conclusions about relative donor-acceptor bond strengths from studies of equilibria in solution.

Lappert (27) and Cook (28) have used the shift in the carbonyl stretching frequency to investigate the acceptor properties of various Lewis acids. By making the assumption that the stronger Lewis acid will shift the carbonyl infrared stretch to lower frequency upon complexation, they have found the same qualitative trends in acidity along a series of Lewis acids from this spectroscopic method as those indicated from measurements of condensed-phase heats of formation. Drago and

co-workers (26) have shown that a linear correlation exists between the carbonyl frequency shift upon complexation and the enthalpy of adduct formation for a series of Lewis acids.

A wide range of stabilities has been encountered in studies of boron trihalide adducts. The most stable complex of a given acceptor is usually that with 1:1 proportions of donor and acceptor. Thus, tensimetric studies of the alkylated di- and tri-N-substituted ureas and thioureas at -78^{o} suggest the formation of weak 2:1 BF_3 adducts, with the second mole of BF_3 being rapidly lost above this temperature (21). The coordinate bond of BF_3 complexes with oxygen donors is generally suffeciently weak that there is some dissociation into the free acid and base at room temperature.

(ii) Donor Site in Ureas

There are two possible donor sites in ureas. While oxygen coordination has been established in the related amide adducts of BF_3 and BCl_3 (18), considerable evidence exists to suggest that in closely related series of simple oxygen and nitrogen compounds, such as amines and ethers, nitrogen is the better donor (16). However, the effect of the donor atom can be greatly out-weighed by the effect of donor substituents in determining base strength. Electron withdrawing substituents or bulky substituents which cause steric hindrance at the donor site can greatly decrease the donor atom's strength. In the case of alkylated ureas and thioureas, Greenwood and Robinson (21) suggest that nitrogen is also the preferred donor in these

structures. If resonance stabilization of the adduct is important enough (Structures Ia-Ic), oxygen donation, rather than nitrogen donation, may be preferred.

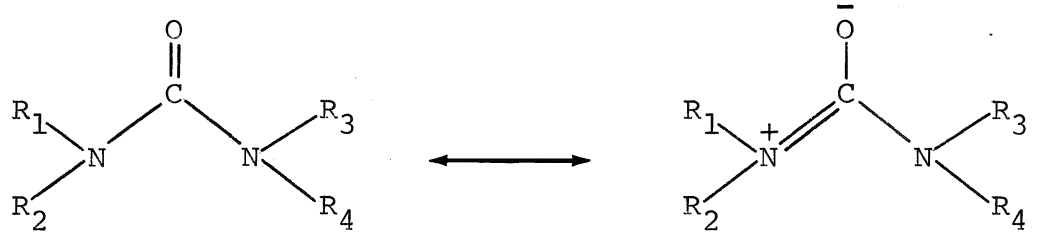

Ia Ib

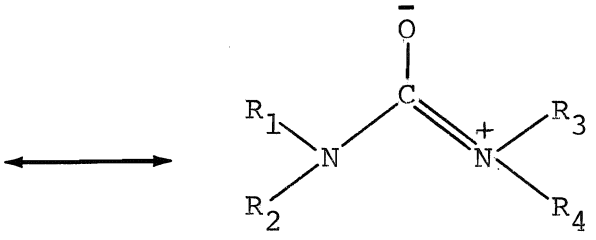

Ic

The site of protonation in ureas and thioureas has also been controversial. Several conflicting interpretations of the infrared spectra of the protonated species in strong acid media have been published, but NMR studies of the ions present in fluorosulfuric acid solutions have shown that protonation is on oxygen or sulfur (29). Further studies show diprotonation in very strong acids with nitrogen being the second donor (30).

It is evident from the considerable number of structural and chemical studies (31-33) on urea and thiourea complexes of the transition metals that oxygen or sulfur is the preferred

donor atom. Few adducts with the main group elements have been studied comprehensively, but again, the majority seem to be oxygen or sulfur coordinated (34). A considerable portion of this thesis is concerned with the problem of donor site in boron trihalide adducts of ureas and related structures.

(iii) Exchange Reactions

Exchange or redistribution reactions are very common in groups II-VII among the non-transition elements and have been reviewed by Lockhart (35). The boron trihalides (36,37) and their adducts (38-40) undergo rapid exchange. Two basic mechanistic types *could* account for halogen and donor exchange in these systems, a four-center associative mechanism and/or a dissociative mechanism.

It is usually assumed that the mechanism for halogen redistribution in free boron trihalides involves a four-center boron-halogen bridged intermediate (16)

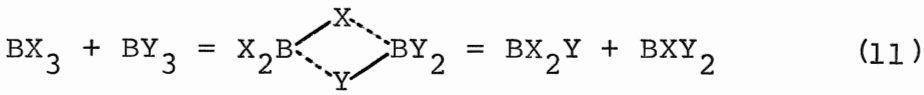

$$BX_3 + BY_3 = X_2B(X,Y)BY_2 = BX_2Y + BXY_2 \qquad (11)$$

Halogen redistribution in the adducts of trimethylamine (a strong donor) in the presence of excess Lewis acid may also involve a halogen-bridged intermediate (40)

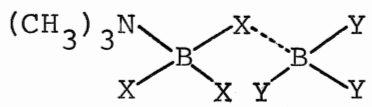

II

Mixtures of the solid adducts in solution do not undergo redistribution even at elevated temperatures, showing that halogen exchange requires free acid. In contrast, the low temperature ^{1}H, ^{19}F, and ^{11}B spectra reveal that mixtures of $(CH_3)_2O \cdot BF_3$ and $(CH_3)_2O \cdot BCl_3$ undergo rapid redistribution in the presence of excess base when their methylene chloride solutions are warmed briefly to room temperature (39). Halogen exchange presumably occurs through a halogen scrambling mechanism involving the free trihalides formed by dissociation of the weak donor-acceptor bond and/or through a halogen-bridged intermediate similar to that proposed for trimethylamine.

Dissociation of either a boron-halogen bond or a donor-acceptor bond in the adduct followed by nucleophilic attack or recombination could give rise to exchange in these systems. In BF_3 adducts, the breaking of the B-F bond is less likely to occur than the breaking of the weaker donor-acceptor bond (38), though such a mechanism has been proposed to explain the slow fluorine exchange process in solutions of BF_4^- (41).

Kemmitt, Milner, and Sharp (42) have observed that both the ^{19}F and ^{11}B NMR spectra of solutions containing BF_4^- and BCl_4^- show a single exchange-averaged peak, the chemical shift of which varies systematically with the relative concentrations of BF_4^- and BCl_4^-. This is the expected behavior if a series of mixed tetrahaloborates of very short lifetimes were formed in solution. It is suggested that a mechanism in which BCl_4^- dissociates to BCl_3 and Cl^- with subsequent attack of the BCl_3

upon BF_4^- (presumably through a halogen-bridged intermediate) could explain the exchange process. This system has been re-investigated and a revised interpretation presented in Chapter III of this thesis.

(C) HIGH-RESOLUTION NMR STUDIES OF BORON TRIHALIDE COMPLEXES

(i) Complexation Shifts as a Measure of Donor-Acceptor Interaction

The formation of a donor-acceptor bond decreases the density of electronic charge at the donor site and increases the density at the acceptor site as a result of the sharing of an electron pair which was previously localized on the donor. Changes in electron density on complex formation should result in "complexation shifts" to higher field in the acceptor resonance, and to lower field in the donor resonance (12,19,20, 43,44). The changes in electron density should be greatest at the donor site but should still be significant at other sites in the molecule due to inductive and, in some cases, mesomeric effects. In cases in which the inductive effect alone is operative, the complexation shift attenuates rapidly as the distance from the donor site increases.

Fluorine-19 complexation shifts are generally found to be a very sensitive measure of donor strength. A complexation shift of 20-30 ppm to high field is observed in the ^{19}F resonance of BF_3 upon adduct formation with many common donors. This large shift indicated that a considerable fraction of the gain in electron density on BF_3 is delocalized from the boron to the

fluorines.

Good correlations of bond strengths with complexation shifts to low field have been obtained in several studies of ^{1}H resonances of donor molecules (20,43,45). The relative magnitudes of the shifts for different trihalides correlate well with estimates of relative bond strengths by other methods, and increase in the order $BF_3 < BCl_3 < BBr_3$.

Boron-11 resonance studies have shown that complexation shifts to high field occur in boron containing Lewis acids. Mooney and co-workers (46) have estimated donor strengths based on the relative magnitudes of chemical shifts to high field of a single acceptor such as BF_3 upon its complexation with different donors. The relative magnitude of ^{11}B shifts to high field of different Lewis acids upon complexation with the same donor appear to yield only a rough estimate of relative acid strengths. In a series of boron trihalide adducts, BF_3 occupies an anomalous position, the boron atom being too shielded if judged purely on electronegativity grounds.

(ii) Measures of Boron-Halogen $p_\pi - p_\pi$ Bonding

Boron-halogen π bonding allows some electron density to be present in the $2p_z$ orbital on boron, resulting in a shielding of the boron nucleus and deshielding of the halogen nuclei. The expectation of greater orbital overlap, and hence stronger π bonding, in the case of fluorine, has been integrated in terms of ^{19}F chemical shift trends observed for the mixed boron trihalides (36). As fluorine is progressively replaced in BF_3 by

more weakly π bonding halogen substituents such as chlorine and bromine, the ^{19}F resonance moves down field due to deshielding of the remaining fluorine atoms arising from increased fluorine-boron π bonding. Boron-11 NMR studies (37) have likewise provided evidence for the postulated π bonding contribution in the mixed boron trihalides.

Trends in ^{19}F chemical shifts of the dimethyl ether-mixed boron trihalide adducts resemble the trends previously observed in the free mixed boron trihalides (39). It is suggested that some measure of π bonding survives even in tetrahedral boron compounds. Mooney's estimates of acid strengths based on ^{11}B complexation shifts discussed above fail to account for this.

An almost linear relationship exists between the ^{19}F chemical shift and the boron-fluorine coupling constant in the mixed trihalides and their dimethyl ether adducts (39). It has been suggested that the boron-fluorine coupling is also dependent on the boron-fluorine $p_\pi - p_\pi$ interaction (16).

(iii) Rapid Equilibration in Solution

Several studies of the ^1H NMR spectra of mixtures of an organic base and a boron trihalide in which $[D] > [BX_3]$, where D = donor, did not yield separate resonances for the free and complexed base, but yielded a single set of resonances having chemical shifts intermediate between those of the free base and the 1:1 complex (38,45). This indicates a rapid exchange of BX_3 among base molecules. This rapid exchange reaction could be slowed down at low temperatures, yielding separate signals due

to free and complexed base. In some cases (7) the averaged chemical shifts were found to vary linearly with the acid-base ratio as acid was added until 1:1 proportions of acid and base were present. Addition of more acid had no effect on the chemical shift(s) of the base, indicating that additional acid does not complex.

A similar exchange phenomenon has been observed in the ^{19}F spectrum in the presence of excess BF_3 where a single exchange-averaged peak is observed that shifts to lower field with increasing proportions of free BF_3, approaching the free BF_3 resonance (7). In some cases this exchange can be slowed down at low temperatures, yielding separate resonances for free and complexed BF_3. Variations in chemical shift may then be used to confirm the stoichiometries of the complexes.

CHAPTER II

EXPERIMENTAL

(A) MATERIALS

(i) General

Manipulations involving moisture sensitive materials were carried out under anhydrous conditions on a vacuum line or in a dry box. All materials, except where indicated, were stored over diphosphorus pentoxide.

(ii) Boron Trihalides

Boron trifluoride (Matheson) was triply distilled under vacuum from a trap at -78° to a trap at liquid nitrogen temperature, the initial and final cuts being rejected each time. The molecular weight was determined by direct weighing of an accurately known volume of gas at a known temperature and pressure. The measured molecular weight was 67.8 ± 0.4 g/mole.

Boron trichloride (Matheson) was distilled under vacuum from a 0° trap through a dry ice-acetone trap and a liquid nitrogen trap connected in series. The BCl_3 collected in the dry ice-acetone trap was stored at liquid nitrogen temperature under vacuum until used.

Boron tribromide (Alfa Inorganics) was treated with mercury to remove bromine and then purified by the technique used for BCl_3.

Boron triiodide (Alfa Inorganics) was used without further purification.

(iii) Tetrahaloborates

Tetra-*n*-butylammonium tetrafluoroborate was prepared by an ion exchange method. An aqueous slurry of Dowex 50W X-8 (100-200 mesh) cation exchange resin (J. T. Baker) in its silver form was treated with an excess of solid tetra-*n*-butylammonium bromide (Eastman). The resulting $n\text{-}Bu_4N^+$ form of the resin and silver bromide precipitate were filtered off and rinsed with distilled water until the filtrate gave a negative silver nitrate test for bromide ion. The washed resin and AgBr were placed in a saturated aqueous solution of ammonium tetrafluoroborate (Alfa Inorganics) and extracted with sucessive portions of benzene. The benzene extract was filtered and evaporated to dryness on a steam bath. The resulting crude $n\text{-}Bu_4N^+BF_4^-$ was recrystallized twice from ethanol-water mixtures. The monoclinic crystals were crushed and dried overnight under vacuum; m.p. 161.5-162.0° (lit. 161.8° (48)).

Tetraethylammonium tetrachloroborate was prepared by the direct addition of BCl_3 to tetraethylammonium chloride (Eastman). Finely ground anhydrous $Et_4N^+Cl^-$ was placed in a Pyrex trap which was evacuated and then immersed in a dry ice-acetone bath. Pure BCl_3 was distilled in at 0° until an excess was present. After standing overnight at 0°, the excess BCl_3 was pumped off and the residue dried at room temperature for two hours under vacuum, leaving a white, free-flowing powder.

Tetra-*n*-butylammonium tetrabromoborate was prepared by a method analogous to that used for $Et_4N^+BCl_4^-$. After allowing n-$Bu_4N^+Br^-$ to stand overnight with BBr_3, excess BBr_3 was removed by pumping on the solid residue for 24 hours. The product was periodically broken up to facilitate drying. Both $Et_4N^+BCl_4^-$ and n-$Bu_4N^+BBr_4^-$ were stored under vacuum in sealed ampoules until used.

Because previous attempts to isolate solid tetraalkylammonium tetraiodoborates proved unsucessful (49), tetra-*n*-butylammonium tetraiodoborate was prepared in solution by mixing BI_3 and tetra-*n*-butylammonium iodide (Eastman) (a 10 mole per cent excess) in NMR sample tubes.

(iv) Donors

Tetramethylurea (Aldrich), dimethylacetamide (Fisher), and dimethylforamide (NMR Specialities) were used without further purification.

sym-Dimethylurea, *unsym*-dimethylurea, *sym*-diethylurea, and *unsym*-diethylurea (Aldrich) were dried overnight as fine powder under high vacuum.

Deuterated *sym*-dimethylurea was prepared by dissolving *sym*-dimethylurea in deuterium oxide (Isomet) and evaporating to dryness. This procedure was repeated three times, giving a 95% N-deuterated product. The final product was twice recrystallized from anhydrous diethylether, powdered, and dried overnight under vacuum.

Tetramethylthiourea (Aldrich) was found to contain sig-

nificant quantities of bis(dimethylthiocarbonyl) sulfide and bis(dimethylthiocarbonyl) disulfide (verified by comparison of the mass spectrum and ^1H NMR spectrum with the spectra of commercial samples of the two impurities (Eastman)). Vacuum sublimation of tetramethylthiourea at room temperature onto a -78° cold finger resulted in a white solid, m.p. 78.0-78.5° (lit. 78° (50)).

Tetramethylselenourea was prepared by heating finely ground phosphorus pentaselenide (K & K Laboratories) with an excess of tetramethylurea in an evacuated sealed tube. The mixture was heated for one week at 70-80° and then transfered to a vacuum line where most of the excess tetramethylurea was removed by vacuum distillation at room temperature. The residue was stirred with hexane, previously dried and distilled over P_2O_5, and filtered. On recrystallization twice from hexane at -78°, very light pink crystals were obtained. The crystals were dried under vacuum for one hour and than sublimed at 50° onto a dry ice-acetone cold finger. The resulting white solid, m.p. 78.5-79.0° (lit. 78-79° (51)), was stored in sealed ampoules under vacuum until used. All manipulations involving the selenourea were carried out in a dry, oxygen free atmosphere.

Practical grade tetramethylguanidine (Eastman) was distilled under reduced pressure at 25-30° in a moisture and carbon dioxide free atmosphere. The distillation was repeated three times, rejecting the first and final cuts each time.

(v) Crystalline Tetramethylurea Adducts

TMU·BF_3. Three procedures were used for the preparation of the BF_3 adduct of tetramethylurea (TMU). Pure TMU·BF_3 was obtained by carrying out the preparation under rigidly anhydrous conditions on a vacuum line. An excess of pure BF_3 was condensed onto a solution of TMU in dry, vacuum distilled CH_2Cl_2. The solvent was removed under vacuum and the viscous residue dried at 80° under vacuum for three hours.

The second method involved slow vacuum addition of pure BF_3 directly to liquid TMU with constant stirring. The temperature of the reaction mixture was maintained near room temperature with the aid of an ice bath. After uptake had ceased, the temperature was raised to 60° and the BF_3 pressure maintained at 0.5 atmosphere until uptake was complete. Excess BF_3 was removed by pumping on the molten adduct at 80° with constant stirring for one hour. The adduct prepared by this method contained small quantities of $(TMU)_2 \cdot BF_2^+BF_4^-$ and is discussed in Chapter 6.

The third method used to prepare TMU·BF_3 was that of Greenwood and Robinson (21) who used commercial BF_3 direct from the cylinder. The adduct prepared by this method was found to contain significant quantities of $TMU \cdot H^+BF_4^-$ and is discussed in Chapter 4.

In each case, the low melting, extremely hygroscopic adduct crystallized at room temperature and was stored under vacuum over P_2O_5 until used.

TMU·$H^+BF_4^-$. Treatment of a CH_2Cl_2 solution of TMU·BF_3 (first

preparative method) with hydrogen fluoride (Matheson) in a polyethylene vessel gave, upon standing, colorless monoclinic crystals that were moderately soluble in CH_2Cl_2, m.p. 113-115°. The melting point compared favorably with that of material isolated from impure TMU·BF_3 (third preparative method) which had been allowed to stand for one month over anhydrous calcium sulfate in a desiccator. Recrystallization of filtered CH_2Cl_2 solutions of the aged adduct gave a moderately soluble fraction m.p. 110-112°. In addition, boric acid, m.p. 168.0-168.5° (lit. 169 ± 1° (52)) was isolated as an insoluble residue.

TMU·BCl_3. The BCl_3 adduct of TMU was prepared using the first method outlined above. The dried product was recrystallized from CH_2Cl_2 a total of three times to remove occluded BCl_3 and finally dried overnight under vacuum, m.p. 145.5-146.0°.

(vi) Trimethylsilyl Halides

Trimethylsilyl chloride (Alfa Inorganics) was used without further purification. Trimethylsilyl iodide was prepared from hexamethyldisiloxane (NMR Specialities) using the method of Voronkov, *et al*. (53).

(vii) Solvents and NMR References

Reagent grade methylene chloride (British Drug Houses), tetramethylsilane (Stohler Isotope Chemicals), and trichlorofluoromethane (K & K Laboratories) were allowed to stand over

Linde 4A Molecular Sieves before use. Trimethoxyboron (Chem Service) was prepared as a 10% v/v solution in CH_2Cl_2 and sealed in capillary tubes. Methylene bromide (Eastman), methylene iodide (Fisher), hydrogen iodide (Matheson), and d_3-nitromethane (Diaprep) were used without further purification.

(B) NMR

(i) Sample Preparation

All materials used in the preparation of NMR samples were routinely checked for purity by recording their high gain ^1H NMR spectra.

Most BF_3-containing NMR samples (with the exception of those prepared from the solid adducts) were prepared by standard high vacuum techniques (54,55). The BF_3 complexes were prepared by condensation of known amounts of purified BF_3 from a calibrated volume directly into 5 mm o.d. precision Pyrex sample tubes (Wilmad) containing a degassed solution of the base. A known weight of base was added to the sample tube prior to attachment to the vacuum line. Tetrahaloborate solutions and solutions of crystalline TMU adducts were prepared directly in precision NMR tubes and degassed by attachment to the vacuum line. Proton and fluorine-19 spectra were referenced by condensing in small quantities of TMS and $CFCl_3$. Boron-11 spectra were referenced to external $(CH_3O)_3B$.

The samples were sealed off under vacuum with the contents still at liquid nitrogen temperature, then warmed to room temperature. Heat sensitive samples such as those containing HI solvent were warmed to an intermediate temperature in a chlorobenzene slush (-45°) or dry ice-acetone (-78°). Total base concentrations in all samples were ~1.0 M unless otherwise specified.

Changes in solution composition resulting from the addition of free TMU to CH_2Cl_2 solutions of $TMU \cdot BF_3$, $TMU \cdot BF_3$/$TMU \cdot BCl_3$ mixtures, and $TMU \cdot H^+BF_4^-$ were followed by monitoring the NMR spectra. Free TMU was injected into septum-capped NMR sample tubes using a 10 or 50 µl syringe (Hamilton Co.). The solutions were mixed after each addition (in all cases equilibrium was rapidly attained) and the spectra recorded and electronically integrated. Equilibrium compositions were calculated from the initial composition and the relative peak areas.

(ii) Instrumentation

All spectra, unless otherwise indicated, were obtained at ambient temperature (26^o-^{19}F; 30^o-^{11}B, ^1H (100 MHz); 37^o-^1H (60 MHz)) and referenced to TMS, $CFCl_3$ or external $(CH_3O)_3B$.

Fluorine-19 spectra were obtained on a Varian Associates DA-60IL NMR spectrometer (McMaster University) operating at 56.4 MHz in HR sideband mode. The spectra were calibrated by the usual audio sideband method, using a Muirhead-Wigan D-890-A decade oscillator. Sideband frequencies were checked with a General Radio Type 1191 frequency counter. Calibration of large ^{19}F chemical shifts with respect to trichlorofluoromethane was carried out by using 2500 Hz sidebands arising from a Hewlett-Packard 200 CDR audio oscillator which were 180^o out of phase with the normal signals. The method gave chemical shift values for a given sample at a given temperature that were reproducible to within ±0.5 ppm. A Varian V-4540 variable

temperature controller and variable temperature probe were used to adjust the sample tube to the required temperature.

Boron-11 spectra were obtained on a Varian HA-100 NMR spectrometer (McMaster University) operating at 25.1 MHz in centerband mode. Spectra were calibrated with respect to a capillary of $(CH_3O)_3B$ using audio sidebands generated by a Hewlett-Packard 200 CD audio oscillator and the sideband frequencies monitored with a General Radio Type 1191 frequency counter. Reproducibility was approximately ±0.4 ppm for a given sample at ambient temperature.

Proton spectra were recorded at 60 MHz on a Varian A-60 instrument and at 100 MHz on the Varian HA-100 instrument operating in HA frequency sweep mode. Both spectrometers were used in conjunction with V-6040 variable temperature controllers and variable temperature probes. Homonuclear decoupling experiments on the A-60 instrument were performed using a Varian Model V-6058A spin decoupler; difference frequencies were accurately determined using an Eldorado Electronics Model 224 frequency counter. All spectra were recorded on calibrated paper. The estimated error was ±0.05 ppm for the ^1H chemical shifts reported in this work.

Relative peak areas were determined by electronic integration. The estimated experimental error was ±2%.

(C) OTHER TECHNIQUES

(i) CNDO/2 Calculations

The CINDO-CNDO AND INDO PROGRAM was provided by the Quantum Chemistry Program Exchange (56). The calculations were executed for the closed shell configurations on an IBM 360 computer. Input data consisted of the wavefunction option, the open-closed shell option, the number of atoms, the molecular charge, the multiplicity, the atomic number of the atoms, and the Cartesian coordinates of the atoms in their molecular geometry.

(ii) Mass Spectra

Mass spectra were recorded on a Bendix Model 10 time of flight spectrometer or on an AEI MS-12 spectrometer (Trent University), both operating at an ionizing voltage of 70 ev. High resolution spectra were recorded on the MS-12 instrument. Since the compounds studied were solids or high-boiling liquids, heated direct insertion probes were used.

(iii) Infrared Spectra

All infrared measurements were done on a Perkin-Elmer Model 237B grating spectrophotometer operating at ambient temperature. Spectra were recorded in CH_2Cl_2 solutions against a solvent blank using 0.1 mm solution cells with potassium bromide windows.

(iv) Tensimetric and Electrical Conductivity Measurements

A Beckman Model RC-18 conductivity bridge with an oscillator

frequency setting of 1 KHz was used for conductivity measurements. The conductivity cell was of the variable path length type described elsewhere by Gillespie and co-workers (57). Cell constants were compared before and after low temperature titrations by thermostating a 0.2000 M potassium chloride solution in distilled water at 25.00 ± 0.05°. The cell constants did not change by more than ±1%.

Tensimetric and conductometric titrations of $Et_4N^+Cl^-$ in CH_2Cl_2 with BF_3 were carried out by condensation of known quantities of BF_3 into the tensimeter or conductivity cell at liquid nitrogen temperature. Measurements at -78.5° were made by immersing the frozen solution in a dry ice-acetone bath; the temperature of the bath was measured with a toluene-filled low temperature thermometer and was held constant to within ±0.5°.

Pressure measurements were made at equilibrium with a mercury manometer. The high vacuum system employed was so designed that a minimum quantity of gas was outside the thermostated container. The system was "calibrated" by measuring the partial pressure of BF_3 over pure solvent at -78.5°; the resulting curve was near linear (Figure 4).

CHAPTER III

MIXED TETRAHALOBORATE IONS

INTRODUCTION

A number of compounds which might contain mixed tetrahaloborate anions are recorded in the literature (16), but only the chlorotrifluoroborate anion appears to have been well characterized (58). A previous report of very rapid exchange in these systems (42) has led to a serious apparent anomaly in relative rates of exchange reactions. It is difficult to explain why the tetrahaloborates, which probably undergo a preliminary dissociation step in the exchange reaction, should undergo exchange much faster than the free boron trihalides. The free trihalides should have available a relatively low energy halogen-bridged intermediate, but, unlike the ^{19}F and ^{11}B NMR spectra reported for the mixed tetrahaloborates (42), their spectra show separate resonances with well-resolved B-F couplings at room temperature (36,37).

In addition, the data obtained in the present Chapter has served to clarify much of the chemistry of tetramethylurea-mixed boron trihalide adduct systems presented in Chapter VI.

RESULTS

(A) MIXED TETRAHALOBORATE IONS BY HALOGEN SCRAMBLING AND SOLVENT EXCHANGE

(i) General

Halogen scrambling in CH_2Cl_2 solution has been observed by NMR techniques in systems containing equimolar mixtures of BF_4^-/BCl_4^-, BF_4^-/BBr_4^-, BF_4^-/BI_4^-, BCl_4^-/BBr_4^-, BCl_4^-/BI_4^-, and BBr_4^-/BI_4^-. The ^{19}F and ^{11}B NMR parameters are listed in Tables II and III, respectively.

(ii) BF_4^-/BCl_4^-

The initial room temperature ^{19}F and ^{11}B spectra of *n*-$Bu_4N^+BF_4^-$ and $Et_4N^+BCl_4^-$ showed only the peaks arising from the unmixed species. Heating the solution at 60° for several minutes led to the appearance of new signals which are assigned to BF_3Cl^-, $BF_2Cl_2^-$, and $BFCl_3$. Three new 1:1:1:1 quartets appeared in the ^{19}F spectrum (Figure 1) while the ^{11}B spectrum became complex due to the overlapping of multiplets which arise from coupling of boron with varying numbers of fluorines. By skewing the BF_4^-/BCl_4^- ratio toward chlorine-containing species, it was possible to identify and assign multiplets in the ^{11}B spectra (Figure 2). The ^1H spectra of the cations remained unchanged during halogen scrambling in this and all subsequent BX_4^- systems reported in this study.

(iii) BCl_4^-/BBr_4^-, BCl_4^-/BI_4^-, and BBr_4^-/BI_4^-

Exchange was found to be considerably faster in these

Table II

Observed and Calculated ^{19}F Chemical Shifts and ^{11}B-^{19}F Coupling Constants for BX_4^- Ions

BX_4^-	^{19}F Chemical Shift (ppm)		^{11}B-^{19}F Coupling Constant (Hz)	
	obs.	calc.	obs.	calc.
BF_4^-	151.3	151.5	1*	-1.5
BF_3Cl^-	124.6	123.9	25.2	25.7
BF_3Br^-	113.8	113.3	-	37.8
$BF_2Cl_2^-$	104.1	104.6	54.2	53.8
BF_2ClBr^-	95.7	96.3	65.1	65.2
$BFCl_3^-$	94.0	93.6	79.4	79.8
$BF_2Br_2^-$	88.2	88.9	76.1	75.9
$BFCl_2Br^-$	87.8	87.6	91.3	91.0
$BFClBr_2^-$	-	82.5	-	101.5
$BFBr_3^-$	78.6	78.3	111.3	111.3

* estimate; not visible in these samples; seen in other work in CH_2Cl_2 and other solvents (41).

Table III

Observed and Calculated ^{11}B Chemical Shifts for BX_4^- Ions

BX_4^-	^{11}B Chemical Shift (ppm)	
	obs.	calc.
BCl_4^-	11.6	11.5
$BFCl_3^-$	11.8	12.1
$BF_2Cl_2^-$	13.8	13.7
BCl_3Br^-	15.4	15.5
BF_3Cl^-	16.6	16.3
BF_4^-	19.9	20.0
$BCl_2Br_2^-$	22.1	22.0
$BClBr_3^-$	30.9	31.0
BCl_3I^-	30.9	31.5
BCl_2BrI^-	-	39.6
BBr_4^-	42.4	42.4

Table III (continued)

BX_4^-	^{11}B Chemical Shift (ppm)	
	obs.	calc.
$BCl_2I_2^-$	60.8	60.6
BBr_3I^-	62.8	63.2
$BClBrI_2^-$	-	72.8
$BBr_2I_2^-$	85.8	85.6
$BClI_3^-$	99.1	98.8
$BBrI_3^-$	115.3	115.0
BI_4^-	146.0	146.0

Figure 1. Fluorine-19 spectra (56.4 MHz) of a CH_2Cl_2 solution containing a 1:3 molar ratio of n-$Bu_4N^+BF_4^-$/$Et_4N^+BCl_4^-$ heated at 60° for (a) 5 min.; (b) 10 min.; (c) 20 min. The peak assignments are: BF_4^- (1), BF_3Cl^- (2), $BF_2Cl_2^-$ (3), and $BFCl_3^-$ (4).

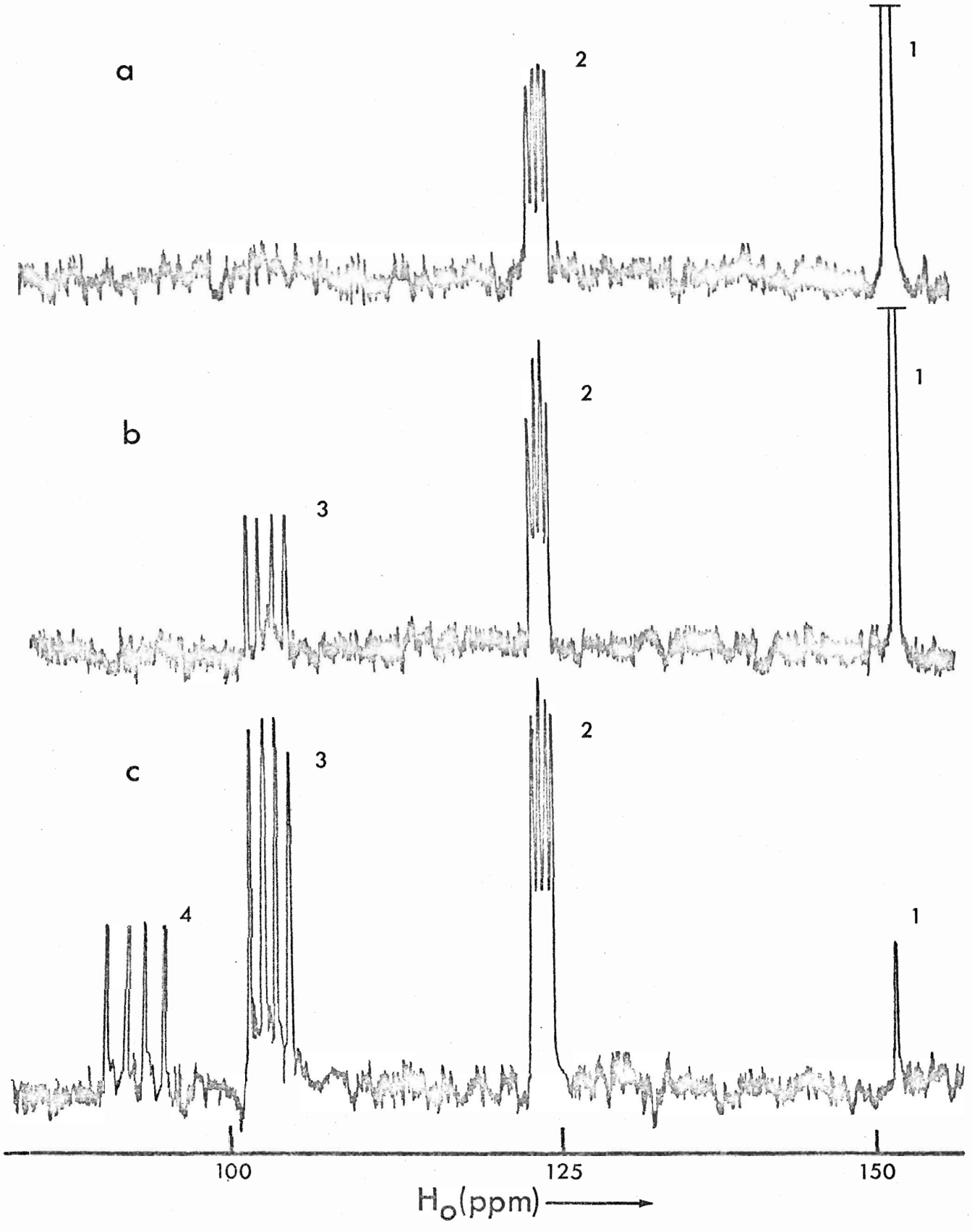
a
1
2
b
1
2
3
c
1
2
3
4
100
125
150
H_o(ppm)

Figure 2. Boron-11 spectra (25.1 MHz) of CH_2Cl_2 solutions of n-$Bu_4N^+BF_4^-/Et_4N^+BCl_4^-$ in the molar ratio (a) 1:1; (b) 3:1 after heating at 60° for 30 minutes. The peak assignments are: BF_4^- (1), BF_3Cl^- (2), $BF_2Cl_2^-$ (3), $BFCl_3^-$ (4), and BCl_4^- (5).

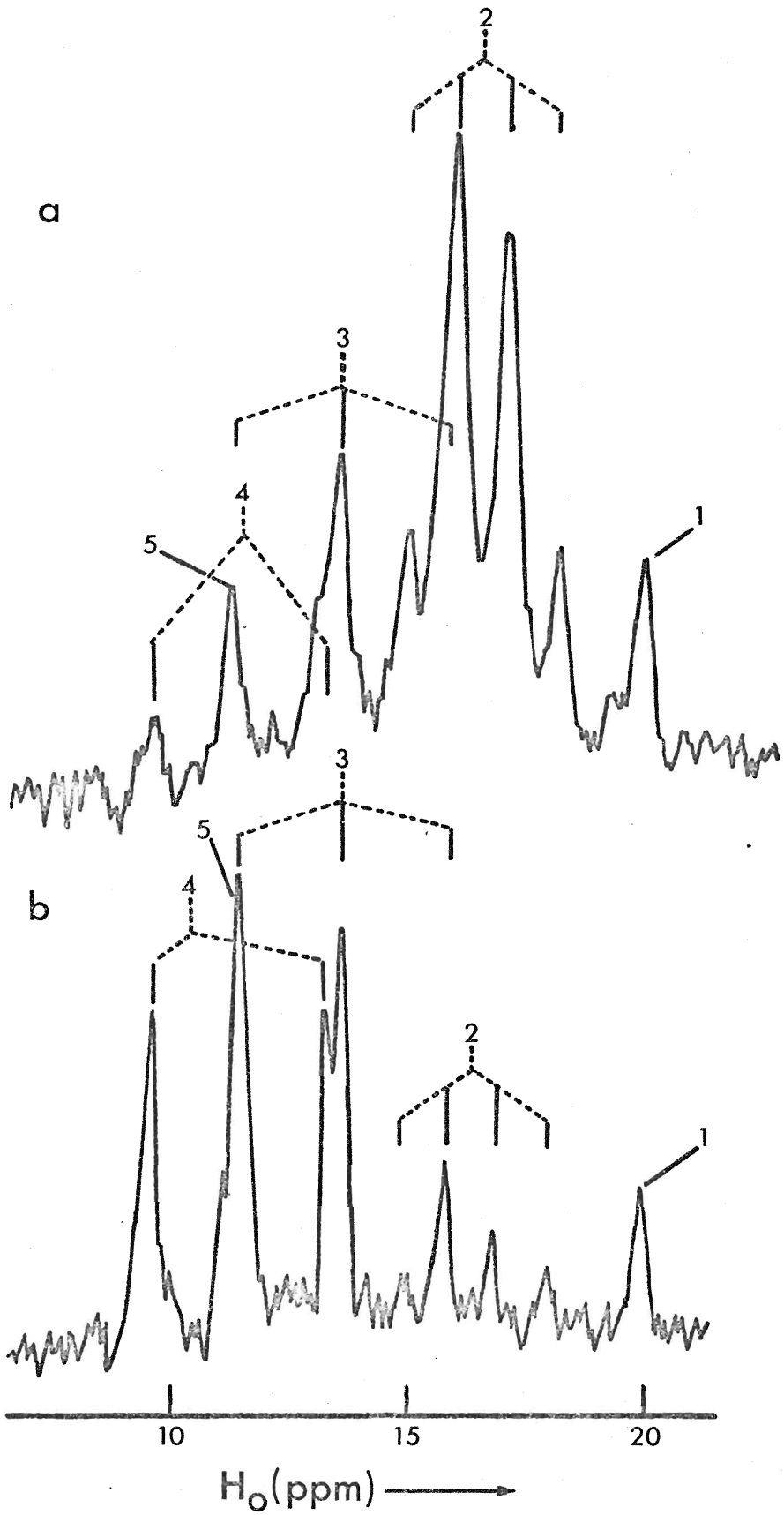
a
2
3
4
5
1
b
3
5
4
2
1
10
15
20
H_o(ppm)

systems than in the BF_4^-/BCl_4^- system. Thus, the initial room temperature ^{11}B spectra of mixtures of the respective tetra-*n*-alkylammonium salts gave near statistical distributions of the mixed tetrahaloborates.

(iv) BF_4^-/BBr_4^- and Ternary F-Cl-Br Systems

The spectra of mixtures of the *n*-Bu_4N^+ salts of BF_4^- and BBr_4^- likewise showed that exchange had occurred readily at room temperature (Figure 3a). The presence of a CH_2ClBr peak in the ^1H spectra of these solutions indicated some solvent exchange. Heating of these solutions to 60° for 15 minutes led to further exchange with the solvent and complication of the room temperature ^{19}F and ^{11}B spectra. The initial ^{19}F spectrum consisted of an exchange-broadened peak at high field. Exchange was slowed sufficiently at -10° to give separate resonances corresponding to BF_3Cl^- and $BF_2Cl_2^-$; in addition, a quartet which did not undergo exchange averaging in the room temperature spectrum was identified as $BFCl_3^-$ (Figure 3b). The -20 - -70° spectra showed no significant changes other than partial collapse of the B-F splittings due to quadrupole relaxation of boron. No BF_4^- peak was observed in any of the samples initially containing BF_4^-/BBr_4^-. The ^{11}B spectra were too complicated for interpretation although BBr_4^- and $BClBr_3^-$ were clearly present. Continued heating of the samples at 60° for five hours resulted in a ^{19}F spectrum showing only the fluorochloroborates and BF_4^-, and a ^1H spectrum with an intensified CH_2ClBr signal.

Figure 3. Fluorine-19 spectra (56.4 MHz) of a CH_2Cl_2 solution containing n-$Bu_4N^+BF_4^-$/$Et_4N^+BCl_4^-$/ n-$Bu_4N^+BBr_4^-$ in the molar ratio 1:1:1 recorded at (a) -10°; (b) 0° after heating for 15 minutes at 60°. The peak assignments are: BF_3Cl^- (1), BF_3Br^- (2), $BF_2Cl_2^-$ (3), BF_2ClBr^- (4), $BFCl_3^-$ (5), $BFCl_2Br^-$ (6).

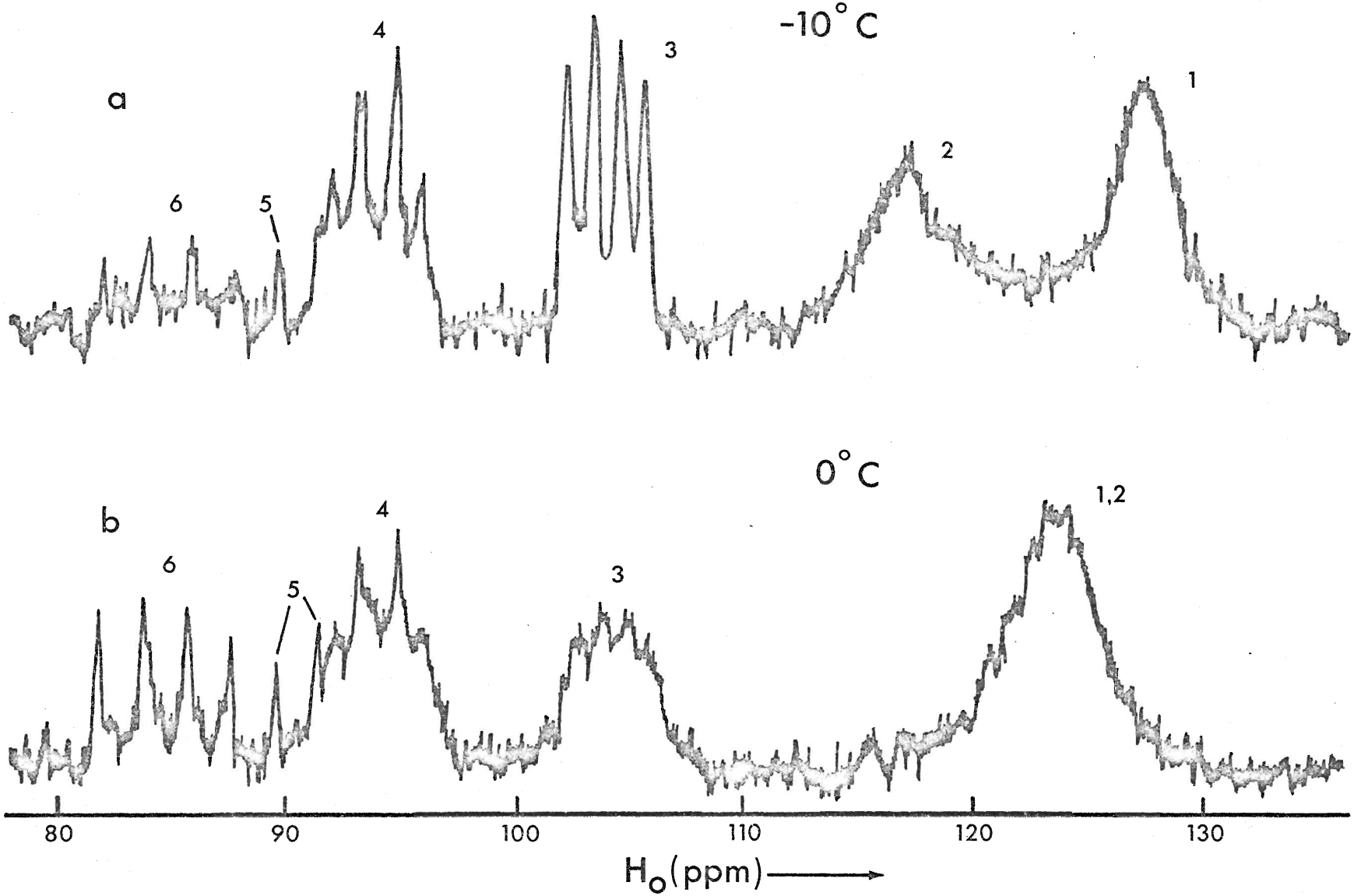
-10° C
a
6
5
4
3
2
1
0° C
b
6
5
4
3
1,2
80
90
100
110
120
130
H_o(ppm)

Nearly identical spectra have been obtained in the case of the ternary system $BF_4^-/BCl_4^-/BBr_4^-$. These samples were prepared either by addition of BBr_4^- to a solution containing BF_4^- and BCl_4^-. In addition to the fluorobromoborates, it is clear that at least two other quartets are present in solvent-exchanged and ternary systems, these have been assigned to two of the three possible ternary species, BF_2ClBr^- and $BFCl_2Br^-$. Confirmation of these and other assignments is dealt with later in this Chapter.

(v) $\underline{BF_4^-/BI_4^-}$

Very rapid exchange occurred in samples containing 1:1:1 and 1:2:1 proportions of $BI_3/n\text{-}Bu_4N^+I^-/n\text{-}Bu_4N^+BF_4^-$ so that even at -90° an averaged ^{19}F signal at 133 ppm was obtained. Warming of these samples to 0° for 30 seconds resulted in the rapid evolution of BF_3. The -90° spectra of the warmed samples revealed an additional broadened peak (~5% of the total fluorine intensity) at 66.4 ppm while the high field peak shifted to 123.2 ppm. Liquid HI solutions of $BI_3/n\text{-}Bu_4N^+I^-/n\text{-}Bu_4N^+BF_4^-$ = 1:1:1 at -40° gave a broad exchange-averaged peak at 119 ppm and a small broadened peak at 44.6 ppm; unfortunately solvent effects do not permit a direct comparison of results obtained in HI with those obtained in CH_2Cl_2. The low field peak in these systems might be due to $BF_2I_2^-$ and/or BFI_3^-.

(vi) Solvent Exchange

Solutions of dihalomethanes in CH_2Cl_2 undergo exchange with BX_4^- (except BF_4^-). The utility of this reaction as a possible means for preparing the non-fluorine-containing mixed tetrahaloborates was briefly explored. Table IV lists the ^1H NMR evidence for exchange in these systems. Even after standing for two months at room temperature and further heating at 90° for several more hours, BBr_4^- did not exchange halogen with CH_2Cl_2. Exchange, however, took place readily upon warming to 90° for 15 minutes in the presence of BF_4^- or BCl_4^-. Solutions giving evidence for solvent exchange contained, after several hours of standing at room temperature, a significant amount of crystalline material. As a result, ^{11}B spectra obtained later from these samples were of little value.

Solutions of the corresponding tetra-*n*-alkylammonium halides in neat dihalomethane solvents also underwent exchange (Table V).

Table IV

^{1}H NMR Evidence for Halogen Exchange in BX_4^-/CH_2X_2 Systems

BX_4^-	CH_2X_2[a]	^{1}H Chemical Shift (δ) of the New Signal[b]	Assignment[c]
F	Cl	-	-
F	Br	-	-
F	I	-	-
Cl	Br	5.17	CH_2ClBr
Cl	I	4.99	CH_2ClI
Br	Cl	-	-
Br	I	4.50	CH_2BrI
F/Br	Cl	5.15	CH_2ClBr
Cl/Br	Cl	5.18	CH_2ClBr

[a] 10% v/v solutions in CH_2Cl_2.

[b] exchange was effected by heating at 90° for 15 minutes; systems which did not exchange after 15 minutes did not exchange when heated an additional 2 hours at 90°.

[c] reference (59).

Table V

^{1}H NMR Evidence for Halogen Exchange in X^-/CH_2X_2 Systems

X^-	CH_2X_2	^{1}H Chemical Shift(s) (δ) of the New Signal(s)[a]	Assignment(s)[b]
Cl	Br	5.16,	CH_2ClBr, CH_2Cl_2
Cl	I	4.97,	CH_2ClI, CH_2Cl_2
Br	I	4.48	CH_2BrI
I	Br	4.49	CH_2BrI
Br	Cl	5.18	CH_2ClBr*
I	Cl	5.00	CH_2ClI*

[a] solutions were heated for one hour at 80°; chemical shifts are given for a 10% v/v solution of the exchanged CH_2X_2 solution dissolved in CH_2Cl_2.

[b] reference (59).

* only small amounts were observed after 1 hour at 80°.

(B) MIXED TETRAHALOBORATES BY OTHER PREPARATIVE METHODS

(i) Halogen Exchange of Trimethylhalosilanes with BF_4^-

Mixed tetrafluorohaloborates can be prepared by halogen exchange between BF_4^- and a trimethylhalosilane at room temperature. Thus, in the case of $(CH_3)_3SiCl/BF_4^-$ in CH_2Cl_2, the ^1H spectrum gave a sharp doublet attributed to $(CH_3)_3SiF$ at 0.21 δ, $J_{^1H-^{19}F}$ = 7.4 Hz (60a) and a singlet corresponding to unreacted $(CH_3)_3SiCl$ at 0.42 δ. The ^{19}F spectrum showed three signals, a decet (eight peaks resolved) corresponding to $(CH_3)_3SiF$ at 159.0 ppm (60b), $J_{^1H-^{19}F}$ = 7.4 Hz; a BF_3Cl^- peak at 125.0 ppm, $J_{^{11}B-^{19}F}$ = 25.0 Hz; and a peak due to unreacted BF_4^-.

Tetrafluoroborate was found to undergo rapid halogen exchange with $(CH_3)_3SiI$. The ^1H spectrum revealed an exchange-averaged signal just to low field of TMS. At -40^o exchange was slowed sufficiently to observe a sharp $(CH_3)_3SiF$ doublet and a singlet at 0.80 δ corresponding to unreacted $(CH_3)_3SiI$. The room temperature and -40^o ^{19}F spectra gave a BF_4^- peak shifted to slightly lower field (146.0 ppm) and a $(CH_3)_3SiF$ signal which was consistent with the expected decet fine structure, suggesting rapid fluorine exchange among BF_4^- and the fluoroiodoborates. Cooling to -90^o failed to slow the exchange process sufficiently to observe other peaks that might be attributed to the fluoroiodaborates.

(ii) BF_3 Adducts of Cl^-, Br^-, and I^-

Both tensimetric and conductometric data indicate that

the direct addition of BF_3 to CH_2Cl_2 solutions of $Et_4N^+Cl^-$ resulted in the uptake of one mole of BF_3 (Figure 4).

The -80^o ^{19}F spectrum at 1:1 proportions of $BF_3/Et_4N^+Cl^-$ and $BF_3/n\text{-}Bu_4N^+Br^-$ gave peaks corresponding to BF_4^-, BF_3X^-, and $BF_2X_2^-$. In both systems the BF_4^- peak corresponded to 30% of the total fluorine intensity. The relative peak areas of the trifluoro- and difluoro- compounds were $BF_3X^-/BF_2X_2^- \simeq 3:1$. Direct addition of BF_3 to $n\text{-}Bu_4N^+I^-$ solutions also gave the same broad, exchange-averaged ^{19}F peak at 131 ppm observed previously in $BI_3/I^-/BF_4^-$ systems. A small broadened peak at 66.9 ppm was observed at -90^o as well.

DISCUSSION

(A) EMPIRICAL CORRELATIONS

(i) General Considerations

The initial phases of the investigation were motivated by the observation that B-F coupling constants and ^{19}F chemical shifts in the fluorine containing BX_4^- ions vary in an almost linear fashion (Figure 5), similar to a trend noted for the mixed boron trihalides (47) and their adducts (Chapter VI). A similar treatment can be extended to ^{11}B NMR parameters in which B-F couplings exist.

Müller and co-workers (61) have noted a linear relationship between the ^{19}F chemical shifts and the sums of the electronegativities of the substituents about boron in the mixed fluorine containing boron trihalides. In the case of

Figure 4. (a) tensimetric titration of Et_4NCl (17.50 mmoles in 25.0 ml CH_2Cl_2) at 194 ^{o}K; (b) conductimetric titration of Et_4NCl (9.89 mmoles in 25.0 ml CH_2Cl_2) at 193.7 ^{o}K.

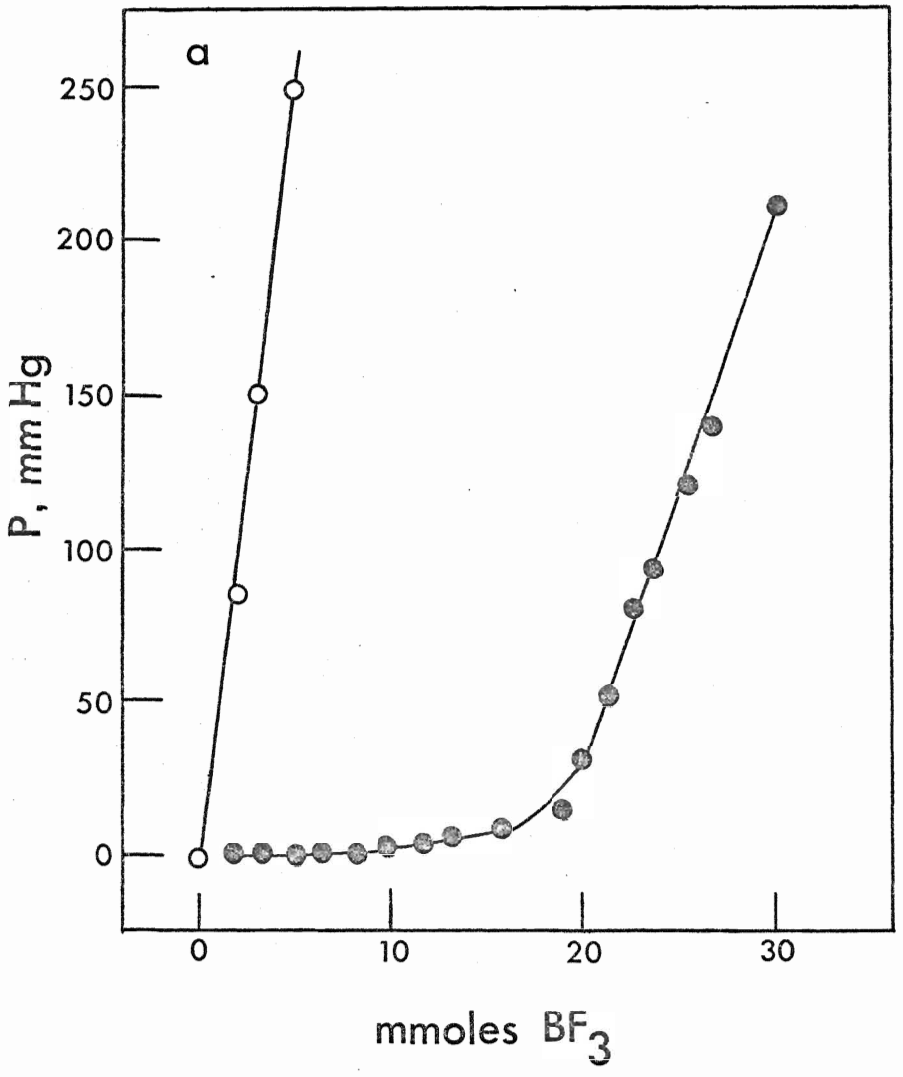
a
250
200
150
100
50
0
P, mm Hg
0
10
20
30
mmoles BF_3

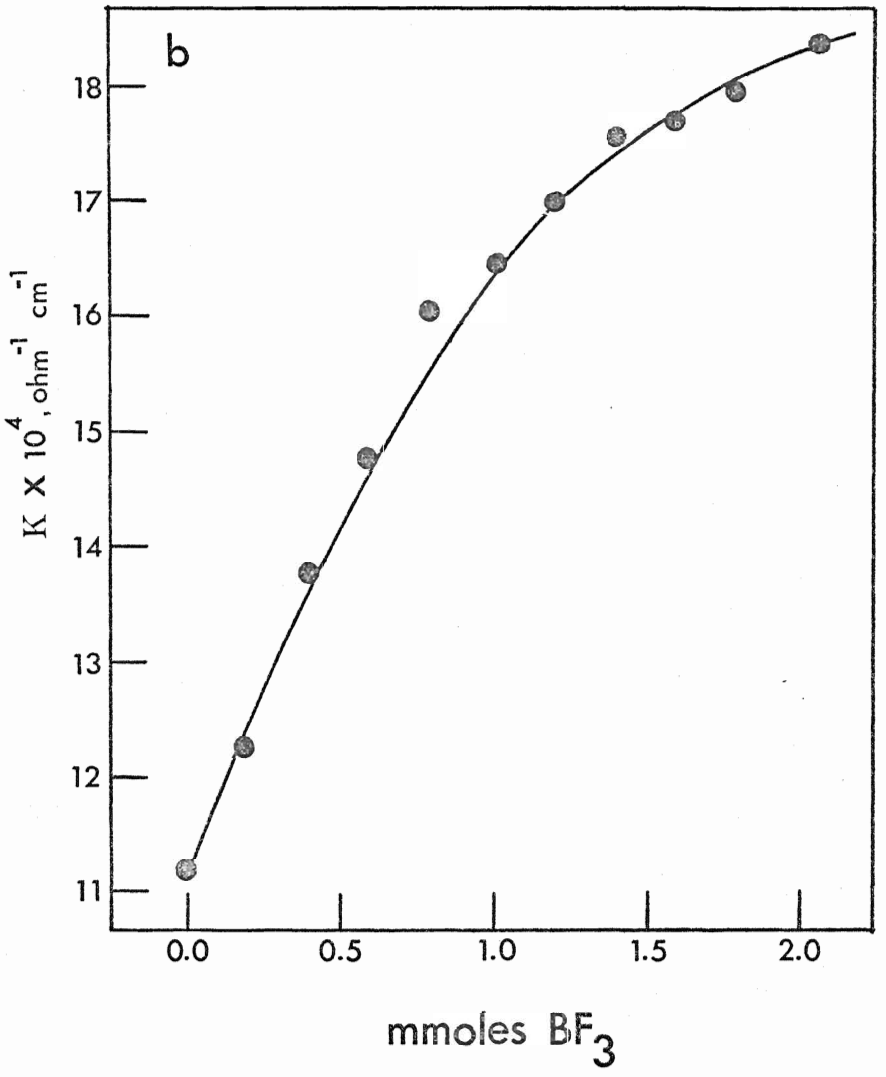
b
18
17
16
15
14
13
12
11
K X 10^4, ohm^{-1} cm^{-1}
0.0
0.5
1.0
1.5
2.0
mmoles BF_3

Figure 5. Variation of ^{19}F chemical shifts and ^{11}B-^{19}F coupling constants of BX_3 (16) and BX_4^- (data from Table II) for X = F and Cl, Br.

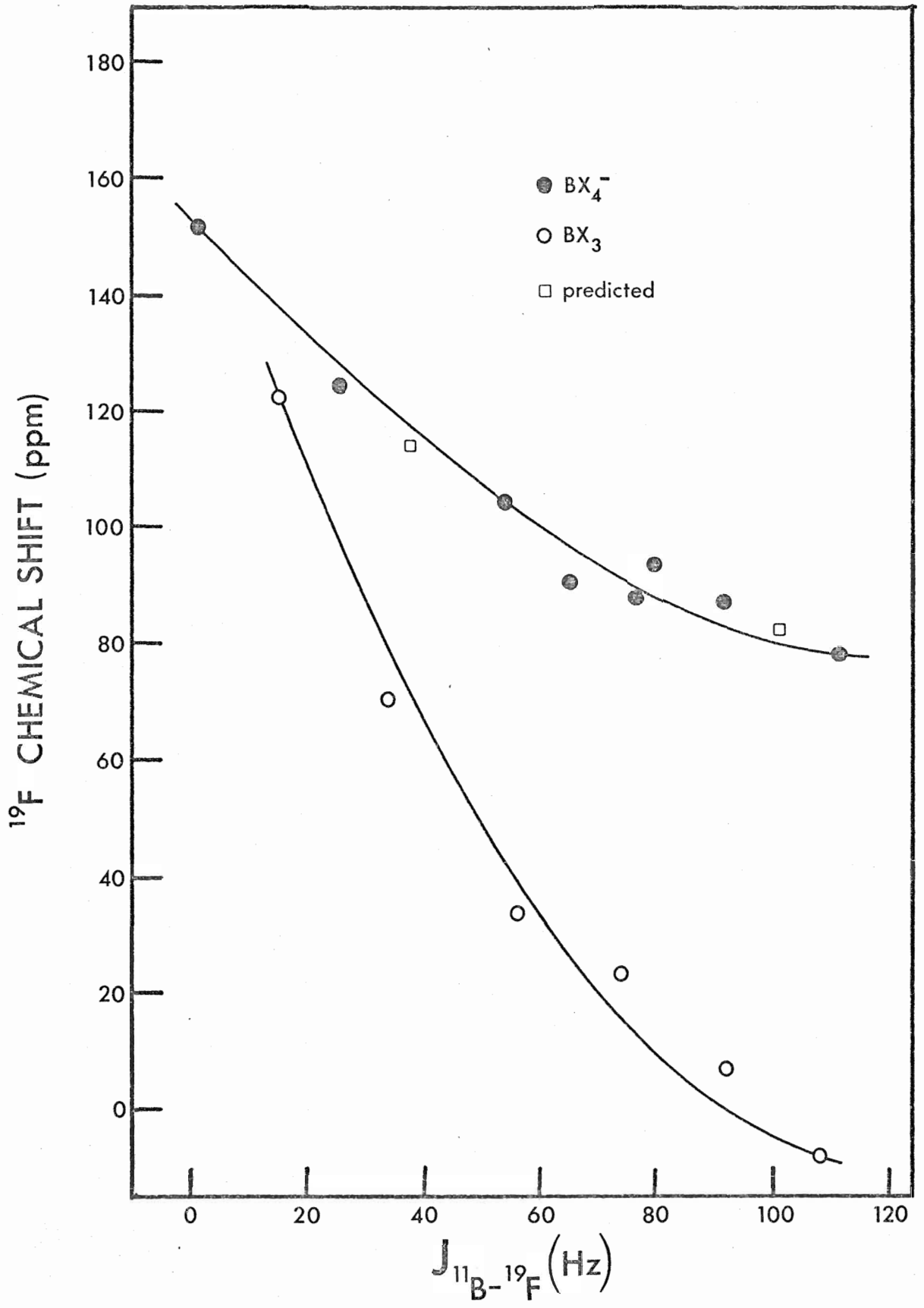
180
160
140
120
100
80
60
40
20
0
^{19}F CHEMICAL SHIFT (ppm)
BX_4^-
BX_3
predicted
0
20
40
60
80
100
120
$J_{^{11}B-^{19}F}$ (Hz)

both fluorine and non-fluorine containing BX_4^- ions, the substituent electronegativity sum becomes a convenient parameter to plot versus the ^{11}B chemical shift (Figure 6).

Similar trends in ^{19}F chemical shifts, ^{13}C-^{19}F coupling constants, and ^{13}C chemical shifts are observed in the tetrahalomethanes (Figure 7).

The mixed tetrahaloborates, the isoelectronic tetrahalomethanes, other adducts of the mixed boron trihalides, and the uncomplexed mixed boron trihalides all show similar trends in ^{19}F and ^{11}B (or ^{13}C) chemical shifts and in ^{11}B-^{19}F (or ^{13}C-^{19}F) coupling constants. Substitution of fluorine by heavier halogens causes a low field shift of the remaining fluorines and an increase in the magnitude of the B-F coupling constant. The trend in the chemical shifts, which is especially pronounced in the free boron trihalides, has been explained in terms of π bonding from fluorine to boron in these compounds, with much of the π bonding surviving in the adducts (39). Similarly, it has been suggested that double bond character is the most important single factor affecting ^{19}F chemical shifts and ^{13}C-^{19}F coupling constants in the fluoromethanes (63). Analogous attempts to estimate π bonding in the mixed tetrahaloborate anions should be facilitated by the availability of data for trigonal planar mixed halogen compounds of boron in which π bonding is well established (16).

Two widely different trends exist in the ^{11}B chemical shifts of the boron trihalides and the tetrahaloborates (Fig-

Figure 6. Variation of ^{11}B chemical shifts and electronegativity sums (using the values of Allred and Rochow) of the halogen atoms for BX_3 (16) and BX_4^- (data from Table III) for X = F, Cl, Br, and I.

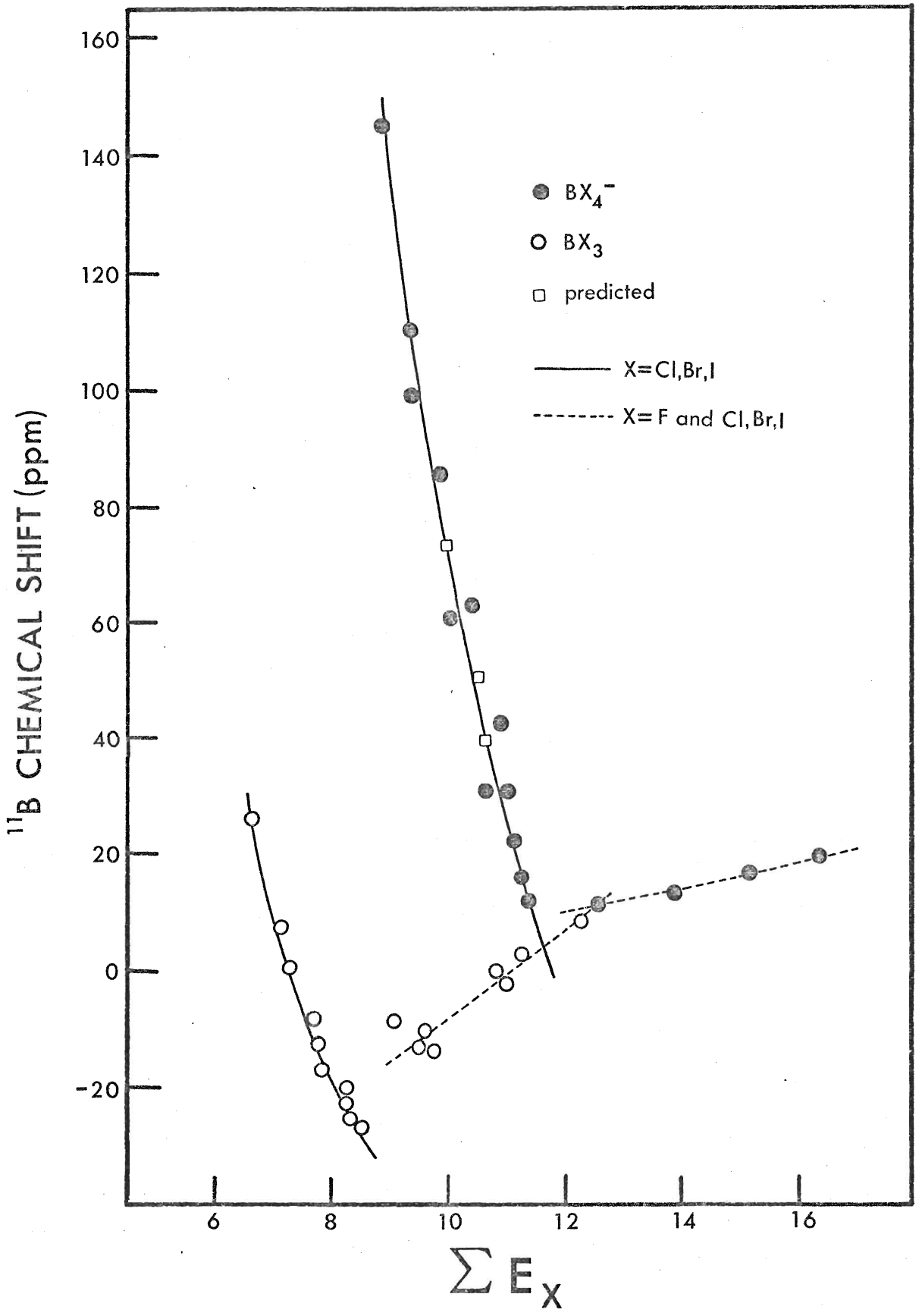
160
140
120
100
80
60
40
20
0
-20
^{11}B CHEMICAL SHIFT (ppm)
BX_4^-
BX_3
predicted
X=Cl,Br,I
X= F and Cl,Br,I
6
8
10
12
14
16
$\sum E_X$

Figure 7. (a) variation of ^{19}F chemical shifts and ^{13}C-^{19}F coupling constants of CX_4 for X = F and Cl, Br and CF_3I (63); (b) variation of ^{13}C chemical shifts with the number of chlorine atoms (n) for CCl_nBr_{4-n} (62).

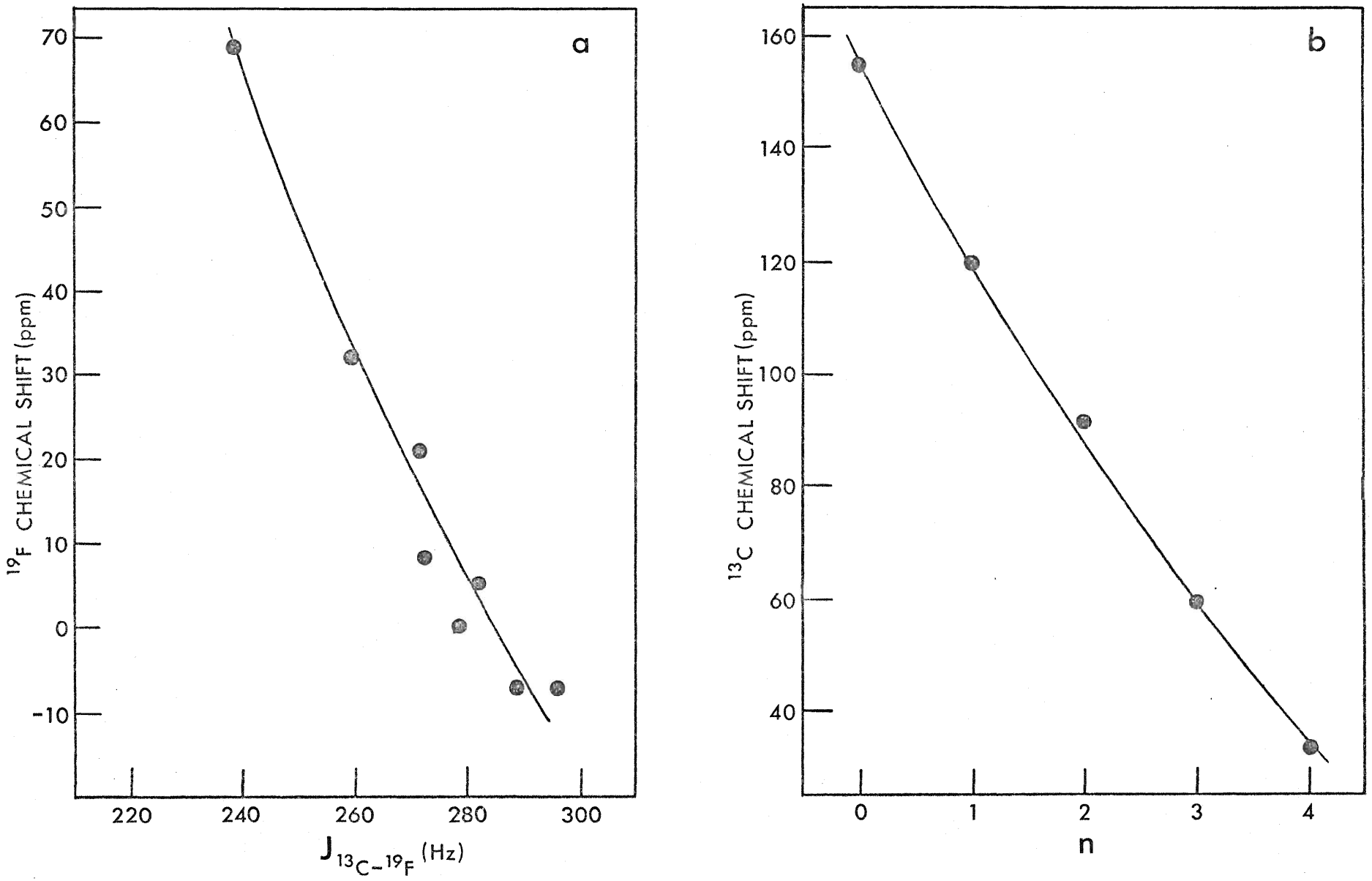
a
70
60
50
40
30
20
10
0
-10
^{19}F CHEMICAL SHIFT (ppm)
220
240
260
280
300
$J_{^{13}C-^{19}F}$ (Hz)
b
160
140
120
100
80
60
40
^{13}C CHEMICAL SHIFT (ppm)
0
1
2
3
4
n

ure 6) as well as in the mixed boron trihalide adducts (39). Fluorine containing species are clearly anomalous on the basis of electronegativity considerations alone. The anomalously high shielding of the boron nucleus in the fluorine containing species may also be assessed in terms of fluorine-boron π bonding.

(ii) Pairwise Additivity

In NMR spectroscopy, nuclear spin-spin coupling constants and chemical shifts have been observed which are pairwise additive with respect to the substituent groups (64). That is, the chemical shift (or spin-spin coupling) can be expressed as

$$\delta = \Sigma\eta_{ij} \tag{12}$$

where η_{ij} is a parameter associated with substiutents i and j, and independent of all other substituents. The sum is taken over all substituents about a central atom, excluding the nucleus observed in the NMR experiment. In the case of $BF_2Cl_2^-$

$$\begin{aligned} \delta_{^{11}B} &= \eta_{F,F} + 4\eta_{F,Cl} + \eta_{Cl,Cl} \\ \delta_{^{19}F} &= 2\eta_{F,Cl} + \eta_{Cl,Cl} \end{aligned} \tag{13}$$

where η_{ij} is different for each nucleus observed.

Theoretical justification of the pairwise additivity rule for chemical shifts and nuclear spin-spin couplings can be found in the work of Vladimiroff and Malinowski (64). Accordingly, pairwise contributions arise because the wave function

of each substituent group suffers a linear correction due to the presence of each neighboring substituent group. In general chemical shifts are expected to be at least pairwise additive. If the substituent is far removed from the nucleus is question, then direct additivity is expected. Some insight into the type of coupling mechanism involved can also be deduced by considering substituent effects. The local nature of the Fermi contact term reduces a pairwise rule to a direct additivity rule. On the basis of the above generalizations and observed additivity behavior in a wide range of systems, Malinowski and Vladimiroff have been able to arrive at two sets of criteria for assessing the nature of the spin-spin coupling: (1) if the coupling is directly additive and the chemical shifts of both of the coupled nuclei are pairwise additive, the Fermi contact term is dominant for this coupling; (2) if the chemical shifts of both of the coupled nuclei and their spin-spin coupling constant obey the same type of additivity rules, the Fermi contact term is not dominant.

A recent observation by Malinowski (65) of pairwise additivity in the ^{27}Al chemical shifts of the mixed tetrahaloaluminate ions has demonstrated the utility of this principle in confirming tentative chemical shift assignments. Pairwise parameters for ^{11}B chemical shifts of some of the non-fluorine containing mixed boron trihalides have been presented by Vladimiroff and Malinowski (64). The present study reveals that the chemical shifts and B-F coupling constants of

BX_4^- systems can be correlated by pairwise additivity relations and provide useful confirmations of their assignments. The empirical parameters were calculated using a least squares technique. Calculated values are compared to the observed values to give an estimate of the reliability of the correlation (Tables II and III). The parameters are also presented (Table VI) since they can be used to estimate the chemical shifts of yet unmeasured ions.

Table VI

Pairwise Substituent Parameters for the ^{19}F and ^{11}B NMR Parameters of BX_4^- Ions

Substituents i,j	$\eta_{i,j}$ Chemical Shift (ppm) ^{19}F	^{11}B	^{11}B-^{19}F Coupling Constant (Hz)
F,F	50.5	3.34	-0.5
F,Cl	36.7	2.11	13.6
F,Br	31.4	-	19.4
Cl,Cl	31.2	1.91	26.6
Cl,Br	28.2	3.25	32.2
Br,Br	26.1	7.07	37.1
Cl,I	-	8.60	-
Br,I	-	14.0	-
I,I	-	24.3	-

On the basis of the criteria set forth by Malinowski and Vladimiroff, the B-F coupling constants in the fluorinated tetrahaloborates do not arise from a dominant Fermi contact term, and the remaining orbital and spin-dipolar contributions must be considered. Similarly, the contact term is probably not dominant in ^{13}C-^{19}F couplings, since ^{19}F chemical shifts (64) and ^{13}C-^{19}F coupling constants (66) are both pairwise additive. Recently a self consistent field perturbation theory has been applied to calculate the orbital and spin-dipolar as well as the contact term of ^{13}C-^{19}F coupling constants in the fluorinated methanes (67). The results confirm that the Fermi contact term is incapable by itself of reproducing the experimental trends of ^{13}C-^{19}F values in a wide range of molecules. It is only when the other two usually neglected terms are included that the experimental trends are obtained.

Both the expression for the orbital contribution and the spin-dipolar contribution consider only the 2p functions (68, 69). The resulting p_σ- p_σ and p_π- p_π bond order terms in the expressions determine the degree of mixing of the ground and excited states. Furthermore, the orbital contribution is non-zero only if there is multiple bonding between the coupled atoms. If the observed trends in ^{11}B-^{19}F (and ^{13}C-^{19}F) coupling constants truly reflect boron-fluorine (and carbon-fluorine) p_π- p_π bonding, the relative p_π- p_π contributions in the theoretical expressions should be dominant.

(B) CALCULATION OF ^{11}B AND ^{19}F CHEMICAL SHIFTS

(i) Theory

The theory of the ^{19}F chemical shift is most conveniently discussed along lines first suggested by Saika and Slichter (70), that is, in terms of an atomic breakdown of diamagnetic currents. The screening constant for the nucleus of fluorine atom A may be written (71)

$$\sigma^A = \sigma_d^{AA} + \sigma_p^{AA} + \sum_{B(\neq A)} \sigma^{AB} + \sigma^{A,ring} \qquad (14)$$

where σ_d^{AA} is the contribution arising from the diamagnetic Langevin-type circulation on atom A, σ_p^{AA} is due to opposing paramagnetic currents on this atom which result from the mixing of ground and excited electronic states by the magnetic field, $\sum \sigma^{AB}$ is the contribution from currents on other atoms, and $\sigma^{A,ring}$ the contribution from ring currents which cannot be localized on individual atoms as in aromatic molecules. Saika and Slichter (70) first showed that for fluorine chemical shifts, the second-order paramagnetic term in Ramsay's general equation for nuclear screening σ_p^{AA} is usually the most sensitive to details of chemical structure. In the remainder of this discussion, only variations of the local paramagnetic term will be considered.

The screening coefficient σ^A is a tensor, of which only the average value is observed in the conventional solution NMR experiment. By second-order perturbation theory (71), the zz-component of the local paramagnetic contribution can be

expressed in terms of ground state molecular orbitals

$$(\sigma_p^{AA})_{zz} = \frac{-e^2h^2}{2m^2c^2(\Delta E)}\langle r^{-3}\rangle_{2p} \quad (Q_{AA})_{zz} + \sum_{B(\neq A)} (Q_{AB})_{zz} \qquad (15)$$

where

$$(Q_{AA})_{zz} = 2-2(P_{x_Ax_A})(P_{y_Ay_A}-1) + 2P_{x_Ay_A}^2 \qquad (16)$$

and

$$(Q_{AB})_{zz} = -2P_{x_Ax_B}P_{y_Ay_B} + 2P_{x_Ay_B}P_{y_Ax_B} \qquad (17)$$

with corresponding expressions for other components. Summations are over all atoms other than A, $\langle r^{-3}\rangle_{2p}$ is the average value of the inverse cube radius of the fluorine 2p orbitals, ΔE is the average electronic excitation energy, and $P_{\mu\nu}$ are elements of the charge density matrix in the molecular orbital theory of the unperturbed molecule. The diagonal element $P_{\mu\mu}$ is a measure of electron population for this orbital, the off-diagonal elements $P_{\mu\nu}$ are overlap populations and are referred to as bond orders. The suffixes $x_A, x_B, y_A, y_B, z_A, z_B$ correspond to the 2p atomic orbitals of atoms A and B (or 3p, 4p, --- if heavier atoms are present). Positive and negative values correspond to bonding and antibonding interaction, respectively.

The factor $\langle r^{-3}\rangle_{2p}$ and the term $(Q_{AA})_{zz}$ depend primarily on the local electron density on the fluorine atom. As the

total electronic charge on atom A increases, the 2p orbitals are expected to expand as electrons are added to the atom. If the net charge on the atom is $-q_A e$, the magnitude of the effect may be estimated by using Slater atomic 2p orbitals (with assumed linear dependence of the Slater atomic screening constant on q_A) to calculate $\langle r^{-3} \rangle_{2p}$ (72) by choosing the nuclear charge Z_A according to Slater's rules (73). Since these yield a Z_A value of 5.20 for a neutral fluorine atom and a screening of 0.35 per 2p electron

$$Z_A = 5.20 - 0.35(q_A - 1) \tag{18}$$

For a Slater 2p orbital, $\langle r^{-3} \rangle_{2p}$ is given by

$$\langle r^{-3} \rangle_{2p} = \frac{1}{24}\left(\frac{Z_A}{a_o}\right)^3 \tag{19}$$

for small q_A, a_o being the Bohr radius.

The atomic term $(Q_{AA})_{zz}$ takes the value of +2 if the electron density in each 2p function is unity. It should be noted that for fluorine atoms, the variation of Q_{AA} gives a significant contribution to the chemical shift.

The terms involving Q_{AB} with A≠B are of considerable interest. Physically they arise because the external field acting on atom B mixes in certain excited electronic states of the molecule inducing a current flow on A. Such terms can occur only if atom B possesses p atomic orbitals, and contain the p_π- p_π contributions to the chemical shift. If B is a neighboring atom and the x-axis is chosen along the

bond, the cross term $P_{x_A y_B} P_{y_A x_B}$ will usually be small and the average value of Q_{AB} may be written

$$Q_{AB(av)} = -\frac{2}{3} \; P_{x_A x_B}{}^{\sigma} (P_{y_A y_B}{}^{\pi}) + P_{y_A y_B}{}^{\pi} P_{z_A z_B}{}^{\pi} \qquad (20)$$

The bond order between the two $2p_\sigma$ atomic orbitals forming the σ bond are represented by $P_{x_A x_B}{}^{\sigma}$ and the two π bond orders by $P_{y_A y_B}{}^{\pi}$ and $P_{z_A z_B}{}^{\pi}$. From Equation (20) it is clear that this effect of neighboring atoms only occurs if there is both σ and π bonding between A and B and may be termed a multiple bond effect.

The term σ_p^{AA} is the sum of contributions from all the excited states of $p_x \rightarrow p_y$ type (for the lighter elements other than hydrogen), which are mixed with the ground state. The degree of mixing increases with a decrease in the excitation energy. This mixing is due to unquenching of the orbital angular momentum in the applied field. This circulation of charge around the nucleus deshields it by a reinforcement of the field at the nucleus. Calculations of the chemical shift usually employ a ΔE which is constant for a particular series of related compounds (74), but in the present work the change in this quantity from species to species was taken into account by using the calculated singlet-singlet transition energies in each case

$$\Delta E = \varepsilon_j - \varepsilon_i \qquad (21)$$

where ε_i is the energy corresponding to the highest occupied

molecular orbital and ε_j is the energy corresponding to the lowest unoccupied molecular orbital.

Armstrong and Perkins (74) have applied a similar treatment to the calculation of ^{11}B chemical shifts in the mixed boron trihalides. The ^{19}F and ^{11}B chemical shifts for the fluorine-chlorine containing boron trihalides and tetrahaloborates have been calculated in the present work using the molecular orbital theory for ^{13}C chemical shifts set forth by Karplus and Pople (72) and Pople (71).

(ii) Calculations

Calculations using the CNDO/2 method were carried out with a computer program (56) incorporating the theory outlined by Pople, Santry, and Segal (75a) and Pople and Segal (75b,c). A CNDO treatment is intermediate in complexity between full LCAOSCF calculations for π electrons and the simple Hückel approach. It is of particular value since it includes all valence electrons, rather than just π electrons, permitting a full treatment of σ and π electrons in planar molecules and application of the theory to a great range of molecules where σ-π separation is not possible. In the CNDO calculation, no simple hybridization scheme is assumed; boron and halogen atomic orbitals are distributed according to their energies and overlap properties, but always consistent with the symmetry of the molecule. Trends rather than exact chemical shifts should be compared as part of the difference is due to the nature of the calculation itself as well as the inherent

sensitivity of these methods to the chosen geometry.

The B-F and B-Cl bond lengths in BX_3 molecules were taken as 1.291 Å and 1.74 Å, the experimentally determined distances in BF_3 and BCl_3, respectively (76). Bond lengths in the BX_4^- ions were taken as the average B-F and B-Cl internuclear separations in the x-ray crystal structure of BF_4^-, 1.384 Å (77), and BCl_4^-, 1.842 Å (78). Ideal bond angles were assumed, *i.e.*, 120° X-B-X angles in BX_3 and 109°28' X-B-X angles in BX_4^-.

The parameters needed in Equation (15) to calculate the local paramagnetic contribution σ_p^{AA} are listed in Table VII. Calculated values of σ_p^{AA} were scaled by a factor of 1/1.60 in the case of ^{19}F chemical shifts and 1/2.50 in the case of ^{11}B chemical shifts. Contributions other than the paramagnetic contribution were assumed to be constant in both series and were evaluated by taking the difference between the calculated (scaled) BF_3 chemical shift and the observed BF_3 chemical shift (122.2 ppm with respect to $CFCl_3$ in the ^{19}F spectrum (this work) and 6.7 ppm with respect to external $(CH_3O)_3B$ in the ^{11}B spectrum (46)). This difference was then added to the scaled theoretical chemical shift values of the remaining BX_3 and BX_4^- species to give the plots in Figures 8 and 9.

(iii) Conclusions

The main features of the results given in Figures 8 and 9 arise from changes with excitation energy ΔE (Table VII),

Table VII

Calculated Parameters (in au) for the Paramagnetic Contributions to the ^{19}F and ^{11}B Chemical Shifts

Molecule or Ion	ΔE	Fluorine-19			Boron-11		
		$Q_{AA(av)}$	$\sum_{B(\neq A)} Q_{AB(av)}$	q_A	$Q_{AA(av)}$	$\sum_{B(\neq A)} Q_{AB(av)}$	q_A
BF_3	0.9016	0.6667	0.1958	0.2324	1.5752	0.5499	-0.6971
BF_2Cl	0.6415	0.7060	0.2112	0.1940	1.6157	0.5619	-0.5645
$BFCl_2$	0.5407	0.7480	0.2268	0.1544	1.6711	0.6246	-0.4171
BCl_3	0.5140	-	-	-	1.7412	0.6603	-0.2522
BF_4^-	0.9717	0.5233	0.1394	0.4015	1.6243	0.5544	-0.6059
BF_3Cl^-	0.6862	0.5680	0.1492	0.3609	1.6386	0.5607	-0.5560
$BF_2Cl_2^-$	0.5924	0.6080	0.1554	0.3241	1.6657	0.5657	-0.4795
$BFCl_3^-$	0.5687	0.6480	0.1618	0.2902	1.7059	0.5654	-0.3781
BCl_4^-	0.5564	-	-	-	1.7570	0.5492	-0.2539

Figure 8. Comparison of experimental and theoretical ^{19}F chemical shifts of BX_3 (16) and BX_4^- (X = F,Cl).

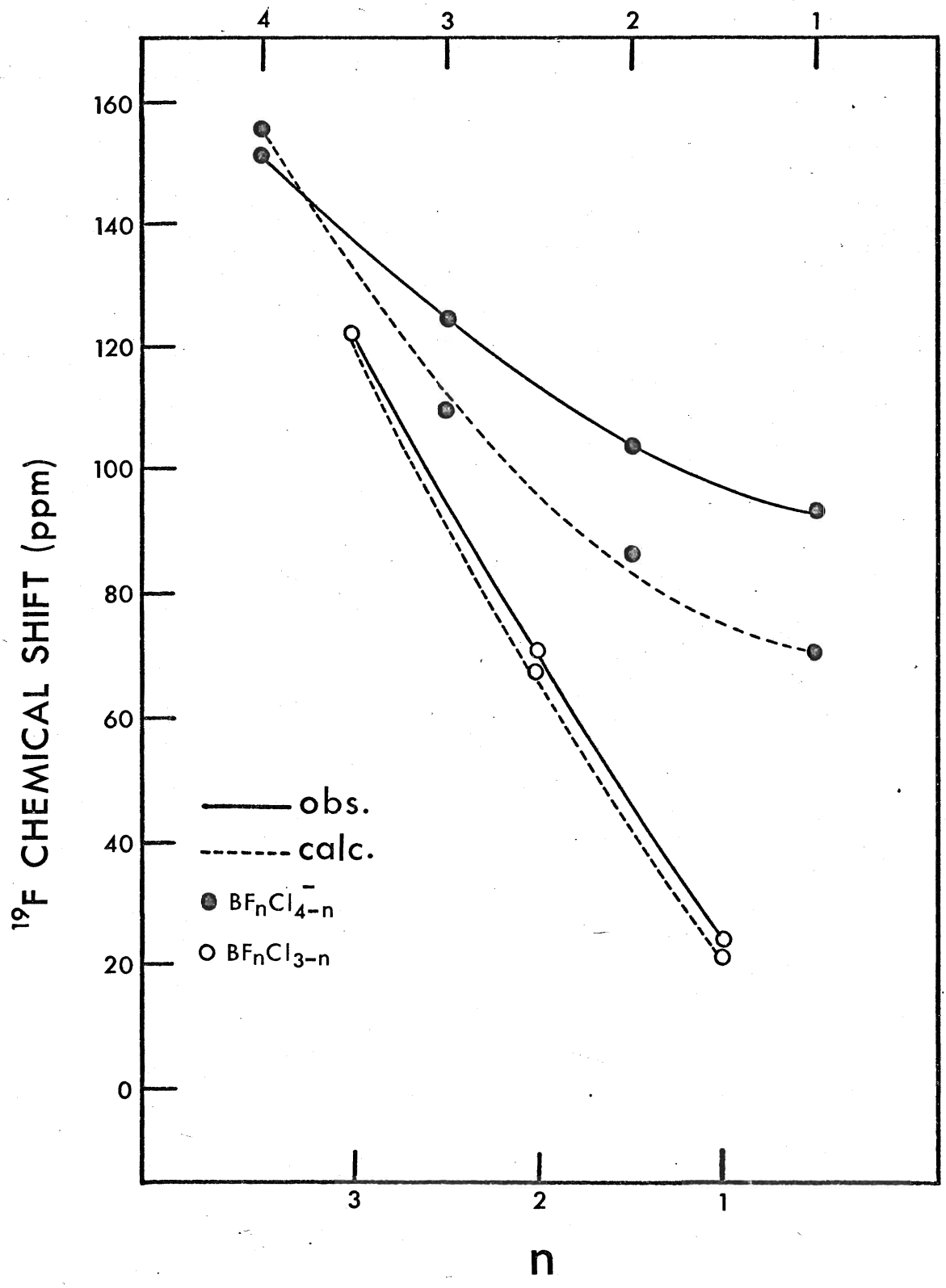
4
3
2
1
160
140
120
100
80
60
40
20
0
^{19}F CHEMICAL SHIFT (ppm)
obs.
calc.
$BF_nCl_{4-n}^-$
BF_nCl_{3-n}
3
2
1
n

Figure 9. Comparison of the experimental and theoretical ^{11}B chemical shifts of BX_3 (16) and BX_4^- (X = F,Cl).

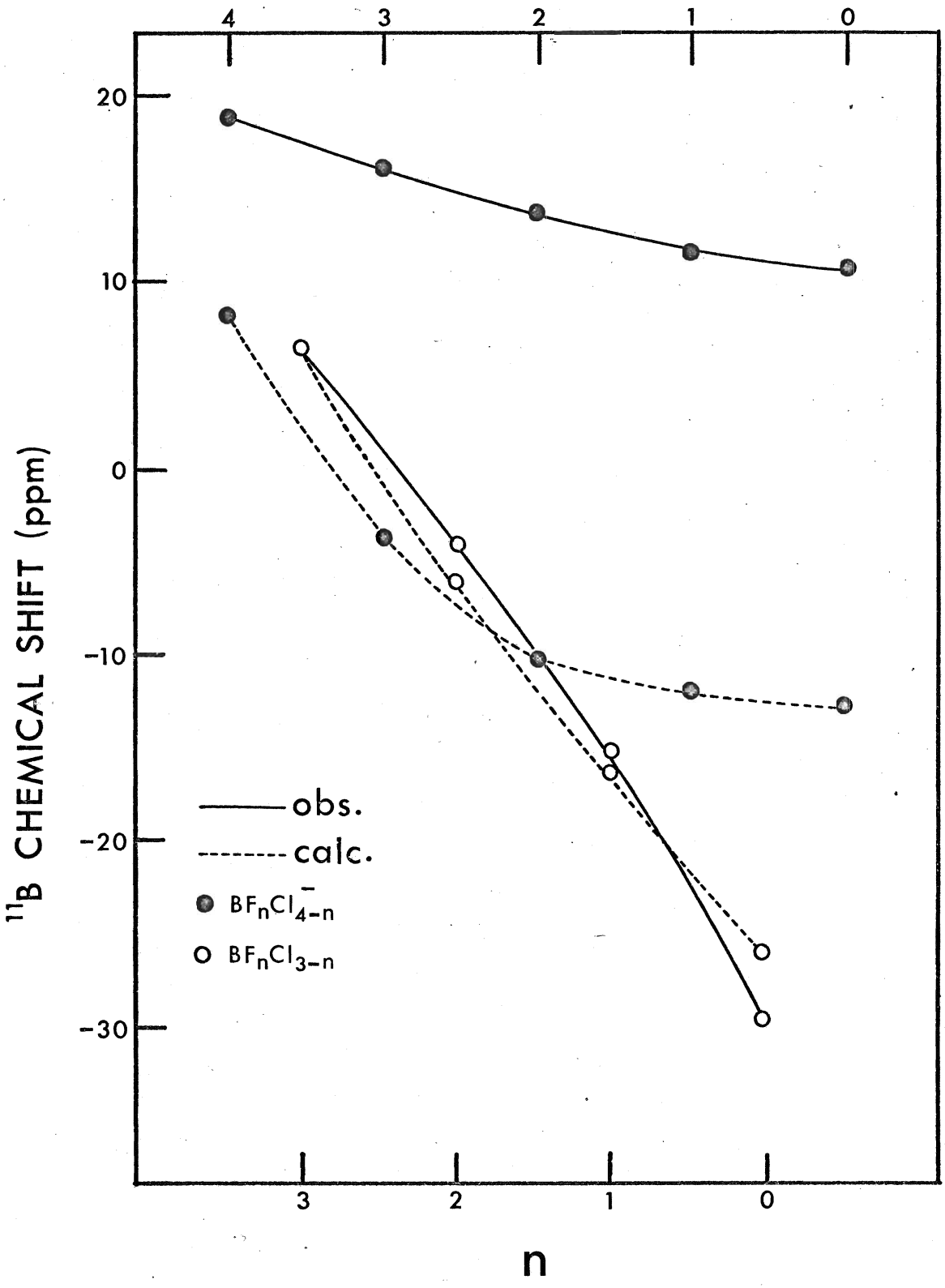
4
3
2
1
0
20
10
0
-10
-20
-30
^{11}B CHEMICAL SHIFT (ppm)
obs.
calc.
$BF_nCl_{4-n}^-$
BF_nCl_{3-n}
3
2
1
0
n

though the multiple bond terms Q_{AB} and the atomic term Q_{AA} also give negative contributions to the paramagnetic shift with decreasing numbers of fluorine substituents. The ability of this method to predict the correct trends in ^{11}B and ^{19}F chemical shifts suggests that assessment of boron-fluorine p_π- p_π bonding in these systems in terms of ^{11}B and ^{19}F chemical shifts may be better understood if the nature of the dominant term, ΔE, is known.

Fluorine containing systems are clearly anomalous by electronegativity considerations (Figure 6). Thus, electronegativity trends in non-fluorine containing species predict more negative ^{11}B chemical shifts for fluorine containing species than are actually observed. This suggests that ΔE is anomalously large in the fluorine cases and that the nature of the excitation is different when fluorine is present. The large drop in ΔE upon going from BF_3 to BF_2Cl or from BF_4^- to BF_3Cl^- (Table VII) and subsequent leveling off as more chlorines are substituted for fluorines suggest that ΔE is dominated by low-lying chlorine excitation when chlorine is present.

The nature of the highest occupied molecular orbital is important when considering the effects of ΔE. Bassett and Lloyd (79) suggest, on the basis of photoelectron spectroscopy studies, that the highest occupied molecular orbital in BF_3 is of the π type. If the average excitation energy is made up of, *e.g.*, $\pi \rightarrow \pi^*$ contributions from fluorine and

$n \rightarrow \pi^*$ or $\pi \rightarrow \pi^*$ contributions of very much lower energy from the heavier halogens, compounds of the heavier halogens and those containing fluorine might be expected to give different trends in the two series. A similar rationale may be extended to ^{19}F chemical shift trends in these systems, which increase with increasing total substituent electronegativity, as well as to analogous trends in the adducts of the mixed boron trihalides (39) and the isoelectronic tetrahalomethanes (63).

(C) MECHANISMS FOR HALOGEN EXCHANGE

(i) General

While it is impossible to discuss reaction mechanisms with certainty in the absence of rate data, it appears that a mechanism in which a tetrahaloborate ion dissociates to boron trihalide and halide ion is operative. The present study eleminates the previously existing anomaly by putting the relative exchange rates, at least in the fluorine-chlorine system where dissociation of halide ion from BX_4^- does not occur too readily, in the expected order $BX_4^- < BX_3$.

Assuming prior dissociation of tetrahaloborate, two mechanisms can be given. The first involves a halogen-bridged intermediate

$$BX_4^- \rightleftharpoons BX_3 + X^-$$

$$BX_3 + BY_4^- \rightleftharpoons \left[\begin{array}{c} X \quad Y \quad Y \\ B \quad\quad B \\ X \quad X \; Y \quad Y \end{array} \right]^- \rightleftharpoons \Big] \qquad (22)$$

$$\left.\begin{array}{l} BX_3Y^- + BY_3 \\ \\ BY_3 + X^- \rightleftharpoons BY_3X^-, \; etc. \end{array}\right] \quad (22)$$

The second mechanism, which is formally S_N1, would involve the rapid reassociation of the boron trihalide with a different halide ion

$$\left.\begin{array}{l} BX_4^- \rightleftharpoons BX_3 + X^- \\ BY_4^- \rightleftharpoons BY_3 + Y^- \\ BX_3 + Y^- \rightleftharpoons BX_3Y^-, \; etc. \end{array}\right] \quad (23)$$

Lockhart (35) suggests that the rapid dissociation step might give a powerful enough nucleophile to allow S_N2 attack on tetrahaloborate ion by halide ion. While plausible in other systems, S_N2 attack on a negatively charged-species by a negatively charged nucleophile seems unlikely since it would give the highly unfavorable situation of a doubly charged transition state.

(ii) Bridge Mechanism

Although boron-halogen dissociation is least likely to occur in the B-F case, slow fluorine exchange involving prior dissociation of BF_4^- has been reported (41). Equation (23) may then be most applicable when both X and Y are good leaving groups. While Equation (22) may be applicable in all systems under consideration, fluorine bridging with boron is a strong probability in the case of fluorine containing systems. Brown-

stein and Paasivirta (23) have presented strong evidence for fluorine bridging in BF_3/BF_4^- systems. They have postulated the existence of $B_2F_7^-$ in ion pairs in CH_2Cl_2 solutions at low temperatures, and have proposed the bent fluorine bridged structure

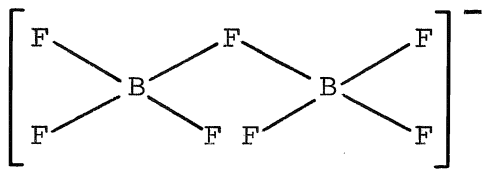

III

Further work by Harris (24) showed that $B_2F_7^-$ can exist at room temperature if the cation is sufficiently large.

(iii) Preferential Exchange

The observed sequence for the formation of the fluorochloroborate ions, BF_3Cl^- - $BF_2Cl_2^-$ - $BFCl_3^-$ (Figure 1), may reflect the relative Lewis acidities of the corresponding boron trihalides as well as a mechanism involving a dissociative step. As chlorine is replaced by fluorine in BCl_3, the observed Lewis acidity decreases (39,40) and the relative ease of Cl^- ion dissociation is expected to increase in the series $BCl_4^- < BFCl_3^- < BF_2Cl_2^- < BF_3Cl^-$. Thus, in the following sequence, where Equation (22) has been assumed to represent the mechanism, BF_3Cl^- is formed with little $BF_2Cl_2^-$ and $BFCl_3^-$ being observed in the initial stages of the reaction

$$\left.\begin{array}{l} BCl_4^- \rightleftharpoons BCl_3 + Cl^- \\ BCl_3 + BF_4^- \rightleftharpoons \left[BF_4\text{-}BCl_3^-\right] \rightleftharpoons BF_3 \\ +BFCl_3^- \end{array}\right] \quad (24)$$

$$\left.\begin{array}{l} BFCl_3^- \rightleftharpoons BFCl_2 + Cl^- \\ BF_2Cl + BF_4^- \rightleftharpoons \left[BF_4\text{-}BF_2Cl^-\right] \rightleftharpoons BF_3 \\ +BF_3Cl^- \end{array}\right] \quad (25)$$

$$BF_3 + Cl \rightleftharpoons BF_3Cl^- \quad (26)$$

Comparable reaction sequences can be written for $BF_2Cl_2^-$ when $\left[BF_3Cl^-\right]$ is large and for $BFCl_3^-$ when $\left[BF_2Cl_2^-\right]$ is large.

In the ternary F-Cl-Br systems, relative rates of fluorine exchange among various tetrahaloborate species can be inferred from exchange behavior over a range of temperatures (Figure 3). The relative rates of fluorine exchange closely parallel the Lewis acidities of their respective trihalides (Table VIII), and are indicative of a mechanism requiring the prior dissociation of tetrahaloborate (Equations (22) and (23)). A similar trend is noted in BF_4^-/BI_4^- systems. If the assignments are correct, the $BF_2I_2^-$ and BFI_3^- ions reflect their reduced lability by their reluctance to undergo exchange averaging with rapidly exchanging BF_4^- and BF_3I^- ions to higher field.

(iv) Solvent Exchange

Complications arising from halogen exchange with the solvent may be interpreted in light of a prior dissociation of

Table VIII

Observed Relative Rates of Fluorine Exchange in Ternary F-Cl-Br Containing Systems of BX_4^- Ions

BX_3	$BX_4^-(BX_3 \cdot X^-)$	Rate of Fluorine Exchange
BF_3	BF_3Cl^-	rapid
	BF_3Br^-	
BF_2Cl	$BF_2Cl_2^-$	
BF_2Br	BF_2ClBr^-	intermediate
	$BF_2Br_2^-$	
$BFCl_2$	$BFCl_3^-$	
$BFBr_2$	$BFCl_2Br^-$	slow
	$BFBr_3^-$	

Increasing Lewis Acidity*

* inferred from ^1H complexation shifts of the $(CH_3)_2O$ (39) and $(CH_3)_3N$ (40) adducts.

tetrahaloborate to boron trihalide and halide ion; analogous interpretations may be applicable to the tetrahaloaluminate systems (80) where similar behavior has been observed.

Dihalomethanes apparently undergo nucleophilic attack by free halide ion (Table V). The expected order of increasing nucleophilicity is $I^- < Br^- < Cl^-$ while the expected order of leaving ease is $I^- > Br^- > Cl^-$. Bromide ion displaces Cl^- in CH_2Cl_2 with difficulty; thus, it is not surprising that BBr_4^- does not solvent exchange in CH_2Cl_2 solutions. In the presence of BF_4^- solvent exchange takes place readily. The prior formation of the mixed fluorobromoborates appears to be necessary in this case. Relative fluorine exchange rates for these systems (Table VIII) indicate that bromide ion dissociation will be favored in the order $BF_3Br^- > BF_2Br_2^- > BFBr_3^- > BBr_4^-$. The relative ease of solvent exchange in the presence of BF_4^- may also involve participation of the dissociated boron trihalide, *e.g.*,

$$BF_3Br^- \rightleftharpoons BF_3 + Br^-$$

$$Br^- + CH_2Cl_2 + BF_3 \rightleftharpoons \left[Br\text{----}C(H)(H)\text{----}Cl\text{----}BF_3 \right]^- \qquad (27)$$

$$\rightleftharpoons CH_2ClBr + BF_3Cl^-$$

There is some evidence from ^{11}B NMR that CH_2Cl_2 can complex with other boron trihalides (49). Any such complex with BF_3 would be very weak since the differential heat of solution of BF_3 in CH_2Cl_2 is only 2.8 Kcal./mole (23). Similar arguments

may be applied to BCl_4^-/BBr_4^- systems where halogen exchange with CH_2Cl_2 has also been observed (Table IV).

(v) Comparison with Previous Work

Wharf and Shriver (22) have presented tensimetric and infrared evidence for the formation of BF_3Cl^- by low temperature additions of BF_3 to CH_2Cl_2 solutions of $SnCl_3^-$, $GeCl_3^-$, and Cl^-. In the case of chloride ion, they inferred the presence of a considerable amount of BF_4^-. The low temperature ^{19}F spectra of similar $BF_3/Et_4N^+Cl^-$ solutions in CH_2Cl_2 show in addition to BF_3Cl^- and BF_4^-, a considerable proportion of $BF_2Cl_2^-$. The presence of both BF_4^- and $BF_2Cl_2^-$ may be rationalized on the basis of the previously discussed redistribution mechanisms (Equations (22) and (23)), thus BF_3 arising from either dissociation of initially formed BF_3Cl^- or from direct addition may react with another mole of BF_3Cl^-

$$\begin{aligned} BF_3 + BF_3Cl^- &\rightleftharpoons BF_4^- + BF_2Cl \\ BF_2Cl + Cl^- &\rightleftharpoons BF_2Cl_2^- \end{aligned} \qquad (28)$$

The relative concentrations, $\left[BF_4^-\right]/\left[BF_2Cl_2^-\right] \simeq 2:1$, derived from the integrated ^{19}F intensities are in agreement with the proposed stoichiometry. A parallel interpretation is given to the BF_3/Br^- system where similar relative proportions of BF_4^- and $BF_2Br_2^-$ were observed.

CHAPTER IV

THE BORON TRIFLUORIDE ADDUCT OF TETRAMETHYLUREA

INTRODUCTION

The existence of the boron trifluoride donor-acceptor complex of tetramethylurea (TMU) has been well established (45). In addition, Greenwood and Robinson (21) have prepared a variety of boron trihalide adducts of other substituted ureas and thioureas and have examined their ^{1}H, ^{19}F, and ^{11}B spectra to determine whether nitrogen or oxygen (sulfur) is the donor atom.

The work presented in this Chapter and in Chapters V and VII was undertaken in an effort to establish the donor site in urea structures.

RESULTS

(A) TMU·BF_3

(i) NMR Spectra

The ^{1}H and ^{19}F NMR parameters for the solid adduct prepared from pure BF_3 (first preparative method, Chapter II) are listed in Table IX. In some cases, a second minor peak

Table IX

^{1}H and ^{19}F NMR Data for TMU, $TMU \cdot BF_3$, and $TMU \cdot H^+BF_4^-$ in CH_2Cl_2

Compound	^{1}H Chemical Shift (δ) of the N-Methyl	Relative ^{1}H Peak Areas	Relative ^{19}F Peak Areas[a] ($TMU \cdot BF_3 : BF_4^-$)
TMU	2.75	-	-
$TMU \cdot BF_3$ (pure; 1st preparative method)	3.02	-	0.99:0.01
$TMU \cdot H^+BF_4^-$	3.12	-	0.00:1.00
$TMU \cdot BF_3$ (impure; 3rd preparative method)	3.03 (adduct) 3.11 ($TMU \cdot H^+$)	0.86 0.14	0.82:0.18
$TMU \cdot BF_3$ (impure; aged sample; hydrolyzed)	3.02 (adduct) 3.09 ($TMU \cdot H^+$ + TMU)	0.72 0.28	0.65:0.35

[a] ^{19}F chemical shifts of $TMU \cdot BF_3$ and BF_4^- were 149.2 ± 0.2 ppm and 151.2 ± 0.2 ppm, respectively; $J_{^{11}B-^{19}F}$ for BF_4^- was 0.97 ± 0.05 Hz.

(<1% of the total intensity) was observed to high field in the ^{19}F spectrum (Figure 10c). At -70^{o} the adduct signal was split into two peaks of relative areas (low field peak)/(high field peak) = 1:4 and of relative chemical shift 0.064 ppm. This splitting is of the correct magnitude and direction to be attributed to an isotope shift. The ^{1}H-^{13}C coupling constants were 136.8 and 140.0 Hz for TMU and TMU·BF_3, respectively. The ^{11}B chemical shift was also determined and found to be 19.0 ppm.

Vacuum line samples of TMU·BF_3 in the presence of excess TMU gave sharp methyl singlets corresponding to the adduct and the free base, with a complexation shift of 16.2 Hz. Only a single exchange-averaged peak was visible when $[BF_3]/[TMU] > 1$ in the ^{19}F spectrum, while the ^{1}H chemical shift for the adduct peak remained invariant.

(ii) Infrared Spectra

Infrared data for two prominent features of the TMU and TMU·BF_3 spectra, the Amide I band (mainly C=O stretch) and the Amide II band (mainly N-CH_3 bend), are given in Table X.

(B) TMU·$H^{+}BF_4^{-}$

(i) ^{1}H NMR Spectra

The ^{1}H spectrum of material prepared as described in Chapter II consisted of a sharp methyl singlet (Table IX) and a broadened oxygen proton singlet of variable chemical shift with relative peak intensities 12:1. The oxygen and

Table X

Amide I and Amide II Bands [a]

of TMU and $TMU \cdot BF_3$

Mode	TMU (cm^{-1})	$TMU \cdot BF_3$ (cm^{-1})
C-O stretch	1636	1605
C-N bend	1497	1550

[a] reference (21).

Figure 10. Fluorine-19 spectra (56.4 MHz) of CH_2Cl_2 solutions of TMU·BF_3 (a) prepared from commercial (HF contaminated) BF_3; (b) prepared from commercial BF_3 + n-$Bu_4N^+BF_4^-$; (c) prepared from pure BF_3.

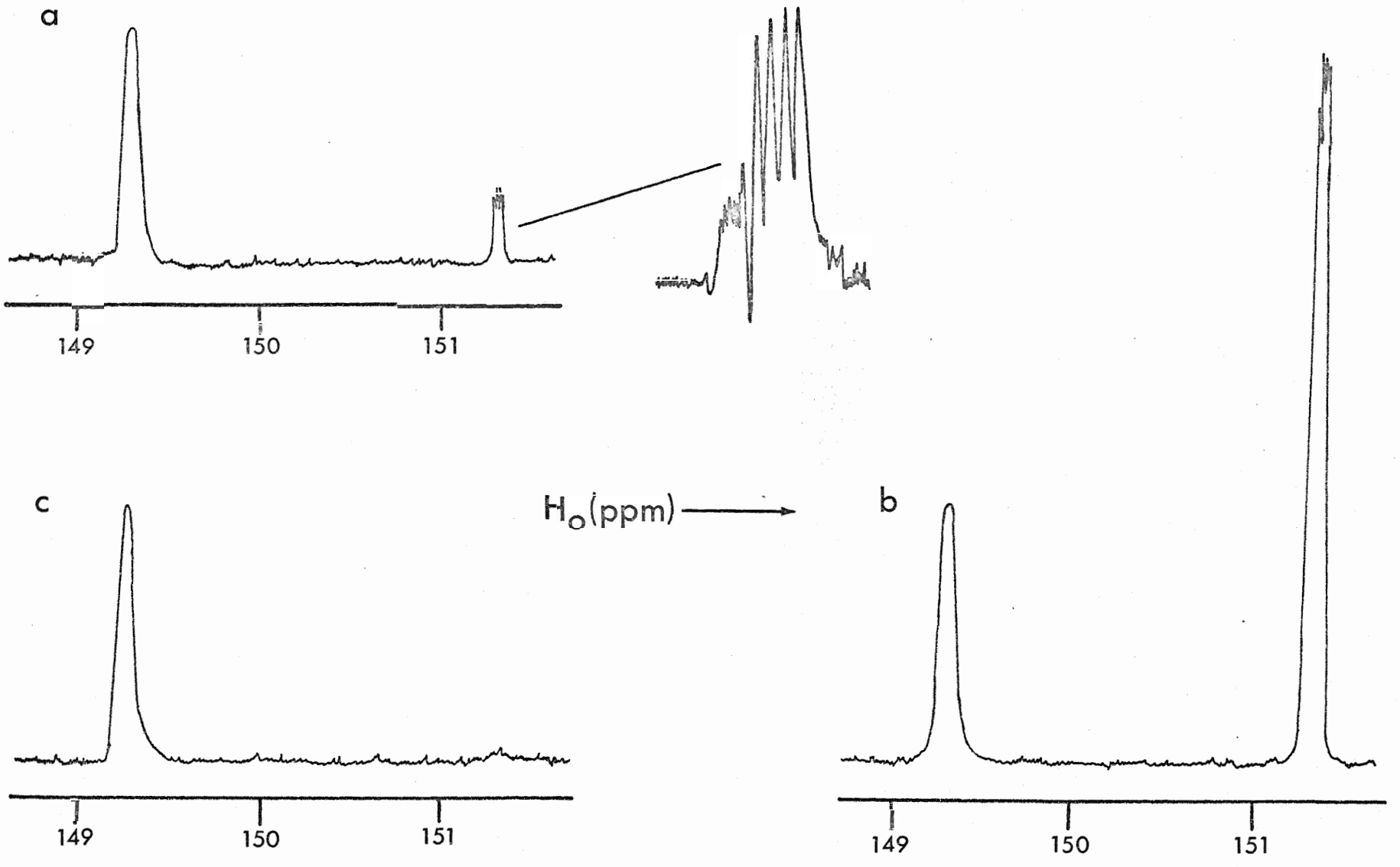
a
149
150
151
c
149
150
151
H_o(ppm) ⟶
b
149
150
151

methyl proton chemical shifts were dependent both upon the concentration of $TMU \cdot H^+BF_4^-$ and the concentration of free TMU. Titration of CH_2Cl_2 solutions of $TMU \cdot H^+BF_4^-$ (saturated at 37°) with free TMU led to a down-field shift for the oxygen proton followed by a reversal at higher proportions (Figure 11a), while a single exchange-averaged peak that shifted to higher field with increasing proportions of TMU was observed for the methyl protons (Figure 11b).

(ii) ^{19}F NMR Spectra

Fluorine-19 spectra of solutions of $TMU \cdot H^+BF_4^-$ in CH_2Cl_2 gave a broadened singlet ($w_{\frac{1}{2}}$ = 3.4 Hz) corresponding to BF_4^- (Table IX); no fine structure or isotope shift were observed. However, in the presence of TMU (~0.5 M) the normal B-F coupling and isotope shift of 0.055 ppm (10) could be resolved.

(C) $TMU \cdot BF_3$ PREPARED DIRECTLY FROM COMMERCIAL BF_3

(i) General

In previous work by Greenwood and Robinson (21), commercial BF_3 was used without further purification in the preparation of various urea adducts. There was reason to suspect contamination of their BF_3 by HF, which might affect the interpretation of their results. Boron trifluoride is capable of acting as a co-solvating agent for HF. In a non-aqueous medium like CH_2Cl_2, the pair HF-BF_3 is a strong acid capable of protonating TMU on oxygen. The present work shows that considerable amounts of $TMU \cdot H^+BF_4^-$ are present in $TMU \cdot BF_3$ adduct

Figure 11. Variation of the ^1H chemical shift of (a) the oxygen proton of pure $TMU \cdot H^+$; (b) the CH_3 protons of pure $TMU \cdot H^+$ and $TMU \cdot H^+$ contaminant in $TMU \cdot BF_3$ with $\left[TMU\right] / \left[TMU \cdot H^+\right]$.

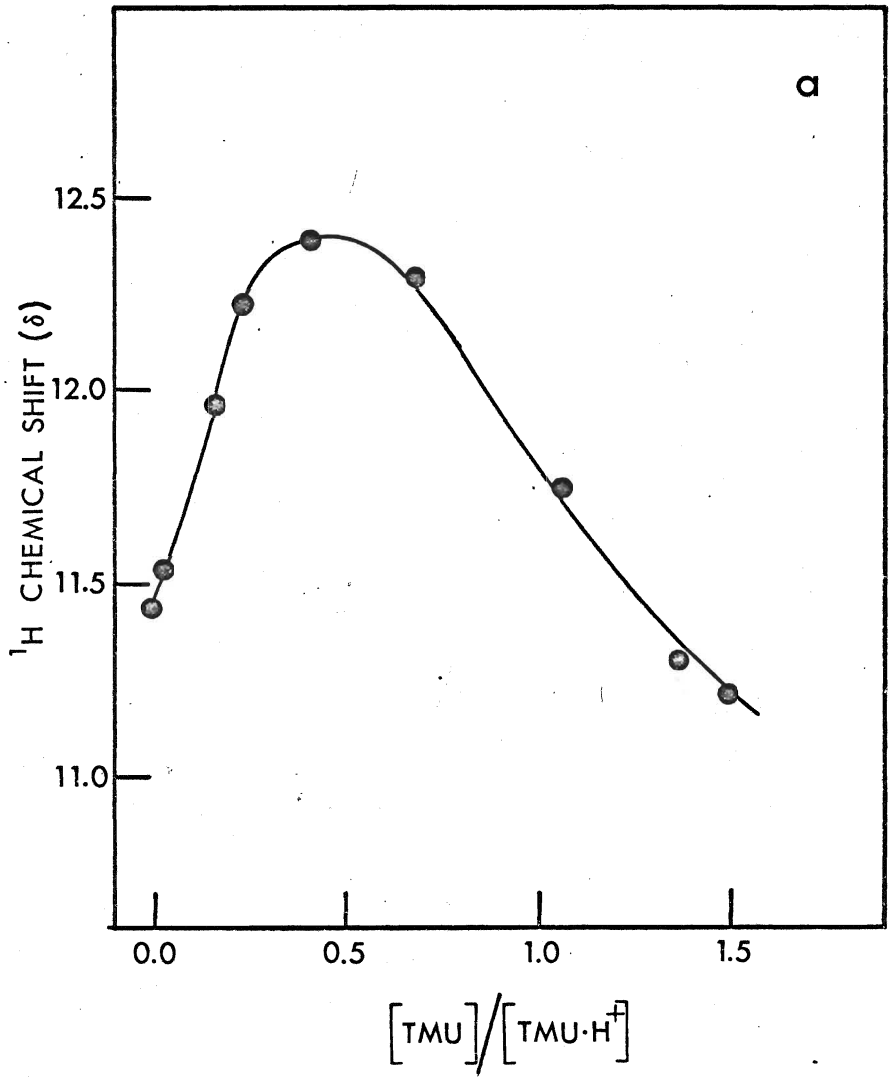
a
12.5
12.0
11.5
11.0
^{1}H CHEMICAL SHIFT (δ)
0.0
0.5
1.0
1.5
[TMU]/[TMU·H$^+$]

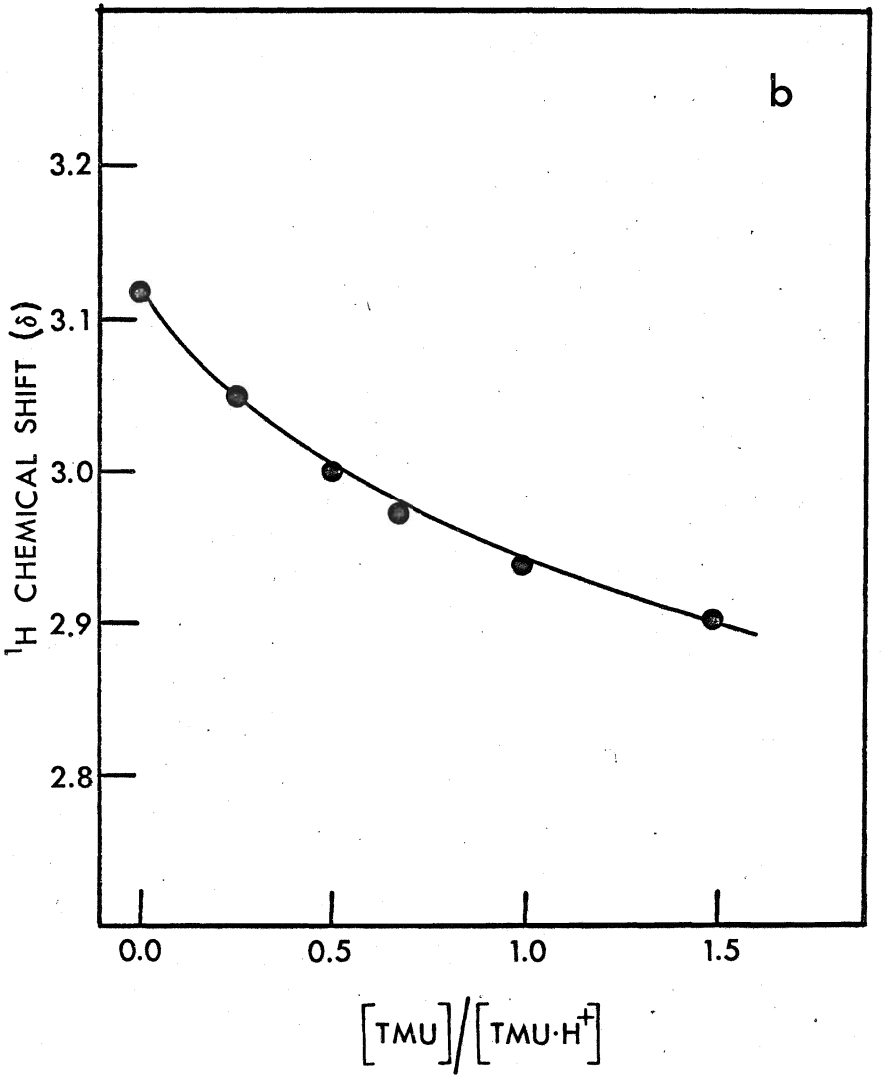
b
3.2
3.1
3.0
2.9
2.8
^{1}H CHEMICAL SHIFT (δ)
0.0
0.5
1.0
1.5
[TMU]/[TMU·H$^+$]

samples prepared directly from commercial BF_3.

(ii) ^1H NMR Spectra

The solid adduct (third preparative method, Chapter II), when dissolved in dry CH_2Cl_2, gave a normal ^1H spectrum for the 1:1 adduct and an additional small peak (14% of the total intensity) just to low field of the main adduct peak (Table IX). At higher concentrations, a small peak (~1% of the total intensity) of variable chemical shift could be observed just to low field of the CH_2Cl_2 solvent peak.

A standard solution of TMU·BF_3 (assuming a molecular weight of 184.0 g/mole) was prepared in CH_2Cl_2. This solution was subsequently titrated with free TMU and the titration monitored by ^1H NMR. Successive additions of free TMU resulted in migration of the low field peak to higher field, approaching 2.75 δ, the chemical shift of free TMU (Figure 11b).

(iii) ^{19}F NMR Spectra

The ^{19}F spectrum showed the normal two resonances (Table IX); the high field peak had, however, grown considerably in intensity over that of the TMU·BF_3 complex prepared from highly purified BF_3 (Figure 10a and c). The adduct underwent slow fluorine and/or BF_3 exchange at room temperature. At -70° or in the presence of excess TMU (~0.5 M), exchange was slowed sufficiently to show an isotope shift of 0.062 ppm on the low field peak. An isotope shift of 0.052 ppm was resolved on the high field peak at room temperature; the ^{11}B portion of the

peak consisted of a 1:1:1:1 quartet (Table IX) while a multiplet (septet) on the ^{10}B portion was only partially resolved (Figure 10a). The coupling constant, chemical shift, and isotope shift were reminiscent of BF_4^- (10). The presence of BF_4^- was confirmed by a pronounced increase in the size of the high-field peak with no change in fine structure upon addition of *n*-$Bu_4N^+BF_4^-$ to a sample containing excess TMU (Figure 10b). At greater than 1:1 proportions of acid/base, a single exchange-averaged peak was observed.

(iv) Changes Upon Standing

Comparison of the ^1H and ^{19}F NMR spectra of a freshly prepared sample with a month old solid sample stored over anhydrous calcium sulfate showed the expected resonances. The relative peak areas had, however, changed (Table IX). Isolation of TMU·$H^+BF_4^-$ and boric acid from the aged adduct indicates that hydrolysis has taken place. The small shift to higher field in the low field peak is attributed to rapid exchange averaging of TMU (liberated in the hydrolysis) and TMU·H^+.

(D) AMIDES AS MODEL OXYGEN DONORS

(i) Dimethylacetamide

The ^1H spectra of dimethylacetamide (DMAC) and DMAC·BF_3 show two different kinds of methyl protons (*cis* and *trans* to the carbonyl oxygen). These arise from restricted rotation about the carbon-nitrogen bond due to its partial double bond character. The retention of the two separate signals for methyl protons in the BF_3 adduct shows preservation of the

partial double bond character of the C-N bond and indicates oxygen coordination (19).

For 1:1 acid/base proportions or greater, no peaks were observed for uncomplexed DMAC. An excess of DMAC gave two sets of methyl signals, corresponding to the complex and the free base (Table XI). The complexation shifts of the N-methyl peaks were 0.316 ppm (CH_3(b)) and 0.286 ppm (CH_3(c)), while the C-methyl gave a complexation shift of 0.416 ppm.

No proton couplings were observed in the free base, but the high field N-methyl and C-methyl signals were broadened. The adduct, however, showed a quartet structure on CH_3(c) and a partially resolved quartet on CH_3(a), with broadening due to an additional small coupling to CH_3(b) (Table XI). Homonuclear decoupling in field sweep mode resulted in simplification of the CH_3(c) quartet to a singlet at a frequency difference setting of 46.8 Hz, in good agreement with the measured CH_3(a)-CH_3(c) separation of 46.0 Hz.

The room temperature ^{19}F spectra gave a sharp singlet ($w_{\frac{1}{2}}$ = 3.1 Hz) at 149.2 ppm which, under high resolution, revealed a well defined isotope shift of 0.060 ppm.

(ii) Dimethylformamide

Free dimethylformamide (DMF) and DMF·BF_3 also show *cis* and *trans* N-methyl-aldehyde proton couplings. Since coupling constants have not been reported for the adduct, they have been measured in the present work. Coupling constants were measured from a CH_2Cl_2 solution containing $[BF_3]/[DMF]$ = 0.50.

Table XI

Comparison of ^1H NMR Parameters of DMAC [a], DMF, and Their BF_3 Adducts

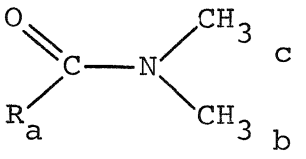

DMAC (R = CH_3)
DMF (R = H)

Base/Adduct	^1H Chemical Shift (δ) R(a)	CH_3(b)	CH_3(c)	$J_{R(a)-CH_3(b)}$ (Hz)	$J_{R(a)-CH_3(c)}$ (Hz)
DMAC	2.02	2.98	2.89	0.0	-*
DMAC·BF_3	2.42	3.25	3.20	-*	0.7
DMF	7.91†	2.95†	2.80†	0.4	0.6
DMF·BF_3	8.07†	3.30†	3.18†	0.6	1.0

a assignments of *cis*- and *trans*- methyl groups are based on the criteria summarized in reference (81).

* coupling too small to be resolved; irradiation of CH_3(a) resulted in sharpening of the signal.

† reference (19).

Both coupling constants compare well with values approximated from the published spectra of Kuhn and McIntyre (19) for $DMF \cdot BF_3$ at 1:1 acid/base proportions in nitropropane and CH_2Cl_2 solvents.

DISCUSSION

(A) IMPURE $TMU \cdot BF_3$; HF CONTAMINATION

Greenwood and Robinson also reported two signals in the ^{19}F spectra of their N-alkylated urea and thiourea adducts, a broad resonance at 148.5 ± 1 ppm and a sharp peak at 150.5 ± 1 ppm. No fine structure or isotope shift were reported. It would appear that Greenwood's extraneous ^{19}F resonance, BF_4^-, was due to HF contamination of BF_3 in the case of the ureas

$$HF + BF_3 + Urea \rightleftharpoons Urea \cdot H^+ + BF_4^- \qquad (29)$$

and/or partial hydrolysis of the adducts

$$\begin{aligned} Urea \cdot BF_3 + 3H_2O &\rightleftharpoons B(OH)_3 + 3HF + Urea \\ HF + Urea \cdot BF_3 &\rightleftharpoons Urea \cdot H^+ + BF_4^- \end{aligned} \qquad (30)$$

Growth of the BF_4^- and $TMU \cdot H^+$ concentrations in solid $TMU \cdot BF_3$ (Table IX) presumably arises from hydrolysis by the water of hydration from the calcium sulfate used as the desiccant.

Samples with $[TMU] > [BF_3]$ gave two major room temperature ^1H peaks corresponding to "free" TMU and $TMU \cdot BF_3$. Since proton exchange is generally very fast, a single averaged meth-

yl proton signal for TMU and $TMU \cdot H^+$ was observed which shifted to high field as the relative amount of TMU increased (Figure 11b). Boron trifluoride exchanges much more slowly than H^+ among TMU molecules, so that a separate $TMU \cdot BF_3$ peak of fixed chemical shift was visible at room temperature. A more complex case of proton transfer affecting chemical shifts of "free" base molecules has been reported in the methanol-BF_3 system (82). Rapid BF_3 and fluorine exchange may be invoked to explain averaging of the room temperature ^{19}F and ^1H spectra beyond 1:1 acid/base proportions.

It is of interest to note that some samples of commercial BF_3, in particular those taken from nearly empty cylinders in which the less volatile HF had become concentrated, contained up to 20 mole % HF. It seems likely that some of the studies reported in the literature have been carried out using impure material.

Variations in chemical shift observed for the oxygen proton of pure $TMU \cdot H^+$ in CH_2Cl_2 solution can be partially explained in terms of hydrogen bonding effects (83). In the presence of excess TMU, the signal initially shifts to higher field. Reversal of the chemical shift trend at higher proportions of TMU may correspond to increased intermolecular hydrogen bonding between oxygen and the oxygen proton.

(B) DONOR SITE

(i) General

The observation of separate TMU and $TMU \cdot BF_3$ peaks at

room temperature for samples containing excess TMU rules out exchange averaging of methyl environments *via* rapid intermolecular exchange of donor molecules. Equivalence of methyl protons in $TMU \cdot BF_3$ at temperatures as low as -100° without any significant broadening has been observed in the present work and is consistent with a system undergoing rapid intramolecular exchange. Methyl group equivalence may be rationalized by invoking rapid intramolecular exchange of BF_3 among oxygen and nitrogen donor sites, and/or rapid rotation about the C-N bond. Oxygen donation might be expected to enhance the C-N double bond character, thereby giving rise to a higher free energy of activation for the rotation process.

The lack of H-B, H-F, and B-F couplings, and the appearance of a boron isotope shift in the ^{19}F spectrum has been a characteristic of oxygen donation, but could equally well be just a characteristic of weak donation together with small coupling constants. For example, the BF_3 adducts of amines, which are strong nitrogen donors, exhibit a B-F coupling constant of 13-18 Hz (84) while acetonitrile, a weak nitrogen donor, apparently gives no splittings (85).

(ii) Infrared Spectra

The infrared spectra of TMU and $TMU \cdot BF_3$ may be useful in identifying the donor site in TMU. Several changes in the spectra might be expected on coordination. First, N-coordination should cause an increase in frequency of the Amide I band (assuming it is predominantly a C-O stretch mode)

because the accompanying loss of resonance gives greater double bond character to the C=O bond; conversely it is known that there is a considerable decrease in the frequency of this bond on oxygen coordination (21). Secondly, there should be little change in the frequency of the Amide I band on nitrogen coordination, but a significant decrease in frequency on oxygen coordination. Table X lists the frequencies of the Amide I and Amide II bands. The general increase in frequency of the Amide II band and decrease in frequency of the Amide I band suggest oxygen coordination.

Greenwood and Robinson have presented infrared evidence for adducts of partially alkylated ureas in the solid phase in which both the Amide I and Amide II bands shift to higher frequencies upon adduct formation. Interpretation of their results is complicated by the added possibility of strong intermolecular association. They have presented evidence for association of the adducts in non-polar solvents; in addition, considerable infrared evidence exists which suggests that partially alkylated ureas are also highly associated in non-polar solvents (86).

(iii) Oxygen Donation in the Amides and the Donor Site in TMU; a Comparison

Spin-spin coupling between the aldehyde proton and *cis* and *trans* methyl protons of DMF has been observed in the free base as well as in $DMF \cdot BF_3$ by Kuhn and McIntyre (19). Their assignment of the high field methyl peak to the methyl group

cis to the aldehyde proton is not correct. Assignments in this work are based on the criteria summarized by Stewart and Siddall (81).

A similar trend in coupling constants is observed in DMAC and DMAC·BF_3 (Table XI), in which the *trans* proton couplings are also larger than the *cis* proton couplings. An increase or appearance of splittings upon adduct formation in the amides may correspond to an increase in the C-N π bond order. An electron-withdrawing group at the carbonyl oxygen would be expected to increase electron density between the carbon and nitrogen nuclei and around the hydrogen nuclei, leading to increased interaction between nuclear and electron spins and a resulting change in the magnitude of the couplings.

Unlike TMU·BF_3 where low temperatures are required to observe the isotopic pattern, DMAC·BF_3 gives a F-on-B isotope shift at room temperature. This suggests a greater degree of dissociation of the donor-acceptor bond in the case of TMU·BF_3, leading to faster fluorine exchange. Ligand preference studies by Fratiello and Schuster (45) show that DMF is a stronger donor toward BF_3 than TMU. Both the ^{19}F chemical shift and isotope shift of DMAC·BF_3 agree closely with those determined for TMU·BF_3.

Further evidence for coordination at the oxygen of TMU comes from a comparison of the increase in ^{1}H-^{13}C coupling constants of TMU, DMAC, and other donors (87). Amines show

a large increase in the ^{1}H-^{13}C coupling constant upon coordination with BF_3 (~6-11 Hz). This increase is probably the result of at least two effects. Coordination to BF_3 would remove electron density from the amine, leading to an increase in the effective nuclear charge (88) for both the carbon and the hydrogen atoms as well as the nitrogen. The reduction of electron density on the nitrogen would make it more electronegative than carbon, which according to Bent's isovalent hydridization scheme (89), would require the methyl carbon to rehybridize, placing more p character in its orbital directed to nitrogen and leaving more s character for its C-H bonds. This increase in s character would lead to a larger value of the ^{1}H-^{13}C coupling constant (90). The very small increases noted upon coordination for the ^{1}H-^{13}C coupling constant in the DMAC (0.8 Hz (87)) and TMU (3.2 Hz) adducts are easily understood if coordination takes place at a position three atoms removed from the methyl groups. The coupling constants for the methyl groups suggest that the N-dimethyl groups in DMAC (138.4 Hz (87)) and TMU (136.8 Hz) are quite similar in nature.

(iv) Rotation About the C-N Bonds in TMU

Drago and co-workers (91) have sought to explain the low barrier to rotation about the C-N bonds of TMU by assuming that steric repulsion between methyl groups prevents TMU from having a completely planar C_2NCONC_2 skeleton as in the case of urea. In order to allow for appreciable π interaction of

both $-N(CH_3)_2$ groups, they have assumed a transition state in which one $-N(CH_3)_2$ group lies in a plane with the C-O bond and the other $-N(CH_3)_2$ group is perpendicular to that plane, its electronic structure being similar to that of an amide group.

More resonance energy would be associated with the C-N π bond in the transition state than with either C-N bond in the ground state (planar) configuration of TMU. The loss of the π bond energy of a C-N bond would be at least partially recovered by the increased π bonding to the other $-N(CH_3)_2$ group in the transition state; and a lower barrier to rotation would be observed in TMU than in a simple amide in which all of the C-N π bond energy is lost in the transition state. Correspondingly, the amide adducts should have higher rotational barriers than the TMU adduct if oxygen is the donor.

(v) Summary

Although unequivocal assignment of the donor site in $TMU \cdot BF_3$ cannot be made on the basis of NMR evidence alone, a pattern has emerged which is consistent with donation at the oxygen. Similarities between the observed NMR parameters of $TMU \cdot BF_3$ and BF_3 adducts of the structurally related amides, known oxygen donors, strongly suggest oxygen donation.

CHAPTER V

BORON TRIFLUORIDE ADDUCTS OF *SYM*- AND *UNSYM*- DIALKYLUREAS

INTRODUCTION

Steric and electronic effects are both important in determining conformations and barriers to rotation in ureas. Simultaneous maximum electron delocalization into both amide bonds of TMU is sterically impossible since it would require complete coplanarity of the urea framework, with crowding of methyl groups (91). Unlike TMU, dialkylurea structures should experience a smaller degree of steric interaction in their planar conformation and would be expected to exhibit a higher barrier to rotation about the C-N bond than TMU. Restricted rotation has not been observed in any of the free dialkylureas in this study, but has been observed in the BF_3 adducts.

The ^1H spectra of the dialkylurea adducts exhibit peaks due to two different kinds of alkyl groups (*cis* and *trans* to the carbonyl oxygen) because there is restricted rotation about the C-N bond. At higher temperatures the rate of rotation becomes sufficiently fast so that only one averaged peak can be observed. The observation of two separate alkyl group environments at higher temperatures in the adducts than in the

free ureas shows survival of the partial double bond character of the C-N bond and is indicative of oxygen coordination.

Donor properties of some dialkylurea structures toward BF_3 were studied in this Chapter. Although this work is less extensive than the TMU work, it establishes that oxygen is the donor site in urea structures.

RESULTS AND DISCUSSION

(A) NMR SPECTRA

(i) Room Temperature Spectra

Samples of the BF_3 adducts of *sym*-dimethylurea (*sym*-DMU), *unsym*-dimethylurea (*unsym*-DMU), *sym*-diethylurea (*sym*-DEU), and *unsym*-diethylurea (*unsym*-DEU) were prepared in NMR tubes on the vacuum line. These gave ^1H and ^{19}F spectra very similar to spectra obtained from BF_3/TMU solutions. Thus, the ^{19}F spectra of the adducts gave a slightly broadened peak at 148.6 ± 0.5 ppm and a peak due to a trace of BF_4^- (<1%) at 151.5 ± 0.5 ppm (*c.f.* Chapter IV) when excess base was present. A single exchange-averaged peak beyond 1:1 acid/base proportions was observed. The room temperature ^1H spectra of the N-alkyl groups were similar to those of TMU·BF_3. Separate peaks corresponding to the chemical shifts of the free base and the complex were observed up to 1:1 acid/base proportions. At 1:1 acid/base proportions or greater, only resonances of fixed chemical shift that were assigned to the complex could be observed. In general, CH_2, NH, and NH_2 proton signals were of

little diagnostic value. The nitrogen proton signals were broad and not easily visible due to quadrupole relaxation of ^{14}N, but were evident as CH_3-NH and CH_2-NH couplings in the *sym*-dialkylureas (Table XII).

In solutions containing both the free *sym*-dialkylurea and its adduct, this coupling was collapsed in the free base portion of the spectrum. Similarly, these proton couplings were easily collapsed in CH_2Cl_2 solutions of the free bases upon addition of a trace of anhydrous HF or commercial BF_3. These couplings survived in the adduct over the entire range of acid/base proportions. Collapse of the NH-CH_3 and NH-CH_2 couplings of the free *sym*-dialkylureas in the presence of BF_3 may be attributed to the presence of small amounts of HF (and hence BF_4^- in the ^{19}F spectrum) which give rise to the protonated ureas (Chapter IV). The proton on oxygen may undergo intramolecular exchange with the N-H protons leading to collapse of the fine structure. Neither rapid intra- or intermolecular exchange of adduct N-H protons occurs even though the basicity of the nitrogens is expected to decrease upon adduct formation at the oxygen. Boron trifluoride may serve to prevent proton exchange in the adduct by blocking protonation of the oxygen and/or decreasing the overall basicity of the nitrogens.

(ii) Low Temperature Spectra

The -20° spectra of all samples containing BF_3 showed additional splittings of the low field adduct peaks, while no change was observed in the free base peaks. Spectra of

Table XII

^{1}H NMR Data for *sym*-DMU, *unsym*-DMU, *sym*-DEU, and *unsym*-DEU and Their BF_3 Adducts

Molecule	Complexation Shift (ppm)[a]		CH_3 Multiplet	Coupling Constant (Hz)		
	CH_3	CH_2	Separation[b] (Hz)	$NH-CH_3$	$NH-CH_2$	CH_2-CH_3
sym-DMU	0.182	-	-	5.0[+]	-	-
sym-DMU·BF_3			2.5			
unsym-DMU*	0.192	-	-	-	-	-
unsym-DMU·BF_3*			1.0			
sym-DEU	0.150	0.19	-	-	5.8[†]	7.0
sym-DEU·BF_3			3.6			
unsym-DEU	0.100	0.14	-	-	-	7.1
unsym-DEU·BF_3			3.2			

[a] measured at 37°.

[b] $[BF_3]/[Donor]$ = 1.00 at -20°.

* solutions in CD_3NO_2/CH_2Cl_2 = 50/50 v/v.

† collapsed in the "free" base portion of the spectrum, but not in the adduct portion of the spectrum when BF_3 is present.

supercooled CH_2Cl_2 solutions of the bases in the absence of BF_3 showed no additional splittings down to a temperature of -80°. Proton NMR data for the methyl group absorptions of the 1:1 adducts are summarized in Table XII. Except in the case of the free *sym*-dialkylureas, no change in the spin-spin couplings was observed upon adduct formation or in the presence of HF.

The BF_3 adduct of *sym*-DMU was investigated in some detail. The 60 and 100 MHz spectra of samples for $\left[BF_3\right]/\left[sym\text{-DMU}\right]$ = 0.50 and 0.75 at -20° are compared in Figure 12. The four peaks associated with the adduct arise from spin-spin coupling of the NH proton with CH_3 protons in magnetically non-equivalent environments and are attributed to hindered rotation about the C-N bond. This was confirmed by observing the spectrum of d_2-*sym*-DMU·BF_3. The -20° spectrum consisted of two methyl singlets of unequal intensities centered about 2.90 δ, $\Delta\nu$ = 2.0 Hz (at 60 MHz). The unsymmetrical nature of the doublets is immediately evident in the 100 MHz spectra (Figure 12c,d). The ratio of the observed doublet intensities was (low field CH_3)/(high field CH_3) = 39/61. A small dependence of the relative doublet separation upon composition was also evident (Figure 12) and may have been due to varying degrees of intermolecular association of the adduct and free urea (Chapter IV).

Hindered rotation effects were also observed at -20° for *unsym*-DMU. Two methyl peaks of the same relative intensities were observed in the adduct spectrum. In the case of

Figure 12. The -20° ^{1}H spectra of *sym*-DMU/BF_3 systems for $[BF_3]/[sym\text{-DMU}]$ = 0.50 (a,c) and 0.75 (b,d) at 60 MHz (a,b) and 100 MHz (c,d).

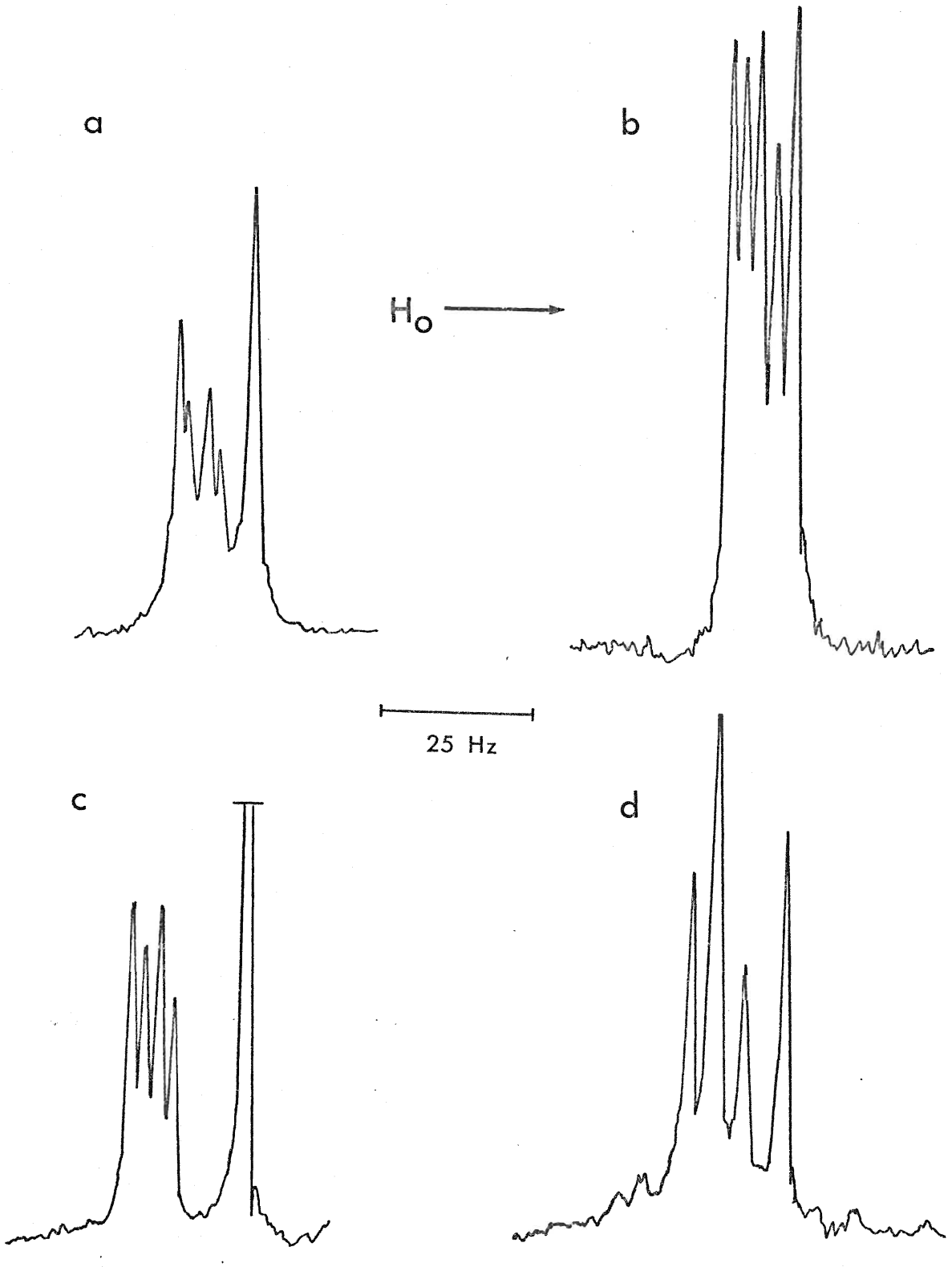
a
b
H_o
25 Hz
c
d

sym-DEU and *unsym*-DEU, hindered rotation effects were most clearly evident in the methyl signals. At -20°, both ureas gave a set of three overlapping methyl triplets (Table XII). The two low field triplets corresponded to the BF_3 adduct. The overlapping triplets could not be sufficiently resolved on the 60 MHz instrument for integration.

(B) DONOR SITE AND ISOMER POPULATIONS

Assignments of the *cis* and *trans* alkyl groups are based on similar assignments for the amides (81) and their BF_3 adducts (Chapter IV); the high field absorption is assigned to the alkyl group *cis* to the oxygen and the low field absorption is assigned to the alkyl group *trans* to the oxygen.

The observation of equal isomer populations in the case of *unsym*-DMU is consistent with two sterically equivalent methyl groups undergoing slow rotation about the C-N bond and rules out the possibility of nitrogen donation. Unequal isomer populations in *sym*-DMU also rule out the possibility of nitrogen donation. Nitrogen donation would be expected to lead to a single N-methyl environment in the fast intramolecular exchange limit (room temperature spectrum) and to at least two N-methyl environments of equal populations in the slow exchange limit (-20° spectrum). A third possibility in the slow exchange limit would allow for hindered rotation about the C-N bond of the uncomplexed $-NHCH_3$ group, giving rise to a third magnetic environment.

The observation of hindered rotation and unequal isomer populations in *sym*-DMU·BF_3 suggests that in oxygen coordinated structures *trans* methyl groups are sterically favored. Four possible structures can be drawn (Structures IVa-d).

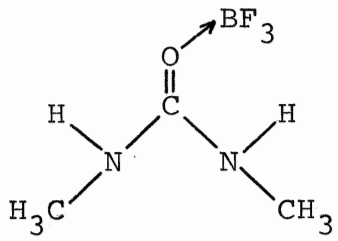

trans-trans 61%

IVa

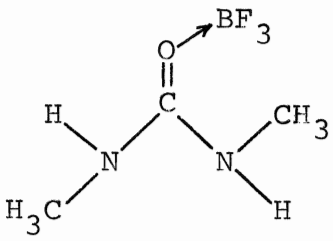

cis-trans 39%

IVb

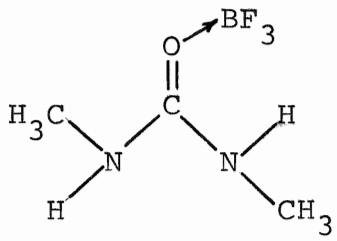

IVc

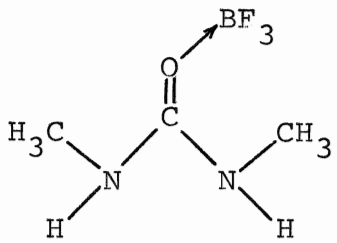

cis-cis 0%

IVd

The *cis-cis* case (Structure IVd) can be eliminated because it would be expected to suffer from severe N-methyl - BF_3 (and N-methyl - N-methyl) steric interactions. Rapid equilibration between the two *cis-trans* structures (IVb and IVc) could

account for the observation of only a single N-methyl doublet at higher field, while the *trans-trans* case would be expected to absorb at lower field.

The importance of steric effects in determining relative *cis-trans* isomer populations in amide structures is seen in the case of N-alkyl formamides. When the formyl hydrogen of an N-alkyl formamide is replaced by an alkyl group, steric interaction between the alkyl group and the N-alkyl group leads to predominance of the *cis* isomer (81). The observation of a higher *trans-trans* isomer population in a case where the *cis* configuration would be expected to predominate suggests a higher degree of steric interaction between BF_3 on oxygen and the methyl group than between the $-NHCH_3$ group and the methyl group (Structure IV). This explanation is consistent with the observed increase in the amount of the *trans* isomer of N-*t*-butylformamide from 18% in dilute benzene solution to 63% in sulfuric acid solution. In this case protonation of the carbonyl oxygen atom increases its effective size and leads to increased steric interaction between the carbonyl oxygen and the *t*-butyl group.

(C) SUMMARY

The complex nature of the spectra arise from a number of possible isomers (*e.g.*, Structures IVa-d). Although no single piece of evidence conclusively proves oxygen donation, all of the data in the TMU case (Chapter IV) and in the case of the dialkylureas, when taken together, present a very strong case

for oxygen donation. Therefore, in succeeding Chapters, oxygen is tacitly assumed to be the donor site in ureas.

CHAPTER VI

MIXED BORON TRIHALIDE-TETRAMETHYLUREA ADDUCT SYSTEMS; DIFLUOROBORON CATIONS

INTRODUCTION

There are many examples of four-coordinated bis(amine)-dihydroboron and bis(amine)dichloroboron cations in the literature (93), but few difluoroboron cations are known. This work describes the characterization of bis(tetramethylurea)-difluoroboron, $(TMU)_2 \cdot BF_2^+$ and related cations. Due to the current interest in the adducts of mixed boron trihalides (39,40), the fluorine-chlorine-containing boron trihalide adducts of TMU have been investigated in some detail and shown to be a convenient source of $(TMU)_2 \cdot BF_2^+$ and the mixed fluorochloroborate ions.

RESULTS

(A) $(TMU)_2 \cdot BF_2^+ BF_4^-$

The ^{19}F spectra of CH_2Cl_2 solutions of $TMU \cdot BF_3$ (second preparative method, Chapter II) showed peaks to high field and to low field of the $TMU \cdot BF_3$ peak. The new signals were broad, comprising 5.0% of the total fluorine intensity, and

integrated in the ratio (low field peak)/(high field peak) = 1:2. The ^1H spectrum showed an additional peak just to low field of $TMU \cdot BF_3$ having an intensity that was 4.5% of the total methyl proton intensity. Unlike the methyl signal observed for $TMU \cdot H^+$, this signal did not undergo exchange averaging in the presence of free TMU (Chapter IV). The new signals have been assigned to $(TMU)_2 \cdot BF_2^+$, low field ^{19}F peak and BF_4^-, high field ^{19}F peak (Table XIII).

(B) MIXED BORON TRIHALIDE - TMU ADDUCT SYSTEMS

(i) ^1H NMR Spectra

Methylene chloride solutions containing $TMU \cdot BF_3$ (first preparative method, Chapter II) and $TMU \cdot BCl_3$ in a molar ratio of $TMU \cdot BF_3/TMU \cdot BCl_3 = 1.74$ were prepared. The $TMU \cdot BCl_3$ adduct was only moderately soluble in CH_2Cl_2, but dissolved over a period of several minutes in the presence of $TMU \cdot BF_3$. Halogen redistribution occurred rapidly at room temperature, giving a series of four closely spaced peaks in the ^1H spectrum (Figure 13a). Upon cooling to 21^o or addition of 5 mole % TMU, a fifth peak appeared in the spectrum (Figure 13b and c). Chemical shifts and assignments are given in Table XIII. Successive additions of TMU resulted in a decrease in the intensity of the $TMU \cdot BF_2Cl$ peak and an increase in the intensity of the $(TMU)_2 \cdot BF_2^+$ peak (Figure 13c-b). A separate TMU peak of variable chemical shift was observed to high field as well as a small dependence of the relative adduct chemical shifts on solvent composition.

Table XIII

^{1}H, ^{19}F, and ^{11}B NMR Parameters for the Binary F-Cl Containing Mixed $TMU \cdot BX_3$ Adduct Systems and Difluoroboron Cations

Adduct/Ion	Chemical Shifts (ppm)			^{11}B-^{19}F Coupling Constant (Hz)
	^{1}H (δ)	^{19}F	^{11}B	
$TMU \cdot BF_3 + TMU$ [a]				
BF_4^-	-	151.9	-	-*
$TMU \cdot BF_3$	3.02	149.2	18.9	-*
$(TMU)_2 \cdot BF_2^+$	3.09	146.1	-	-*
$TMU \cdot BF_3/TMU \cdot BCl_3$ [b]				
$TMU \cdot BF_3$	3.02	149.2	18.9	-*
$(TMU)_2 \cdot BF_2^+$	3.08	146.0	19	12.5
$TMU \cdot BF_2Cl$	3.06	124.3	15.9	28.2
$TMU \cdot BFCl_2$	3.10	105.7	12.9	58.5
$TMU \cdot BCl_3$	3.12	-	10.8	-
BF_3Cl^-	-	126.1	-	24.3
$BF_2Cl_2^-$	-	105.5	-	59.0
$BFCl_3^-$	-	95.4	-	80.1
$TMU \cdot BF_3/TMU \cdot BCl_3$ + DMAC				
$(TMU)_2 \cdot BF_2^+$	-	146.1	-	-*
$(DMAC)(TMU) \cdot BF_2^+$	-	144.8	-	-*
$(DMAC)_2 \cdot BF_2^+$	-	144.2	-	-*

[a] second preparative method for $TMU \cdot BF_3$, Chapter II.

[b] ^{1}H chemical shifts are for a molar ratio $TMU \cdot BF_3/TMU \cdot BCl_3$ = 1.74 and ~1 M in complexed TMU at 21°.

* not visible under these conditions.

Figure 13. Proton spectra (60 MHz) of $TMU \cdot BF_3$/$TMU \cdot BCl_3$ in the molar ratio 1.74:1.00 (a) at 37°; (b) at 21°; and after addition of (c) 5 mole % TMU; (d) 20 mole % TMU; (e) 30 mole % TMU; (f) 50 mole % TMU.

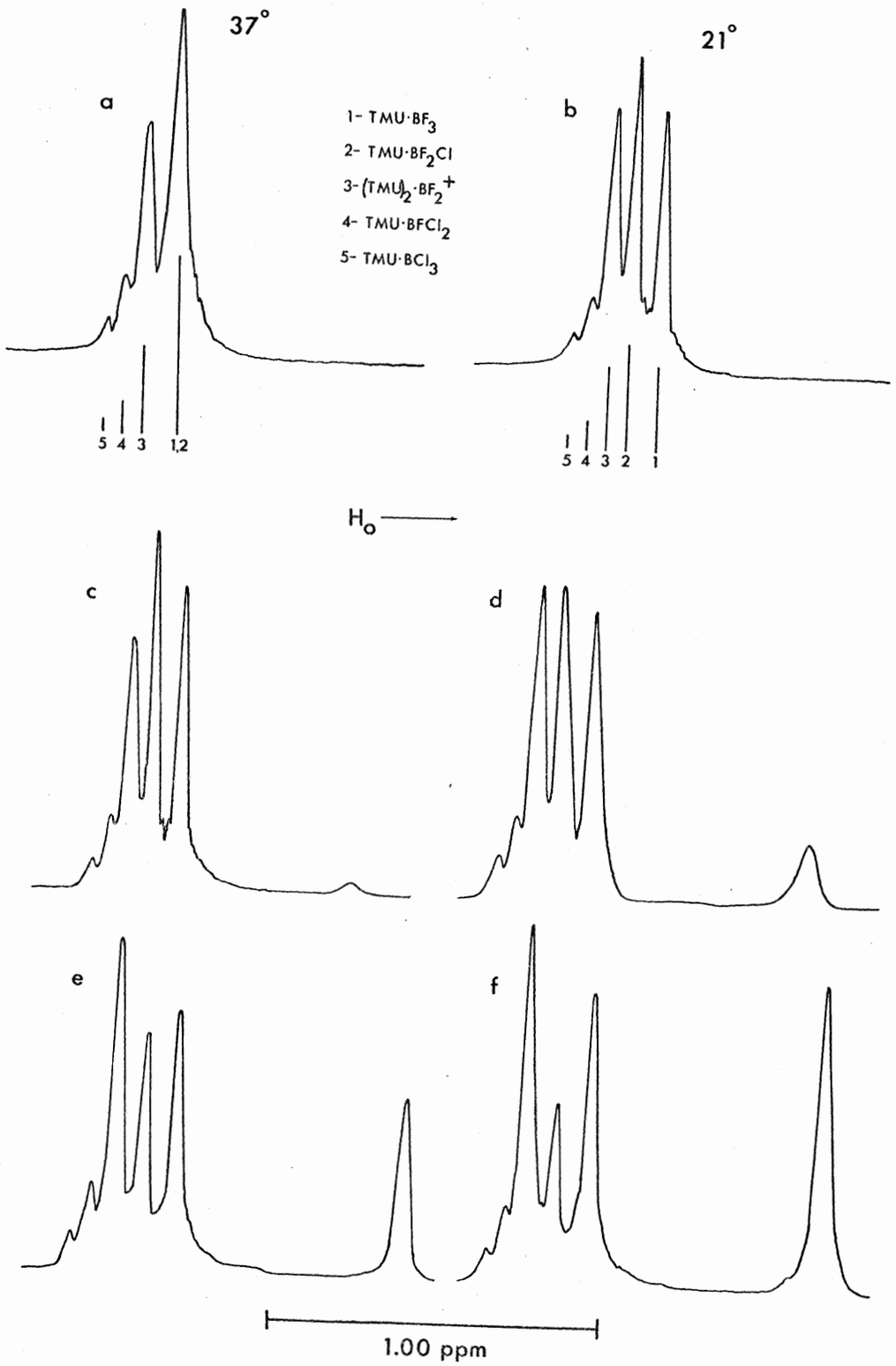
37°
21°
a
b
1- TMU·BF3
2- TMU·BF2Cl
3-(TMU)2·BF2+
4- TMU·BFCl2
5- TMU·BCl3
5 4 3 1,2
5 4 3 2 1
Ho
c
d
e
f
1.00 ppm

Halogen redistribution did not occur when a solution of $TMU \cdot BF_3$ was added to a solution of $TMU \cdot BCl_3$ containing excess TMU or vice versa.

(ii) ^{19}F NMR Spectra

The ^{19}F spectra of the solutions were recorded in the presence of varying proportions of TMU (Figure 14a and b, and Table XIII. Signals corresponding to a broadened $TMU \cdot BF_3$ peak ($w_{\frac{1}{2}}$ = 15.4 Hz); and $TMU \cdot BF_2Cl$, $TMU \cdot BFCl_2$, and $(TMU)_2 \cdot BF_2^+$ peaks having 1:1:1:1 quartet fine structures were observed in the absence of free TMU (Figure 14c). Addition of a small excess of TMU (5 mole %) resulted in a sharpened $TMU \cdot BF_3$ peak ($w_{\frac{1}{2}}$ = 6.1 Hz) and the appearance of BF_3Cl^- and $BF_2Cl_2^-$ quartets (Figure 14b). The presence of BX_4^- ions was confirmed by addition of a solution of the mixed fluorochloroborates to a similar sample and observing the resulting ^{19}F spectrum. No fluorochloroborate ions were observed in the presence of a large excess of TMU, while a large increase in the $(TMU)_2 \cdot BF_2^+$ intensity and a corresponding decrease in the $TMU \cdot BF_2Cl$ intensity were noted (Figure 14a). The results of a quantitative titration of a sample with free TMU are given in Figure 15. Corresponding molar quantities of BF_3Cl^-, $BF_2Cl_2^-$, $BFCl_3^-$, and $TMU \cdot BFCl_2$ are not given in Figure 15 owing to their low initial concentrations and overlap of $BF_2Cl_2^-$ and $TMU \cdot BFCl_2$ quartets. Throughout the titration the fluorochloroborate signals decreased in intensity and finally vanished.

Figure 14. Fluorine-19 spectra (56.4 MHz) of $TMU \cdot BF_3/TMU \cdot BCl_3$ in the molar ratio 1.74:1.00 (a) after addition of 56 mole % TMU; (b) after addition of 10 mole % TMU; (c) in the absence of excess TMU. The peak assignments are: $TMU \cdot BF_3$ (1), $(TMU)_2 \cdot BF_2^+$ (2), BF_3Cl^- (3), $TMU \cdot BF_2Cl$ (4), $TMU \cdot BFCl_2$ (5), $BF_2Cl_2^-$ (6), and $BFCl_3^-$ (7).

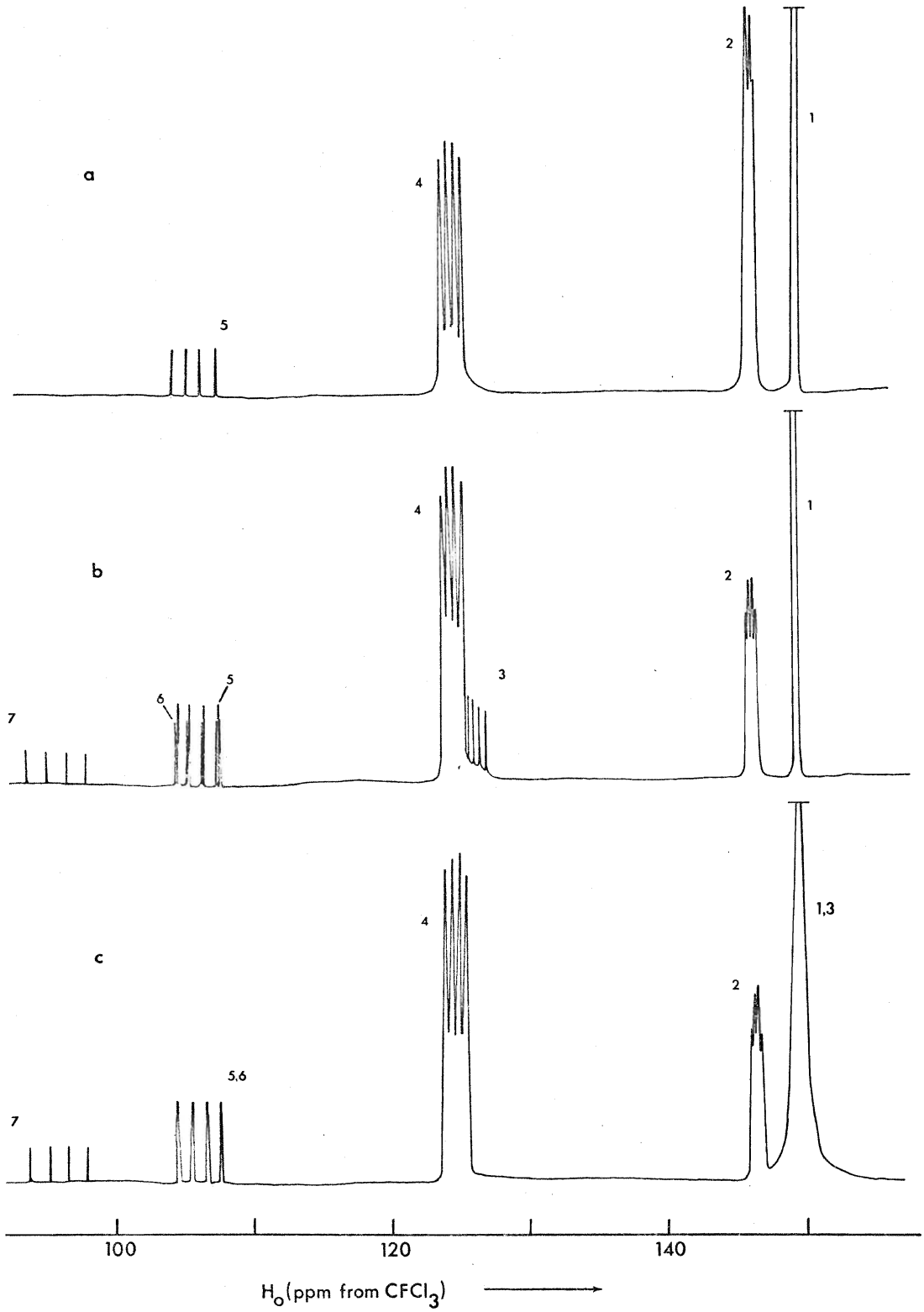
a
2
1
4
5
b
4
1
2
3
6
5
7
c
1,3
4
2
5,6
7
100
120
140
H_o(ppm from $CFCl_3$)

Figure 15. Titration of TMU·BF_2Cl (6.40×10^{-4} mole) with TMU; monitored by ^{19}F NMR.

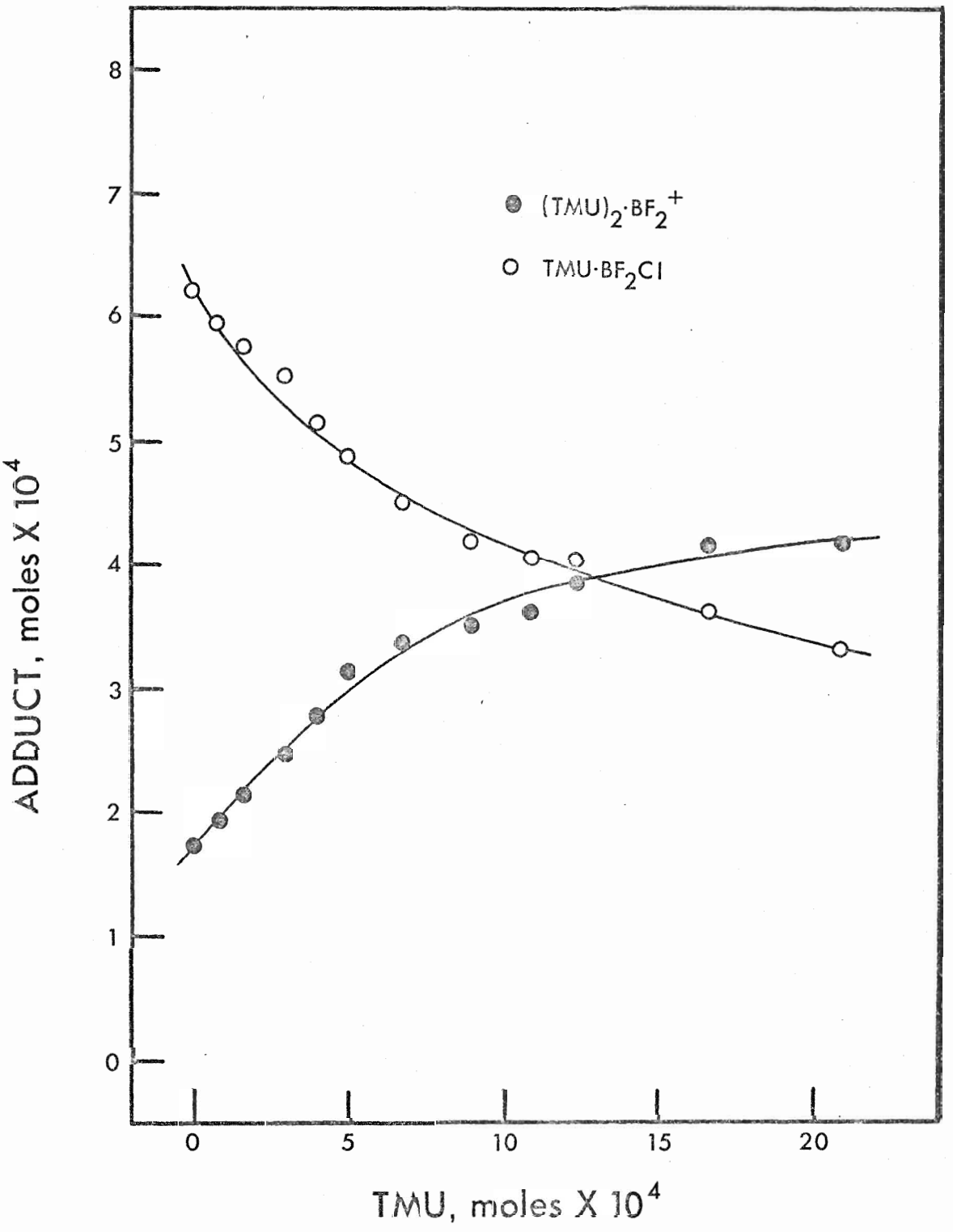
8
7
6
5
4
3
2
1
0
ADDUCT, moles X 10^4
(TMU)2·BF2+
TMU·BF2Cl
0
5
10
15
20
TMU, moles X 10^4

(iii) ^{11}B NMR Spectra

The ^{11}B spectra of $TMU \cdot BF_3/TMU \cdot BCl_3$ solutions were recorded. Chemical shift assignments (Table XIII) were made by skewing relative $TMU \cdot BF_3$ and $TMU \cdot BCl_3$ concentrations so that the 1:2:1 $TMU \cdot BF_2Cl$ triplet and the $TMU \cdot BFCl_2$ doublet could be observed (Figure 16a and b). In some cases, additional overlapping peaks of low intensity that could be assigned to the mixed fluorochloroborate ions were also observed. The addition of a large excess of TMU to such a solution resulted in a decrease in the intensity of the $TMU \cdot BF_2Cl$ triplet and an increase in the intensity of the $(TMU)_2 \cdot BF_2^+$ signal which was coincident with that of $TMU \cdot BF_3$ (Figure 16b and c).

(C) $(TMU)(DMAC) \cdot BF_2^+$ AND $(DMAC)_2 \cdot BF_2^+$ IONS

A quantity of dimethylacetamide (DMAC; ~25 mole %) was added to an equimolar solution of $TMU \cdot BF_3$ and $TMU \cdot BCl_3$. Signals corresponding to $TMU \cdot BF_3$, $DMAC \cdot BF_3$, $(TMU)_2 \cdot BF_2^+$, the mixed fluorochloroborate ions, and badly overlapping quartets arising from the BF_2Cl and $BFCl_2$ adducts were observed in the ^{19}F spectrum. In addition, two new peaks appeared in the $(TMU)_2 \cdot BF_2^+$ region and were assigned to $(TMU)(DMAC) \cdot BF_2^+$ and $(DMAC)_2 \cdot BF_2^+$ (Table XIII). No B-F couplings were observed for the difluoroboron cations in this system.

(D) CHLORIDE ION AS A LEWIS BASE

Solid $Et_4N^+Cl^-$ was added in equimolar amounts to solutions of the mixed fluorine-chlorine containing boron trihalide ad-

Figure 16. Boron-11 spectra (25.1 MHz) of $TMU \cdot BF_3$/$TMU \cdot BCl_3$ in the molar ratio (a) 3:1; (b) 1:1; (c) 1:1 after the addition of ~50 mole % excess TMU. The peak assignments are: $TMU \cdot BF_3/(TMU)_2 \cdot BF_2^+$ (1,2), $TMU \cdot BF_2Cl$ (3), $TMU \cdot BFCl_2$ (4), $TMU \cdot BCl_3$ (5), and external $(CH_3O)_3B$ (6).

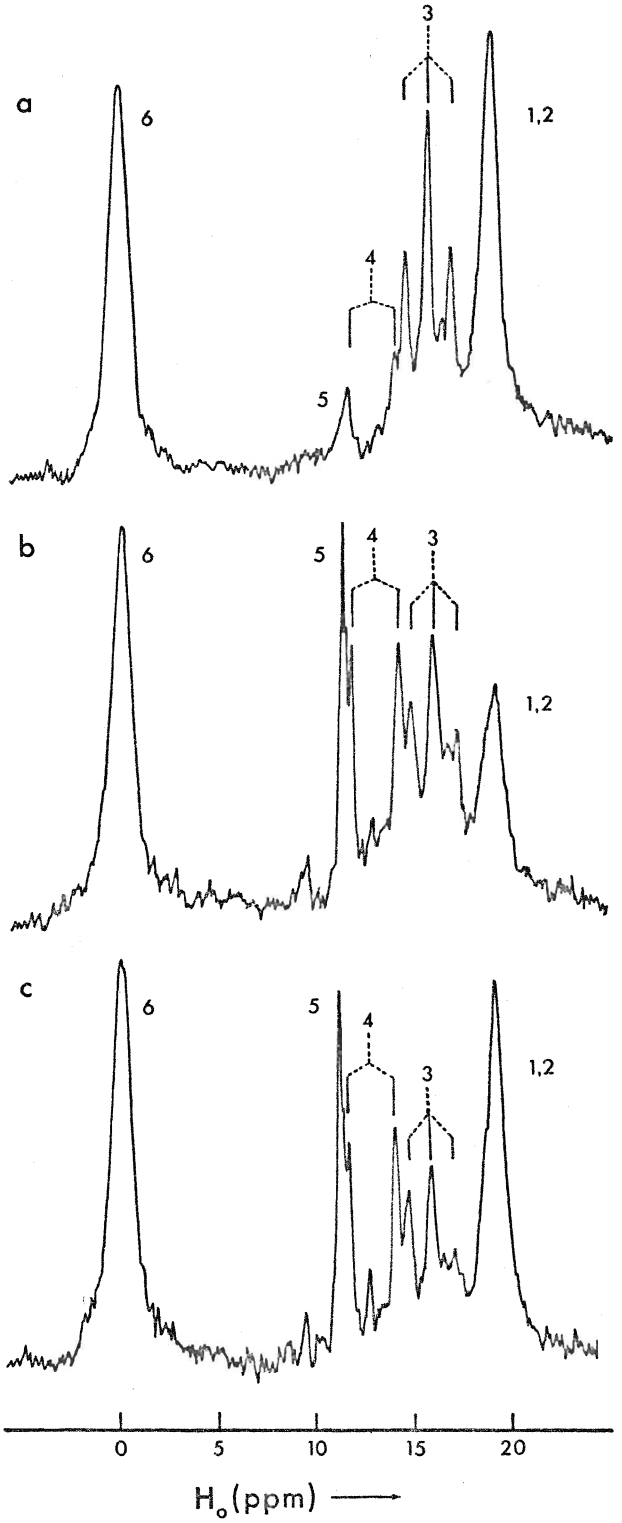
a
6
3
1,2
4
5
b
6
5
4
3
1,2
c
6
5
4
3
1,2
0
5
10
15
20
H_o(ppm) ⟶

ducts of TMU, TMU·BF_3, DMAC·BF_3, and $(CH_3)_3N·BF_3$ (donated by J. M. Miller). Near quantitative displacement of TMU from its mixed adducts and BF_3 adduct took place while no free DMAC or $(CH_3)_3N$ could be detected in their respective ^1H spectra. The ^{19}F spectrum of TMU·BF_3 in the presence of chloride ion showed only a small TMU·BF_3 peak and an intense BF_4^- quartet at 151.0 ppm, $J_{^{11}B-^{19}F}$ = 0.9 Hz.

DISCUSSION

(A) FLUORINE CHEMICAL SHIFT AND BORON-FLUORINE COUPLING CONSTANT TRENDS

(i) Assignments

Plots of ^{19}F chemical shifts versus B-F coupling constants (Figure 17) have been used to arrive at the ^{19}F assignments for the mixed boron trihalide adducts of TMU in Table XIII. In addition, the data for a number of other mixed adduct systems have been included in Figure 17 and in Table XIV (cases in which B-F coupling constants are not available).

Table XIV

^{19}F Chemical Shifts for Some Mixed Boron Trihalide Adducts[a]

	^{19}F Chemical Shift (ppm)		
BX_3	Diethylether	Acetone	Acetonitrile
BF_3	153.7	148.2	142.3
BF_2Cl	129.9	125.6	125.1
$BFCl_3$	116.0	110.7	119.1

[a] reference (85).

Figure 17. Variation of ^{19}F chemical shifts and ^{11}B-^{19}F coupling constants of some BX_3 donor-acceptor complexes where X = F and Cl, Br (85, and this work) and some difluoroboron compounds (94,95).

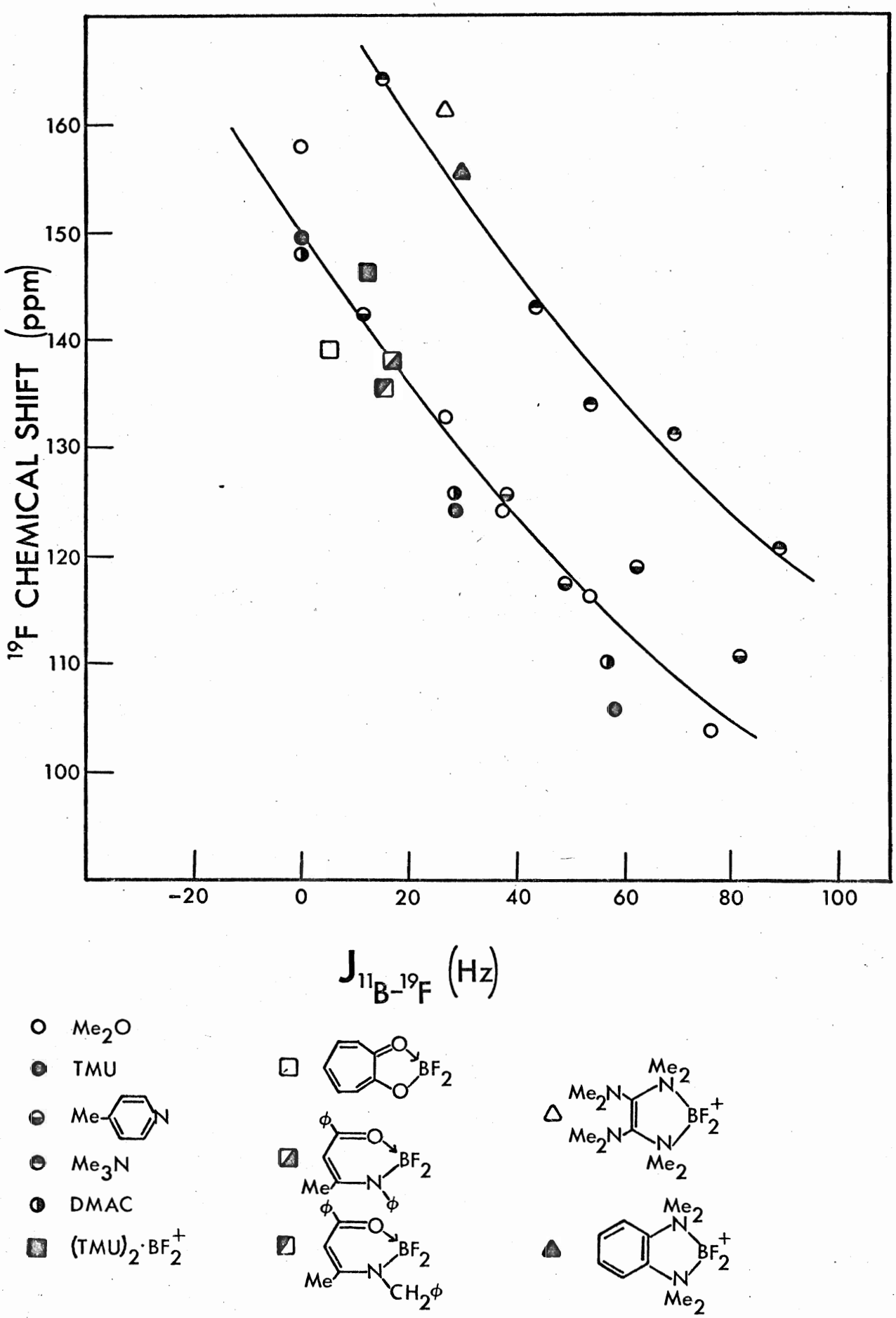
160
150
140
130
120
110
100
^{19}F CHEMICAL SHIFT (ppm)
-20
0
20
40
60
80
100
$J_{^{11}B-^{19}F}$ (Hz)
Me_2O
TMU
Me-
Me_3N
DMAC
$(TMU)_2 \cdot BF_2^+$
BF_2
Me_2N
Me_2
BF_2^+
Me
$CH_2\phi$

The same arguments used to explain trends among BX_4^- and BX_3 species (Chapter III) apply to the boron trihalide adducts.

A similar approach has proven useful when making assignments involving difluoroboron species (Figure 17). The donor atom of the second coordinating group in the cases considered here would be expected to possess π bonding to boron that is intermediate between that with fluorine and that with chlorine, giving a B-F coupling constant and chemical shift that are intermediate between those of $D \cdot BF_3$ and $D \cdot BF_2Cl$.

Assignments of ^1H, ^{19}F, and ^{11}B resonances of $TMU \cdot BF_2Cl$ and $(TMU)_2 \cdot BF_2^+$ were confirmed by changes in their relative peak intensities upon addition of excess TMU and are discussed later in this Chapter. Other ^1H chemical shift assignments were based on the expected Lewis acid strengths increasing in the order $BF_3 < BF_2Cl < BFCl_2 < BCl_3$ (39,40). The assignments were confirmed from the chemical shifts of the individual $TMU \cdot BF_3$ and $TMU \cdot BCl_3$ adducts and by noting that in samples containing a large excess of $TMU \cdot BF_3$ over $TMU \cdot BCl_3$, the signals $(TMU)_2 \cdot BF_2^+$ and $TMU \cdot BF_2Cl$ predominated. On the basis of the ^1H assignments (Table XIII), the moiety, $TMU \cdot BF_2^+$, behaves as if it has a Lewis acid strength intermediate between that of BF_2Cl and $BFCl_2$. Boron-11 assignments of $TMU \cdot BF_2Cl$ and $TMU \cdot BFCl_2$ were confirmed by multiplet fine structures and comparison of the measured B-F couplings with those measured in the ^{19}F spectra.

(ii) Multiple Bond Effect

In general, donor-acceptor species in which the donor atom is multiply bonded absorb at lower field and have smaller coup-

ling constants than donors in which the donor orbital is essentially sp^3 hybridized. The amine adducts form a reasonably distinct region of their own in these plots, while donors containing multiply-bonded donor sites as structurally different as DMAC, TMU, 4-picoline, acetone, (1,3-diketonato)-boron difluorides, and acetonitrile lie in their own region (Figure 17 and Table XIV). If coordination of BX_3 were to occur at the nitrogen in TMU it might be expected that the chemical shift versus B-F coupling constant plot would occur in the amine region, but instead, like other carbonyl donors (Chapters IV and V), it occurs in the multiply-bonded region. The use of such plots as a criterion for establishing donor site is complicated by the fact that amine donation in tetramethylthiourea·BF_3 and tetramethylselenourea·BF_3 where nitrogen donation is proposed (Chapter VII), lead to ^{19}F chemical shifts similar to those observed for carbonyl donors.

(B) MECHANISMS

(i) $(TMU)_2 \cdot BF_2^+ BF_4^-$

Fluorine scrambling mechanisms involving the prior dissociation of the adduct to give $D \cdot BF_2^+$ and F^- are generally less likely to occur in low dielectric constant solvents than breaking of the weaker donor-acceptor bond. The observation of $(TMU)_2 \cdot BF_2^+ BF_4^-$ when TMU·BF_3 is prepared in TMU, a solvent of high dielectric constant, suggests a nucleophilic displacement leading to fluoride ion (X,Y = F)

$$
\left.
\begin{array}{ll}
 & TMU\cdot BX_2Y \rightleftharpoons TMU\cdot BX_2^{+} + Y^{-} \\
S_N1 & TMU + TMU\cdot BX_2^{+} \rightleftharpoons (TMU)_2\cdot BX_2^{+} \\
\text{or} & \\
 & TMU + TMU\cdot BX_2Y \rightleftharpoons \left[\begin{array}{c} \\ C=O\text{----}B\text{----}Y \\ \\ X \quad X \end{array}\right] \\
S_N2 & \rightleftharpoons (TMU)_2\cdot BX_2^{+} + Y^{-}
\end{array}
\right] \quad (31)
$$

followed by nucleophilic attack of fluoride ion on $TMU\cdot BF_3$

$$
\left.
\begin{array}{ll}
 & TMU\cdot BX_3 \rightleftharpoons TMU + BX_3 \\
S_N1 & BX_3 + Y^{-} \rightleftharpoons BX_3Y^{-} \\
\text{or} & \\
 & Y^{-} + TMU\cdot BX_3 \rightleftharpoons \left[\begin{array}{c} X \\ | \\ Y\text{----}B\text{----}O=C \\ X \quad X \end{array}\right]^{-} \\
S_N2 & \rightleftharpoons TMU + BX_3Y^{-}
\end{array}
\right] \quad (32)
$$

Rapid equilibration of $TMU\cdot BF_3$ with the ionic structure $(TMU)_2\cdot BF_2^{+}BF_4^{-}$ could account for fluorine scrambling in low dielectric constant solvents such as CH_2Cl_2. A number of possible mechanisms exist for such a process, though those not involving free fluoride ion are favored since no ionic fluoride is known which is soluble in CH_2Cl_2 (42). One possibility is the prior dissociation of the adduct followed by fluorine ex-

change

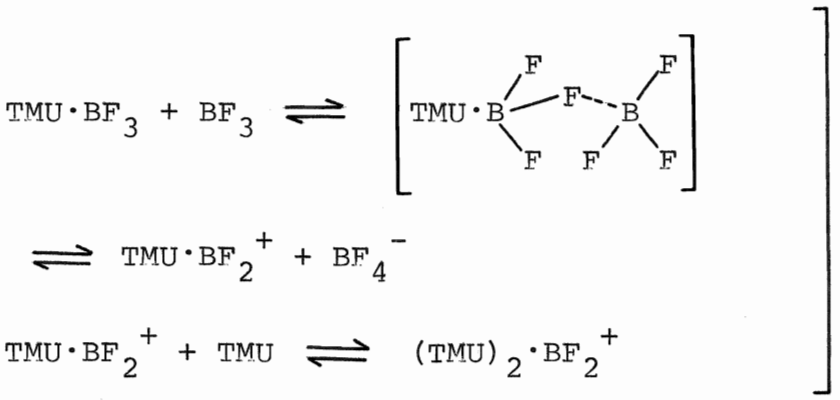

(33)

Alternatively, this reaction might occur through a four-center transition state

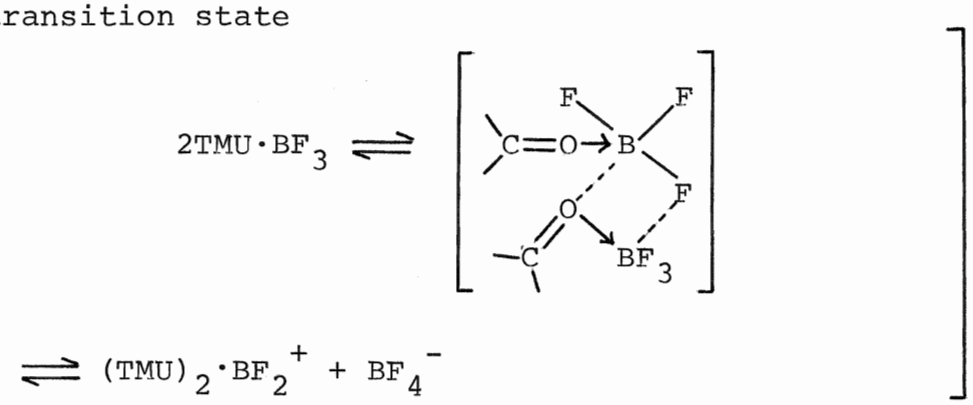

(34)

Wiberg and Buchler (95) have proposed a mechanism for the formation of Structure V having features in common with the above mechanisms.

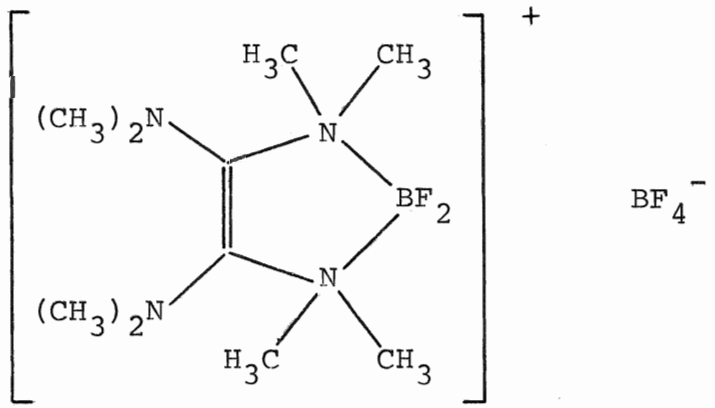

V

(ii) $TMU \cdot BF_3$ - $TMU \cdot BCl_3$ Systems

Halogen redistribution in $TMU \cdot BF_3$ - $TMU \cdot BCl_3$ systems occurs readily at room temperature in the absence of excess Lewis acid, but does not occur in the presence of excess base. A prior dissociation of $TMU \cdot BX_3$ to give the free acid and base could lead to halogen scrambling *via* the halogen-bridged intermediates discussed above and in Chapters I and III. Clearly, the ease of halogen exchange in $TMU \cdot BX_3$ (X = F, Cl) is intermediate between that of BX_4^- ($BX_3 \cdot Cl^-$) which exchanges readily at elevated temperatures (Chapter III) and $(CH_3)_2O \cdot BX_3$ (39) which exchanges readily in the presence of excess base at room temperature. The relative rates of halogen exchange increase in the series $(CH_3)_3N \cdot BX_3$ (40) < $BX_3 \cdot Cl^-$ < $TMU \cdot BX_3$ << $(CH_3)_2O \cdot BX_3$ (39), in agreement with the relative strengths of the donor-acceptor bonds which increase in the order $(CH_3)_2O$ << TMU < Cl^- < DMAC < $(CH_3)_3N$. In the present work, chloride ion has been shown to displace TMU from its fluorochloro-adducts, but not DMAC or $(CH_3)_3N$ from their BF_3 adducts. Thus, the ease of breaking and re-forming of the donor-acceptor bond appears to be the most important single factor when considering halogen redistribution rates among a series of boron trihalide adducts (*c.f.* Chapter III).

The presence of appreciable amounts of $(TMU)_2 \cdot BF_2^+$ in the mixed fluorine-chlorine boron trihalide adducts suggests dissociation of $TMU \cdot BX_3$ followed by nucleophilic attack to give chloride ion, a far better leaving group than fluoride ion in

CH_2Cl_2 (Equations (31) and (32) where X = F and Y = Cl). Trifluorochloroborate ion (Equation (32)) may then undergo halogen redistribution to give the remaining fluorochloroborates (Chapter III).

The stoichiometry of Equation (31) and ^{19}F assignments of $TMU \cdot BF_2Cl$ and $(TMU)_2 \cdot BF_2^+$ are confirmed by the titration curves for $(TMU)_2 \cdot BF_2^+$ and $TMU \cdot BF_2Cl$ (Figure 15). The quantity of $TMU \cdot BF_2Cl$ is found to decrease at the same rate that $(TMU)_2 \cdot BF_2^+$ increases, giving an equivalence point corresponding to the uptake of one mole of TMU per mole of $TMU \cdot BF_2Cl$. Similarly, the addition of excess TMU is shown to diminish the $TMU \cdot BF_2Cl$ concentration and increase the $(TMU)_2 \cdot BF_2^+$ concentration in the ^1H and ^{11}B spectra (Figures 13 and 16, respectively).

Fluorine exchange among $TMU \cdot BF_3$, BF_3Cl^-, and $BF_2Cl_2^-$ is slowed sufficiently in the presence of a small excess of free TMU (Figure 14b and c) to give individual quartets for BF_3Cl^- and $BF_2Cl_2^-$ and a sharpened $TMU \cdot BF_3$ peak. Dissociation of the weak $TMU \cdot BF_3$ bond to give BF_3, which then may exchange with the more labile BF_3Cl^- and $BF_2Cl_2^-$ ions (Chapter III), could account for rapid fluorine exchange in these systems. Fluorine exchange among stronger donor-acceptor species; $(TMU)_2 \cdot BF_2^+$, $TMU \cdot BF_2Cl$, and $TMU \cdot BFCl_2$; and the less labile $BFCl_3^-$ ion is considerably slower.

As noted in Chapter III, chloride ion is expected to be a good leaving group in the fluorochloroborates. Thus, BX_3Cl^- is seen to decrease and vanish in the presence of excess TMU (Figure 14), suggesting nucleophilic attack by TMU on $BX_3 \cdot Cl^-$

to give $TMU \cdot BX_3$ and chloride ion.

The appearance of two new peaks in addition to the $(TMU)_2 \cdot BF_2^+$ peak in the $D_2 \cdot BF_2^+$ region of the ^{19}F spectrum upon addition of DMAC to $TMU \cdot BF_3$/$TMU \cdot BCl_3$ solutions (Table XIII) provides further confirmation of the "$D_2 \cdot BF_2^+$ structure." Dimethylacetamide is a stronger Lewis base than TMU (Chapter IV) and may effectively serve to displace TMU from its neutral adducts and cation, giving $(TMU)(DMAC) \cdot BF_2^+$ and $(DMAC)_2 \cdot BF_2^+$.

CHAPTER VII

BORON TRIFLUORIDE ADDUCTS OF TETRAMETHYLTHIOUREA, TETRAMETHYLSELENOUREA, AND TETRAMETHYLGUANIDINE

INTRODUCTION

The donor properties of the C=S, C=Se, and C=NH analogs of TMU have been investigated in this Chapter. According to Pearson's hard-soft acid-base (HSAB) theory (96) it should be possible to observe nitrogen donation in related thiourea and selenourea structures. Boron trifluoride is a hard acid and would be expected to bind to the hard base (nitrogen) site in these thiourea and selenourea structures. This work indicates that contrary to Greenwood and Robinson's (21) conclusions, sulfur (selenium) rather than nitrogen is the preferred donor site in the 1:1 adduct and that simple HSAB theory alone cannot account for donor site preferences in systems in which a measured degree of resonance stabilization of the adduct is possible (*c.f.* Structure I). The observation of sulfur and selenium donation in these structures lends additional credence to the view that oxygen is the donor site in ureas.

Donor properties of the guanidine structure toward BF_3

are expected to be similar to those of TMU with the added possibility of the guanidine structure behaving as a strong protonic acid.

RESULTS AND DISCUSSION

(A) TETRAMETHYLTHIOUREA AND TETRAMETHYLSELENOUREA

(i) ^{1}H NMR Spectra

Room temperature proton spectra of CH_2Cl_2 solutions of tetramethylthiourea (TMTU) and tetramethylselenourea (TMSeU); and BF_3, in varying molar ratios, contained a single large peak and a very small peak to lower field. The chemical shifts of the major TMTU and TMSeU peaks varied linearly with the ratio $[BF_3]/[Donor]$ as the relative proportion of BF_3 was increased up to the ratio 1:1, as is shown in Figure 18. Since separate resonances were not observed for free and complexed donor in mixtures in which $[Donor] > [BF_3]$, it is evident that a rapid exchange of BF_3 occurs among donor molecules. The linearity of the plots, with a break corresponding to 1:1 proportions, shows that the high field peak corresponds to the 1:1 donor. Further slight changes in the chemical shifts beyond 1:1 proportions indicates a small degree of dissociation of the complexes. The intensity of the low field peak (TMTU, 3.30 δ; TMSeU, 3.32 δ) was found to increase markedly as relative quantities of acid/base were increased beyond 1:1 proportions. A reversible temperature dependence of the relative peak areas was also noted. At lower temperatures, the intensity of the low field peak was further enhanced, and in some

Figure 18. Variation of the TMTU (and TMSeU) ^{1}H (60 MHz) chemical shifts of the high field CH_3 peak with $[BF_3]/[Donor]$.

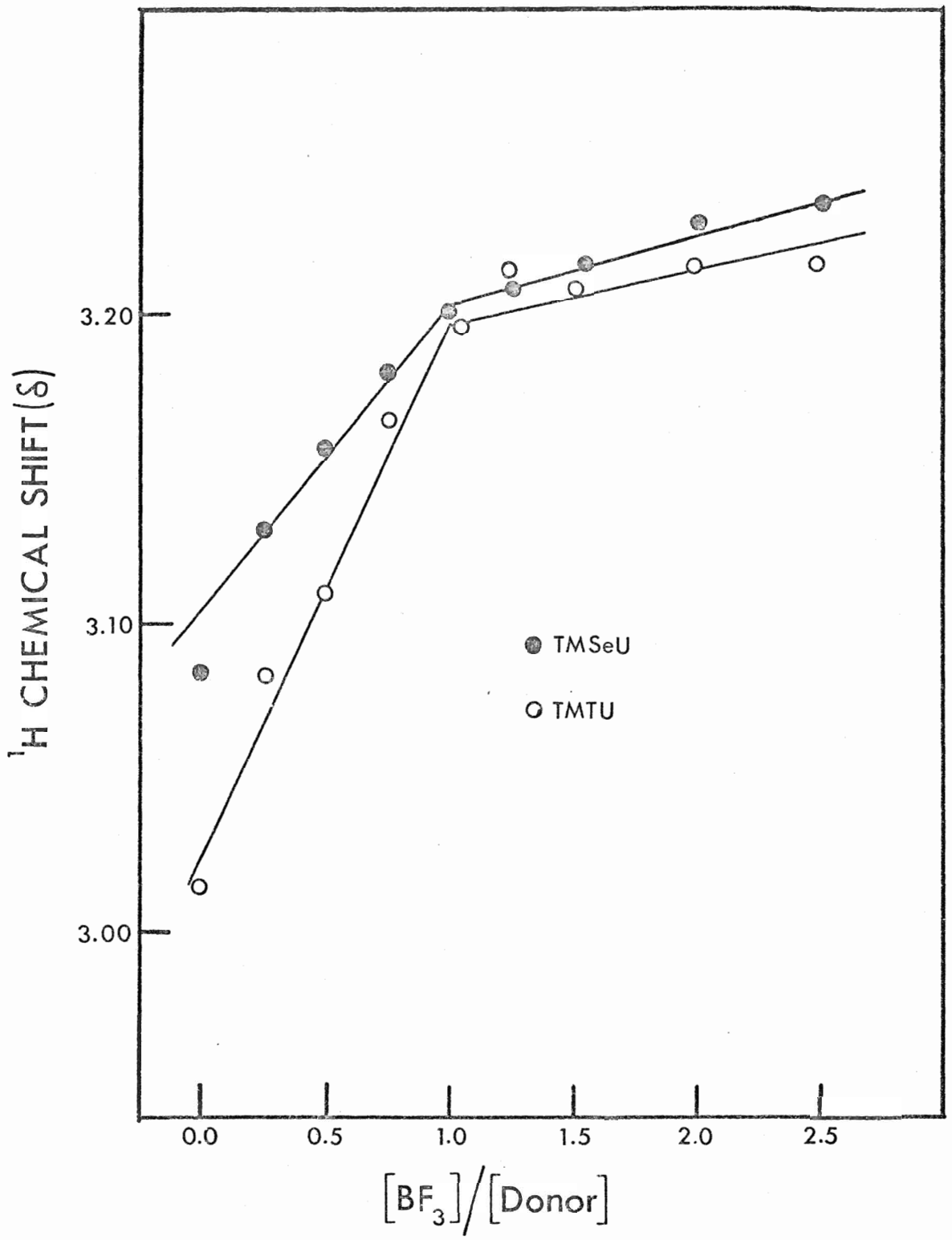
^{1}H CHEMICAL SHIFT (δ)
3.20
3.10
3.00
TMSeU
TMTU
0.0
0.5
1.0
1.5
2.0
2.5
[BF$_3$]/[Donor]

cases reached a limiting value before broadening made accurate integration of relative peak areas impossible (Figures 19 and 20). The limiting values for 1.25 and 1.50 acid/base proportions in the case of TMSeU are reached at 25% and 50%, respectively, while other acid/base proportions are tending toward higher limiting values.

The reversible nature of the temperature variation of the relative proportions of high and low field species is attributed to an equilibrium of the type

$$D \cdot BF_3 + BF_3 \rightleftharpoons D \cdot (BF_3)_2 \qquad (35)$$

Double donation appears to occur to a greater extent in TMSeU. Even at less than 1:1 acid/base proportions, TMSeU·BF_3 apparently dissociates to a sufficient extent to give, *e.g.*, 12% of the low field species at $[BF_3]/[TMSeU] = 1.00$ and -19°.

The BF_3 adducts of TMSeU also exhibited interesting color variations. Thus, solutions of TMSeU were very pale yellow and deepened in intensity up to 1:1 proportions where the pale yellow color diminished slightly as BF_3 was added. Lowering the temperature caused little color change below 1:1 acid/base proportions, but the intensity decreased with decreasing temperatures beyond 1:1 acid/base proportions. In the case of 2:1 acid/base proportions or greater, colorless solutions were obtained at -40°. In all cases, the temperature dependence of color intensity was completely reversible. This behavior parallels the changes observed in the relative ^1H peak areas and suggests that the TMSeU·$(BF_3)_2$ species is the colorless

Figure 19. Temperature dependence of the relative ^1H (60 MHz) peak areas of $TMTU \cdot BF_3$ (high field CH_3 peak) and $TMTU \cdot (BF_3)_2$ (low field CH_3 peak) for systems in which $[BF_3]/[TMTU] > 1$.

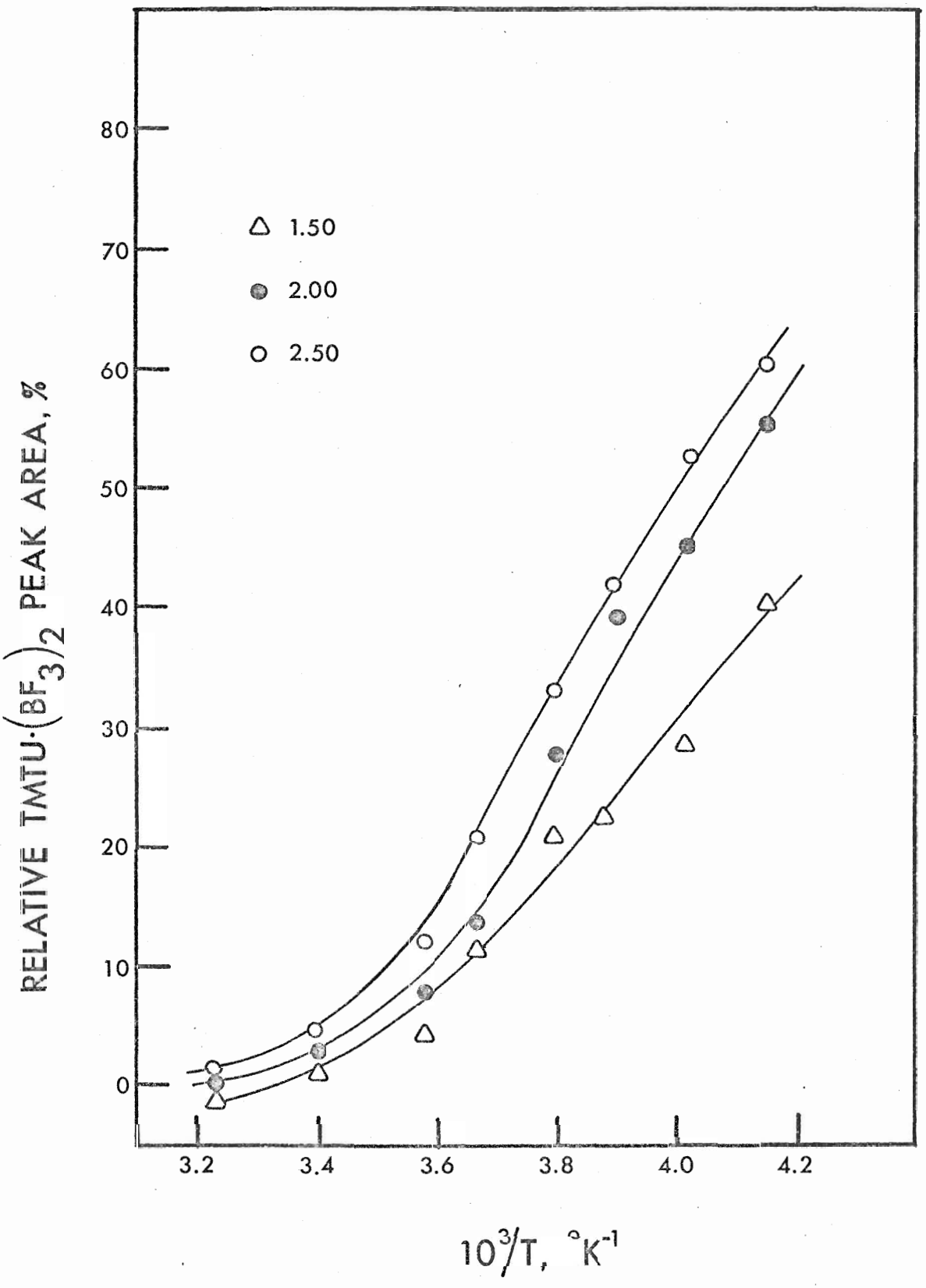
RELATIVE TMTU·(BF3)2 PEAK AREA, %
80
70
60
50
40
30
20
10
0
1.50
2.00
2.50
3.2
3.4
3.6
3.8
4.0
4.2
10³/T, °K⁻¹

Figure 20. Temperature dependence of the relative ^1H (60 MHz) peak areas of $TMSeU \cdot BF_3$ (high field CH_3 peak) and $TMSeU \cdot (BF_3)_2$ (low field CH_3 peak) for systems in which $[BF_3]/[TMSeU] > 1$.

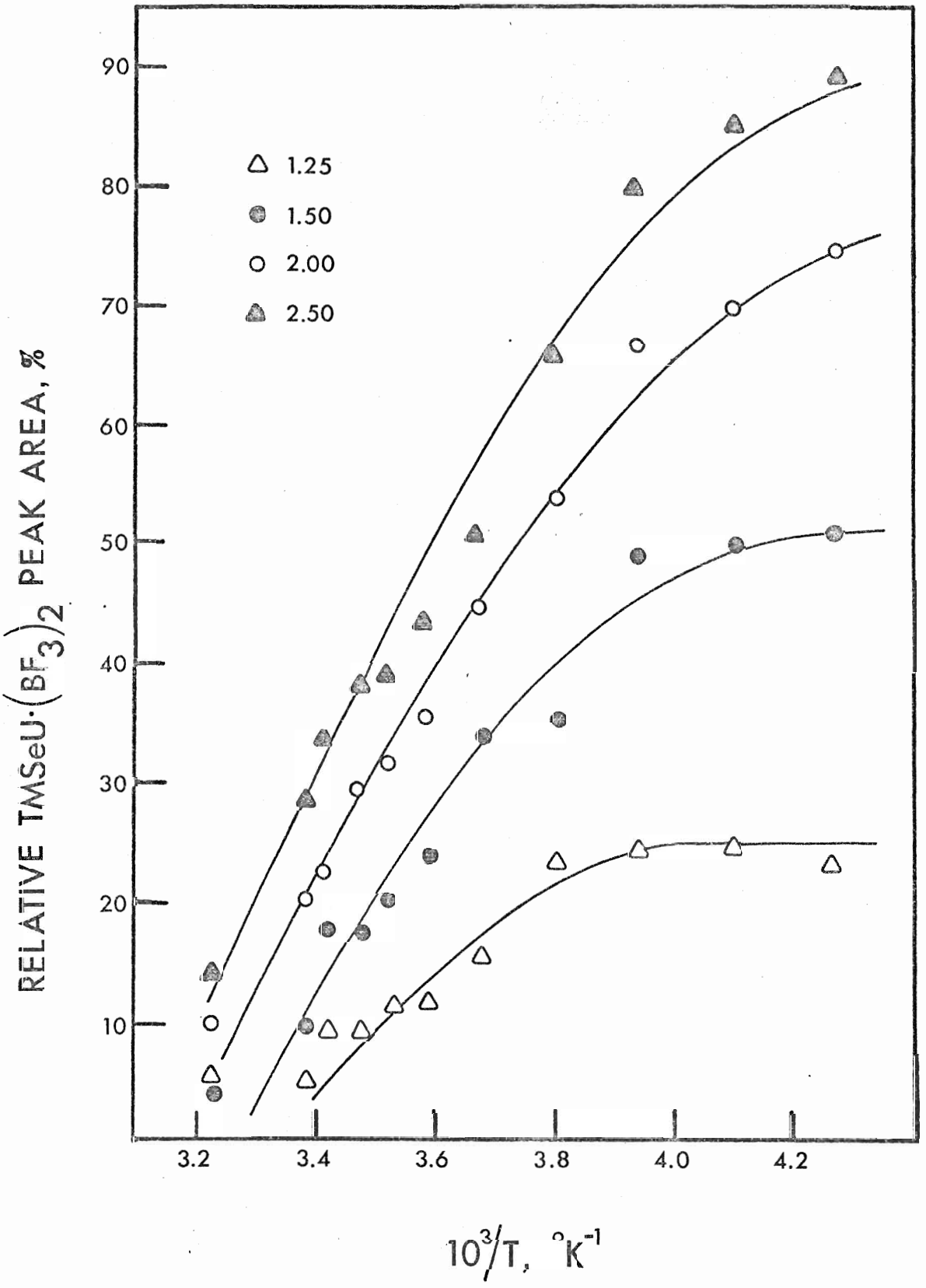
RELATIVE TMSeU·(BF3)2 PEAK AREA, %
90
80
70
60
50
40
30
20
10
1.25
1.50
2.00
2.50
3.2
3.4
3.6
3.8
4.0
4.2
10³/T, °K⁻¹

species and that TMSeU·BF_3 is the yellow species.

(ii) ^{19}F NMR Spectra

The ^{19}F spectra were complex and some of the assignments given are only tentative. At room temperature only a single exchange-averaged peak was observed in all samples. Samples in which $[Donor] > [BF_3]$ gave two peaks at -85° (sulfur compound) and -100° (selenium compound), a broadened peak at 124.4 ± 0.3 ppm (sulfur compound) or 118.0 ± 0.4 ppm (selenium compound), and a small sharp peak (~20% of the total intensity) common to both compounds at 150.8 ± 0.5 ppm. The high field peak position is reminiscent of BF_4^- (Chapters III and IV) although samples were prepared from highly purified BF_3 (Chapter II). The major low field peaks occur at too low a field to be attributed to nitrogen donation (*c.f.* Chapter VI and are assigned to BF_3 on sulfur or selenium.

In addition to the sulfur and selenium donor peaks, two new peaks appeared in the -90° spectra of both compounds past 1:1 acid/base proportions. The high field peak previously assigned to BF_3 on nitrogen (or BF_4^-) was absent (Figure 21). The new high field peak may arise from BF_3 on nitrogen and may include single nitrogen donor, double nitrogen donor, and sulfur (selenium)-nitrogen donor intensities. The weaker peak at low field may be attributed to simultaneous donation at sulfur (selenium) and nitrogen and represent BF_3 on sulfur (selenium). A reduction in electron density due to the presence of an additional BF_3 molecule could account for the low

Figure 21. Fluorine-19 spectra (56.4 MHZ) of
(a) $[BF_3]/[TMTU]$ = 1.25 and
(b) $[BF_3]/[TMSeU]$ = 1.25 at -90°.

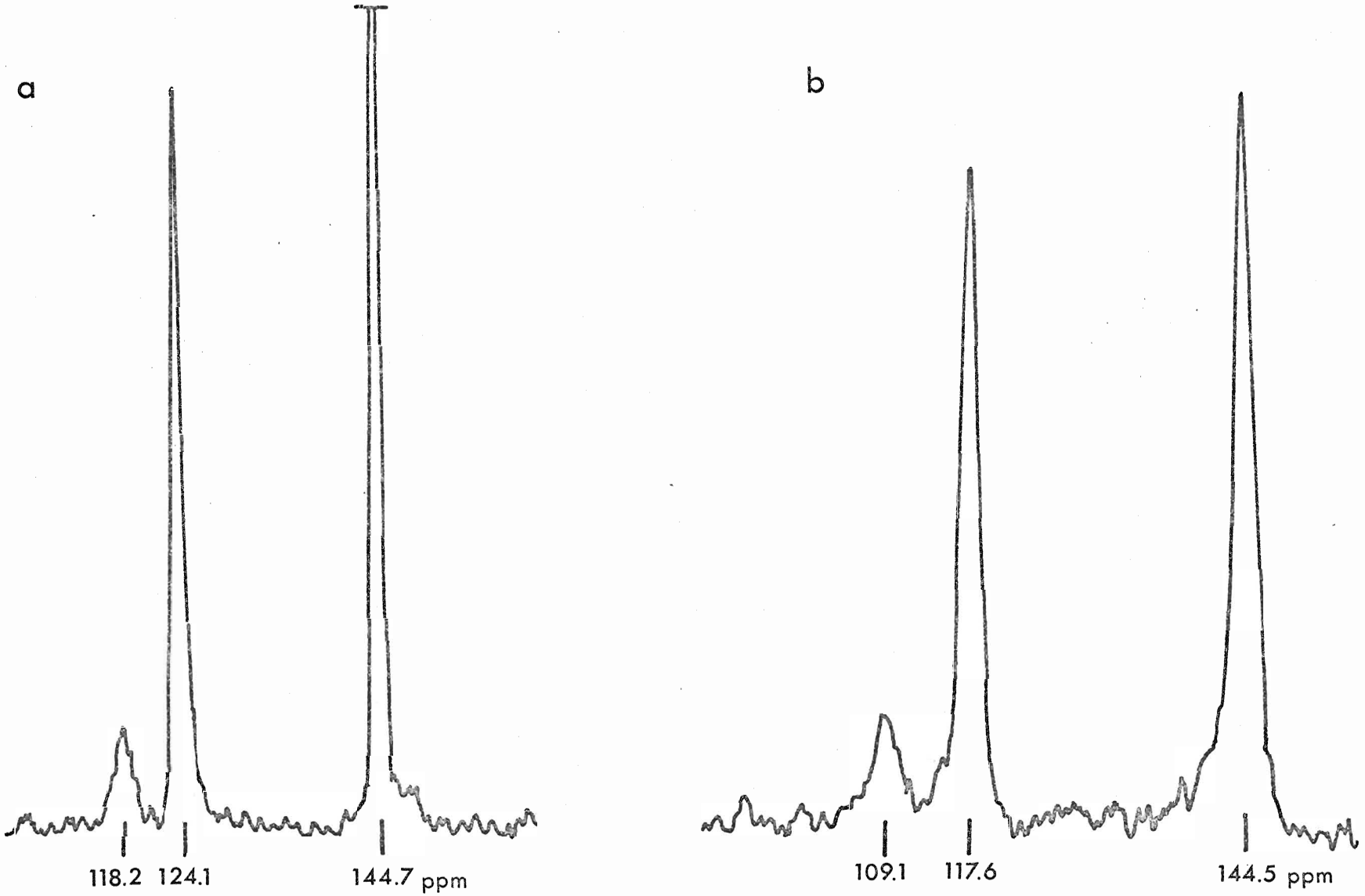
a
118.2
124.1
144.7 ppm
b
109.1
117.6
144.5 ppm

field positions of both of the new peaks. The low relative intensity of the sulfur (selenium)-nitrogen donor peak may similarly be explained in terms of a lowering of the basicity of sulfur (selenium) when a second BF_3 is present. Detailed studies of variations in the relative proportions of different donor-acceptor species were not possible owing to the onset of rapid exchange at acid/base proportions greater than 1.25.

(iii) Comparison with Previous Work

Greenwood and Robinson (21) observed a sharp peak at 150.4 ppm in the ^{19}F spectrum of the BF_3 adduct of *sym*-di-*t*-butyl-thiourea. If rapid exchange occurred, a single peak shifted to lower field by exchange averaging with BF_3 on sulfur should have been observed. The apparent absence of sulfur donation in the *sym*-di-*t*-butylthiourea adduct may be due to unfavorable steric interactions between the BF_3 and the bulky *t*-butyl groups at the sulfur donor site. If BF_4^- was present in these systems, as is suspected in Greenwood's work on the urea adducts (Chapter IV), it very probably would undergo exchange averaging with the nitrogen donor peak. Since both BF_4^- and the nitrogen donor have essentially the same chemical shifts, the presence of BF_4^- contaminant could have easily gone undetected in this system. It seems more likely that the high field peak (150.8 ppm), observed at less than 1:1 acid/base proportions for TMTU and TMSeU complexes, arises from nitrogen coordination than from HF contamination. Thus, it would appear that an equilibri-

um exists between sulfur or selenium donation and nitrogen donation in the 1:1 adducts. In the absence of steric effects, the sulfur or selenium donor site appears to be preferred over the nitrogen donor site.

Isoelectronic donor atoms that are adjacent neighbors in the same period generally give rise to similar ^{19}F chemical shifts for the BF_3 adduct. For example, the chemical shifts attributed to sulfur and selenium donation in the 1:1 adducts, 124.4 ppm and 118.0 ppm, respectively, resemble the chemical shifts of BF_3Cl^- (124.6 ppm) and BF_3Br^- (113.8 ppm).

(B) TETRAMETHYLGUANIDINE

(i) General

Preliminary studies have been carried out on the donor properties of tetramethylguanidine, which is isoelectronic with TMU. Because of recent interest shown in the NMR spectra of guanidine systems (97) and centain parallels which exist between tetramethylguanidine/BF_3 systems and the diphenylketiminoboron dihalides (98), a brief survey of this work is presented here.

(ii) ^1H NMR Spectra

Methylene chloride solutions of the free guanidine, HTMG, where TMG^- is the

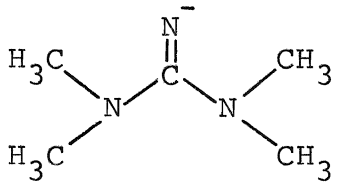

moiety, showed a small broad N-proton peak at 5.06 δ and a sharp methyl singlet at 2.66 δ. Addition of BF_3 to CH_2Cl_2 solutions up to and including 1:1 acid/base proportions resulted in the appearance of a high field peak of fixed chemical shift and migration of the "free" base peak to lower field with increasing proportions of BF_3. The relative peak intensities and chemical shifts up to 1:1 proportions along with their assignments are given in Table XV.

Table XV

^1H NMR Data for the CH_3 Protons when $[BF_3]/[HTMG] \leq 1$

$[BF_3]/[HTMG]$	^1H Chemical Shift (δ)		Relative CH_3 Peak Areas	
	TMG-BF_2	HTMG/HTMG·H^+	(TMG-BF_2)	(Total CH_3 Intensity)
			obs.	calc.
0.00	-	2.66	0.000	0.000
0.26	2.92	2.70	0.116	0.125
0.51	2.92	2.76	0.259	0.250
0.75	2.92	2.82	0.372	0.375
1.00	2.92	2.98	0.502	0.500

Beyond 1:1 acid/base proportions several additional broad CH_3 peaks appeared to lower field and were not readily ammenable to

interpretation. Over the entire range of acid/base proportions, the N-proton peak was broad with a variable chemical shift and was of little diagnostic value.

(iii) ^{19}F NMR Spectra

At less than or equal to 1:1 acid/base proportions, the room temperature spectra consisted of a large BF_4^- signal (verified by its 1 Hz B-F coupling constant and the addition of n-$Bu_4N^+BF_4^-$ (Chapter IV)) and two main quartets of nearly equal intensities having chemical shifts and coupling constants of 141.2 ppm, $J_{^{11}B-^{19}F}$ = 21.9 Hz; and 144.8 ppm, $J_{^{11}B-^{19}F}$ = 16.8 Hz. The magnitudes of the coupling constants are similar to those observed in amine donors (84) while the chemical shifts resemble those of multiply-bonded nitrogen BF_3 adducts (Chapter VI). The low-field quartets were complicated by additional overlapping quartets of low intensity. The relative integrated intensities were (low-field quartets)/(BF_4^-) = 0.29 at $[BF_3]/[HTMG]$ = 0.75. Beyond 1:1 acid/base proportions only a single exchange-averaged peak was observed.

(iv) Interpretations

The spectra are consistent with the reaction sequence

$$2\ HTMG + BF_3 \rightleftharpoons TMG\cdot BF_3^- + HTMG\cdot H^+ \qquad (36)$$

$$TMG\cdot BF_3^- + BF_3 \rightleftharpoons TMG\text{-}BF_2 + BF_4^-$$

where $TMG\text{-}BF_2$ and $HTMG\cdot H^+$ are represented by Structures VIa and VIb, respectively.

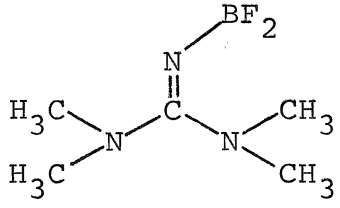

VIa

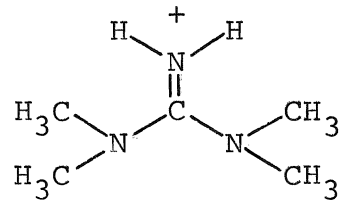

VIb

The concentration dependence of the high field ^{1}H peak (Table XV) closely parallels behavior exhibited by TMU/TMU·H^{+} systems described in Chapter IV and is attributed to rapid proton exchange among HTMG and HTMG·H^{+} species.

The above reaction sequence was confirmed by the mass spectrum of a vacuum dired NMR sample at 1:1 acid/base proportions which gave strong *m/e* values at 164, 163, and 162 and are assigned to HTMG-$^{11}BF_2^{+}$; HTMG-$^{10}BF_2^{+}$, TMG-$^{11}BF_2^{+}$; and TMG-$^{10}BF_2^{+}$, respectively.

Wade and co-workers (98) have described a series of diphenylketiminoboron dihalides. Both the dichloride and dibromide are dimers, while the difluoride appears to be polymeric. The absence of a parent ion attributable to the dimeric form (Structure VII) in the mass spectrum of the HTMG/BF_3 system may be due to the inherent weakness of the boron-nitrogen donor-acceptor bond in these species.

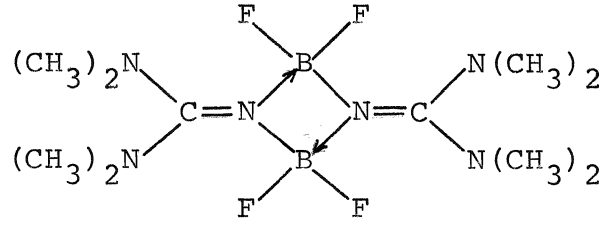

VII

The two main quartets to low field in the ^{19}F spectrum may arise from an equilibrium mixture of the monomer and dimer. Additional quartets and the high intensity of the BF_4^- peak (obs. 71%; theoretical, on the basis of Equation (36, 50%) may arise from further reaction of $TMG\text{-}BF_2$ with BF_3

$$\begin{aligned} &TMG\text{-}BF_2 + BF_3 \rightleftharpoons TMG\text{-}BF^+ + BF_4^- \\ &TMG\text{-}BF^+ + 2HTMG \rightleftharpoons \\ &(TMG)_2BF + HTMG\cdot H^+ \end{aligned} \qquad (37)$$

A similar monomer-dimer equilibrium and similar structures can be invoked to explain the existence of an additional pair of low intensity quartets in the ^{19}F spectrum. Alternatively, quartet pairs may be rationalized in terms of restricted rotation about the B-N bond to give non-equivalent fluorine environments in $TMG\text{-}BF_2$ and $(TMG)_2BF$. However, the temperature variation of this spectrum is required before any firm conclusion can be reached.

BIBLIOGRAPHY

1. J. A. Pople, W. G. Schneider, and H. J. Bernstein, "High-Resolution Nuclear Magnetic Resolution," McGraw-Hill Book Co., New York (1959).

2. A. Abragam, "The Principles of Nuclear Magnetism," Clarendon Press, Oxford (1961).

3. J. W. Emsley, J. Feeney, and L. H. Sutcliffe, "High-Resolution Nuclear Magnetic Resonance Spectroscopy," Vols. I and II, Pergamon Press, Oxford (1966).

4. A. D. Buckingham and K. A. McLauchlan, Proc. Chem. Soc., 144 (1963).

5. J. D. Baldeschwieler and E. W. Randall, Chem. Rev., 63, 81 (1963).

6. R. J. Gillespie and J. W. Quail, J. Chem. Phys., 39, 2555 (1963).

7. R. J. Gillespie and J. S. Hartman, Can. J. Chem., 46, 2147 (1968).

8. J. Bacon, R. J. Gillespie, and J. W. Quail, Can. J. Chem., 41, 3063 (1963).

9. K. Kuhlman and D. M. Grant, J. Phys. Chem., 68, 3208 (1964).

10. R. J. Gillespie and J. S. Hartman, J. Chem. Phys., 45, 2712 (1966).

11. J. H. Beynon, R. A. Saunders, and A. E. Williams, "The Mass Spectra of Organic Molecules," Elsevier Publishing Co., New York (1968), pp. 399, 401.

12. T. D. Coyle and F. G. A. Stone, Progr. Boron Chem., 1, 83 (1964).

13. F. G. A. Stone, Chem. Rev., 58, 101 (1958).

14. N. N. Greenwood and R. L. Martin, Quart. Rev., 8, 1 (1954).

15. A. Finch and P. J. Gardner, Progr. Boron Chem., 3, 177 (1970).

16. A. G. Massey, Advan. Inorg. Chem. Radiochem., 10, 1 (1967).

17. R. W. Taft and J. W. Carten, J. Am. Chem. Soc., 86, 4199 (1964).

18. W. Gerrard, M. F. Lappert, H. Pyszora, and J. W. Wallis, J. Chem. Soc., 2144 (1960).

19. S. J. Kuhn and J. S. McIntyre, Can. J. Chem., 43, 375 (1965).

20. J. M. Miller and M. Onyszchuk, Can. J. Chem., 42, 1518 (1964).

21. N. N. Greenwood and B. H. Robinson, J. Chem. Soc. (A), 511 (1967).

22. I. Wharf and D. F. Shriver, J. Inorg. Nucl. Chem., 32, 1831 (1970).

23. S. Brownstein and J. Paasivirta, Can. J. Chem., 43, 1645 (1965).

24. J. J. Harris, Inorg. Chem., 5, 1627 (1966).

25. F. A. Cotton and J. R. Leto, J. Chem. Phys., 30, 993 (1959).

26. D. G. Brown, R. S. Drago, and T. F. Bolles, J. Am. Chem. Soc., 90, 5706 (1968).

27. (a) M. F. Lappert, J. Chem. Soc., 542 (1962); (b) M. F. Lappert and J. K. Smith, J. Chem. Soc., 5826 (1965).

28. D. Cook, Can. J. Chem., 41, 522 (1963).

29. T. Birchall and R. J. Gillespie, Can. J. Chem., 41, 2642 (1963).

30. G. A. Olah and A. M. White, J. Am. Chem. Soc., 90, 6087 (1968).

31. M. Nardelli and L. Fave, Acta Crystallogr., 12, 727 (1959).

32. A. Lopez-Castro and M. R. Truter, J. Chem. Soc., 1309 (1963).

33. M. Schafer and C. Curran, Inorg. Chem., 5, 265 (1966).

34. I. Lindqvist, "Inorganic Adduct Molecules of Oxo-compounds," Springer Verlag, Berlin (1963).

35. J. C. Lockhart, Chem. Rev., 65, 131 (1965).

36. T. D. Coyle and F. G. A. Stone, J. Chem. Phys., 32, 1892 (1960).

37. N. P. Gates, E. F. Mooney, and D. C. Smith, J. Chem. Soc., 3511 (1964).

38. Reference (7) and references therein.

39. D. E. Hamilton, J. S. Hartman, and J. M. Miller, Chem. Comm., 1417 (1969).

40. J. S. Hartman and J. M. Miller, Inorg. Nucl. Chem. Letters, 5, 831 (1969).

41. R. J. Gillespie, J. S. Hartman, and M. Parekh, Can. J. Chem., 46, 1601 (1968).

42. R. D. W. Kemmitt, R. S. Milner, and D. W. A. Sharp, J. Chem. Soc., 111 (1963).

43. J. M. Miller and M. Onyszchuk, Can. J. Chem., 44, 899 (1966).

44. G. Urry, "The Chemistry of Boron and Its Compounds," E. L. Muetterties, editor, John Wiley and Sons, Inc., New York (1967), Chapter 6.

45. A. Fratiello, T. P. Onak, and R. E. Schuster, J. Am. Chem. Soc., 90, 1194 (1968).

46. W. G. Henderson and E. F. Mooney, Ann. Rev. NMR Spec., 2, 219 (1969).

47. S. A. Fieldhouse and I. A. Peat, J. Phys. Chem., 73, 275 (1969).

48. C. R. Witschonke and C. A. Kraus, J. Am. Chem. Soc., 69, 2473 (1947).

49. R. J. Thompson and J. C. Davis, Inorg. Chem., 4, 1464 (1965).

50. "Handbook of Chemistry and Physics," 51st edition, R. C. Weast, editor, Chemical Rubber Co., Cleveland (1970), p. C-533.

51. K. A. Jensen, G. Felbert, and B. Kägi, Acta Chem. Scand., 20, 281 (1966).

52. Reference (50), p. B-74.

53. M. G. Voronkov, B. N. Dolgov, and N. A. Dimitrieva, Doklady Akad. Nauk S. S. S. R., 84, 959 (1952).

54. R. T. Sanderson, "Vacuum Manipulation of Volatile Compounds," John Wiley and Sons, Inc., New York (1948).

55. D. F. Shriver, "The Manipulation of Air-sensitive Compounds," McGraw-Hill Book Co., New York (1969).

56. Quantum Chemistry Program Exchange, Department of Chemistry, Indiana University, Bloomington, Indiana, U. S. A.

57. J. Barr, R. J. Gillespie, and R. C. Thompson, Inorg. Chem., 3, 1149 (1964).

58. T. C. Waddington and F. Klanberg, J. Chem. Soc., 2339 (1960).

59. Reference (3), Vol. II, Appendix B.

60. (a) H. Schmidbaur, J. Am. Chem. Soc., 85, 2336 (1963); (b) R. B. Johannesen, F. E. Brinckman, and T. D. Coyle, J. Phys. Chem., 72, 660 (1968).

61. A. Müller, E. Niecke, and B. Krebs, Mol. Phys., 14, 591 (1968).

62. Reference (3), Vol. II, p. 996.

63. N. Muller and D. T. Carr, J. Phys. Chem., 67, 112 (1963).

64. T. Vladimiroff and E. R. Malinowski, J. Chem. Phys., 46, 1830 (1967).

65. E. R. Malinowski, J. Am. Chem. Soc., 91, 4701 (1969).

66. E. R. Malinowski and T. Vladimiroff, J. Am. Chem. Soc., 86, 3575 (1964).

67. A. C. Blizzard and D. P. Santry, Chem. Comm., 1085 (1970).

68. J. A. Pople and D. P. Santry, Mol. Phys., 8, 1 (1964).

69. A. C. Blizzard and D. P. Santry, Chem. Comm., 87 (1970).

70. A. Saika and C. P. Slichter, J. Chem. Phys., 22, 26 (1954).

71. J. A. Pople, Mol. Phys., 7, 301 (1963-64).

72. M. Karplus and J. A. Pople, J. Chem. Phys., 38, 2803 (1963).

73. J. C. Slater, Phys. Rev., 36, 57 (1930).

74. D. R. Armstrong and P. G. Perkins, Chem. Comm., 337 (1965).

75. (a) J. A. Pople, D. P. Santry, and G. A. Segal, J. Chem. Phys., 43, S129 (1965);
(b) J. A. Pople and G. A. Segal, J. Chem. Phys., 43, S136 (1965);
(c) J. A. Pople and G. A. Segal, J. Chem. Phys., 44, 3298 (1966).

76. T. L. Cottrell, "The Strengths of Chemical Bonds," Butterworths, London (1958), Table 11.5.1.

77. G. Brunton, Acta Crystallogr., Sect. B, 2161 (1969).

78. O. Glemser, B. Krebs, J. Wegener, and E. Kindler, Angew. Chem., 81, 568 (1969).

79. P. J. Bassett and D. R. Lloyd, Chem. Comm., 36 (1970).

80. R. G. Kidd and D. R. Truax, J. Am. Chem. Soc., 90, 6867 (1968).

81. W. E. Stewart and T. H. Siddall, Chem. Rev., 70, 517 (1970).

82. R. J. Gillespie and J. S. Hartman, Can. J. Chem., 45, 2243 (1967).

83. Reference (83), pp. 534-51.

84. C. W. Heitsch, Inorg. Chem., 4, 1019 (1965).

85. Unpublished work of J. S. Hartman and J. M. Miller.

86. R. L. Werner, V. F. Duckworth, and H. J. Schnitzeling, Austral. J. Chem., 18, 1751 (1965).

87. H. F. Henneike and R. S. Drago, Inorg. Chem., 7, 1908 (1968).

88. D. M. Grant and W. M. Lichtman, J. Am. Chem. Soc., 87, 3994 (1965).

89. H. A. Bent, Chem. Rev., 61, 275 (1961).

90. C. Juan and H. S. Gutowsky, J. Chem. Phys., 37, 2198 (1962).

91. R. L. Middaugh, R. S. Drago, and R. J. Niedzielski, J. Am. Chem. Soc., 86, 388 (1964).

92. L. A. LaPlanche and M. T. Rogers, J. Am. Chem. Soc., 86, 337 (1964).

93. H. Nöth, Progr. Boron Chem., 3, 211 (1970).

94. N. M. D. Brown and P. Bladon, J. Chem. Soc. (A), 526 (1969).

95. N. Wiberg and J. W. Buchler, Chem. Ber., 96, 3000 (1963).

96. R. G. Pearson, J. Am. Chem. Soc., 85, 3533 (1963).

97. H. Kessler and D. Leibfritz, Tetrahedron, 25, 5127 (1969).

98. J. R. Jennings, I. Pattison, and K. Wade, J. Chem. Soc. (A), 565 (1969).